

**CROSS-SECTIONS OF LARGE-ANGLE HADRON PRODUCTION
IN PROTON- AND PION-NUCLEUS INTERACTIONS IV:
COPPER NUCLEI AND BEAM MOMENTA FROM ± 3 GeV/c TO ± 15 GeV/c**

Abstract

We report on double-differential inclusive cross-sections of the production of secondary protons, charged pions, and deuterons, in the interactions with a 5% λ_{abs} thick stationary copper target, of proton and pion beams with momentum from ± 3 GeV/c to ± 15 GeV/c. Results are given for secondary particles with production angles $20^\circ < \theta < 125^\circ$.

The HARP–CDP group

A. Bolshakova¹, I. Boyko¹, G. Chelkov^{1a}, D. Dedovitch¹, A. Elagin^{1b}, M. Gostkin¹,
 A. Guskov¹, Z. Kroumchtein¹, Yu. Nefedov¹, K. Nikolaev¹, A. Zhemchugov¹, F. Dydak²,
 J. Wotschack^{2*}, A. De Min^{3c}, V. Ammosov⁴, V. Gapienko⁴, V. Koreshev⁴, A. Semak⁴,
 Yu. Sviridov⁴, E. Usenko^{4d}, V. Zaets⁴

¹ Joint Institute for Nuclear Research, Dubna, Russia

² CERN, Geneva, Switzerland

³ Politecnico di Milano and INFN, Sezione di Milano-Bicocca, Milan, Italy

⁴ Institute of High Energy Physics, Protvino, Russia

(To be submitted to Eur. Phys. J. C)

^a Also at the Moscow Institute of Physics and Technology, Moscow, Russia

^b Now at Texas A&M University, College Station, USA

^c On leave of absence at Ecole Polytechnique Fédérale, Lausanne, Switzerland

^d Now at Institute for Nuclear Research RAS, Moscow, Russia

* Corresponding author; e-mail: joerg.wotschack@cern.ch

1 INTRODUCTION

The HARP experiment arose from the realization that the inclusive differential cross-sections of hadron production in the interactions of few GeV/c protons with nuclei were known only within a factor of two to three, while more precise cross-sections are in demand for several reasons. Pion production data on a variety of nuclei are required for (i) the understanding of the underlying physics and the modelling of Monte Carlo generators of hadron–nucleus collisions, (ii) the optimization of the design parameters of the proton driver of a neutrino factory, (iii) flux predictions for conventional neutrino beams, and (iv) the calculation of the atmospheric neutrino flux.

Consequently, the HARP detector was designed to carry out a programme of systematic and precise (i.e., at the few per cent level) measurements of hadron production by protons and pions with momenta from 1.5 to 15 GeV/c .

The detector combined a forward spectrometer with a large-angle spectrometer. The latter comprised a cylindrical Time Projection Chamber (TPC) around the target and an array of Resistive Plate Chambers (RPCs) that surrounded the TPC. The purpose of the TPC was track reconstruction and particle identification by dE/dx . The purpose of the RPCs was to complement the particle identification by time of flight.

The HARP experiment was performed at the CERN Proton Synchrotron in 2001 and 2002 with a set of stationary targets ranging from hydrogen to lead.

Here, we report on the large-angle production (polar angle θ in the range $20^\circ < \theta < 125^\circ$) of secondary protons and charged pions, and of deuterons, in the interactions with a 5% λ_{abs} Cu target of protons and pions with beam momenta of ± 3.0 , ± 5.0 , ± 8.0 , ± 12.0 , and ± 15.0 GeV/c .

This is the fourth of a series of cross-section papers with results from the HARP experiment. In the first paper, Ref. [1], we described the detector characteristics and our analysis algorithms, on the example of $+8.9$ GeV/c and -8.0 GeV/c beams impinging on a 5% λ_{abs} Be target. The second paper [2] presented results for all beam momenta from this Be target, and the third paper [3] results from the interactions with a 5% λ_{abs} Ta target.

Our work involves only the HARP large-angle spectrometer, the characteristics of which are described in detail in Refs. [4] and [5].

2 THE T9 PROTON AND PION BEAMS, AND THE TARGET

The protons and pions were delivered by the T9 beam line in the East Hall of CERN’s Proton Synchrotron. This beam line supports beam momenta between 1.5 and 15 GeV/c , with a momentum bite $\Delta p/p \sim 1\%$.

Beam particle identification was provided for by two threshold Cherenkov counters, BCA and BCB, filled with nitrogen, and by time of flight over a flight path of 24.3 m. Table 1 lists the beam instrumentation that was used at different beam momenta for p/π^+ and for π/e separation.

The pion beam had a contamination by muons from pion decays. It also had a contamination by electrons from converted photons from π^0 decays. Only for the beam momenta of 3 and 5 GeV/c were electrons identified by a beam Cherenkov counter and rejected.

The fractions of muon and electron contaminations of the pion beam were experimentally determined [6, 7] and are listed in Table 2 for all beam momenta. For the determination of interaction cross-sections of pions, the muon and electron contaminations must be subtracted from the incoming flux of pion-like particles (except electrons at the beam momenta of 3 and 5 GeV/c).

There is also a kaon contamination of a few per cent in the proton and pion beams. Kaons are suppressed by the beam instrumentation, except at 5 GeV/c beam momentum where they

Table 1: Beam instrumentation for p/π^+ and π/e separation

Beam momentum [GeV/c]	p/π^+ separation	π/e separation
± 3.0	TOF	BCB (1.05 bar)
± 5.0	TOF	BCA (0.60 bar)
± 8.0	BCA (1.25 bar) BCB (1.50 bar)	
± 12.0 and ± 15.0	BCA (3.50 bar) BCB (3.50 bar)	

Table 2: Contaminations of the pion beams by muons and electrons

Beam momentum [GeV/c]	Muon fraction	Electron fraction
± 3.0	$(4.1 \pm 0.4)\%$	rejected
± 5.0	$(5.1 \pm 0.4)\%$	rejected
± 8.0	$(1.9 \pm 0.5)\%$	$(1.2 \pm 0.5)\%$
± 12	$(0.6 \pm 0.6)\%$	$(0.5 \pm 0.5)\%$
± 15	$(0.0 \pm 0.5)\%$	$(0.0 \pm 0.5)\%$

are indistinguishable from pions. Because the kaon interaction cross-sections are close to the pion interaction cross-sections, this kaon contamination is ignored.

The beam trajectory was determined by a set of three multiwire proportional chambers (MWPCs), located upstream of the target, several metres apart. The transverse error of the impact point on the target was 0.5 mm from the resolution of the MWPCs, plus a contribution from multiple scattering of the beam particles in various materials in the beam line. Excluding the target itself, the latter contribution is 0.2 mm for a 8 GeV/c beam particle.

We select ‘good’ beam particles by requiring the unambiguous reconstruction of the particle trajectory with good χ^2 . In addition we require that the particle type is unambiguously identified. We select ‘good’ accelerator spills by requiring a minimal beam intensity and a ‘smooth’ variation of beam intensity across the 400 ms long spill¹⁾.

The target was a disc made of high-purity (99.99%) copper, with a density of 8.91 g/cm³, a radius of 15.1 mm, and a thickness of 7.52 ± 0.05 mm (5% λ_{abs}).

The finite thickness of the target leads to a small attenuation of the number of incident beam particles. The attenuation factor is $f_{\text{att}} = 0.975$.

The size of the beam spot at the position of the target was several millimetres in diameter, determined by the setting of the beam optics and by multiple scattering. The nominal beam position²⁾ was at $x_{\text{beam}} = y_{\text{beam}} = 0$, however, excursions by several millimetres could occur³⁾.

¹⁾A smooth variation of beam intensity eases corrections for dynamic TPC track distortions.

²⁾A right-handed Cartesian and/or spherical polar coordinate system is employed; the z axis coincides with the beam line, with $+z$ pointing downstream; the coordinate origin is at the upstream end of the copper target, 500 mm downstream of the TPC’s pad plane; looking downstream, the $+x$ coordinate points to the left and the $+y$ coordinate points up; the polar angle θ is the angle with respect to the $+z$ axis.

³⁾The only relevant issue is that the trajectory of each individual beam particle is known, whether shifted or not, and therefore the amount of matter to be traversed by the secondary hadrons.

A loose fiducial cut $\sqrt{x_{\text{beam}}^2 + y_{\text{beam}}^2} < 12 \text{ mm}$ ensured full beam acceptance. The muon and electron contaminations of the pion beam, stated above, refer to this acceptance cut.

3 PERFORMANCE OF THE HARP LARGE-ANGLE DETECTORS

Our calibration work on the HARP TPC and RPCs is described in detail in Refs. [4] and [5], and in references cited therein. In particular, we recall that static and dynamic TPC track distortions up to 10 mm have been corrected to better than $300 \mu\text{m}$. Therefore, TPC track distortions do not affect the precision of our cross-section measurements.

The resolution $\sigma(1/p_T)$ is typically $0.2 (\text{GeV}/c)^{-1}$ and worsens towards small relative particle velocity β and small polar angle θ .

The absolute momentum scale is determined to be correct to better than 2%, both for positively and negatively charged particles.

The polar angle θ is measured in the TPC with a resolution of $\sim 9 \text{ mrad}$, for a representative angle of $\theta = 60^\circ$. To this a multiple scattering error has to be added which is on the average $\sim 7 \text{ mrad}$ for a proton with $p_T = 500 \text{ MeV}/c$ in the TPC gas and $\theta = 60^\circ$, and $\sim 4 \text{ mrad}$ for a pion with the same characteristics. The polar-angle scale is correct to better than 2 mrad.

The TPC measures dE/dx with a resolution of 16% for a track length of 300 mm.

The intrinsic efficiency of the RPCs that surround the TPC is better than 98%.

The intrinsic time resolution of the RPCs is 127 ps and the system time-of-flight resolution (that includes the jitter of the arrival time of the beam particle at the target) is 175 ps.

To separate measured particles into species, we assign on the basis of dE/dx and β to each particle a probability of being a proton, a pion (muon), or an electron, respectively. The probabilities add up to unity, so that the number of particles is conserved. These probabilities are used for weighting when entering tracks into plots or tables.

4 MONTE CARLO SIMULATION

We used the Geant4 tool kit [8] for the simulation of the HARP large-angle spectrometer.

Geant4's QGSP_BIC physics list provided us with reasonably realistic spectra of secondaries from incoming beam protons with momentum less than $12 \text{ GeV}/c$. For the secondaries from beam protons at 12 and 15 GeV/c momentum, and from beam pions at all momenta, we found the standard physics lists of Geant4 unsuitable [9].

To overcome this problem, we built our own HARP_CDP physics list for the production of secondaries from incoming beam pions. It starts from Geant4's standard QBBC physics list, but the Quark–Gluon String Model is replaced by the FRITIOF string fragmentation model for kinetic energy $E > 6 \text{ GeV}$; for $E < 6 \text{ GeV}$, the Bertini Cascade is used for pions, and the Binary Cascade for protons; elastic and quasi-elastic scattering is disabled. Examples of the good performance of the HARP_CDP physics list are given in Ref. [9].

5 SYSTEMATIC ERRORS

The systematic uncertainty of our inclusive cross-sections is at the few-per-cent level, from errors in the normalization, in the momentum measurement, in particle identification, and in the corrections applied to the data.

The systematic error of the absolute flux normalization is taken as 2%. This error arises from uncertainties in the target thickness, in the contribution of large-angle scattering of beam particles, in the attenuation of beam particles in the target, and in the subtraction of the muon

and electron contaminations of the beam. Another contribution comes from the removal of events with an abnormally large number of TPC hits⁴⁾.

The systematic error of the track finding efficiency is taken as 1% which reflects differences between results from different persons who conducted eyeball scans. We also take the statistical errors of the parameters of a fit to scan results as systematic error into account [1]. The systematic error of the correction for losses from the requirement of at least 10 TPC clusters per track is taken as 20% of the correction which itself is in the range of 5 to 30%. This estimate arose from differences between the four TPC sectors that were used in our analysis, and from the observed variations with time.

The systematic error of the p_T scale is taken as 2% as discussed in Ref. [4]. For the data from the +15 GeV/c beams, this error was doubled to account for a larger than usual uncertainty of the correction for dynamic TPC track distortions.

The systematic errors of the proton, pion, and electron abundances are taken as 10%. We stress that errors on abundances only lead to cross-section errors in case of a strong overlap of the resolution functions of both identification variables, dE/dx and β . The systematic error of the correction for migration, absorption of secondary protons and pions in materials, and for pion decay into muons, is taken as 20% of the correction, or 1% of the cross-section, whichever is larger. These estimates reflect our experience with remanent differences between data and Monte Carlo simulations after weighting Monte Carlo events with smooth functions with a view to reproducing the data simultaneously in several variables in the best possible way.

All systematic errors are propagated into the momentum spectra of secondaries and then added in quadrature.

6 CROSS-SECTION RESULTS

In Tables A.1–A.45, collated in the Appendix of this paper, we give the double-differential inclusive cross-sections $d^2\sigma/dpd\Omega$ for various combinations of incoming beam particle and secondary particle, including statistical and systematic errors. In each bin, the average momentum at the vertex and the average polar angle are also given.

The data of Tables A.1–A.45 are available in ASCII format in Ref. [10].

Some bins in the tables are empty. Cross-sections are only given if the total error is not larger than the cross-section itself. Since our track reconstruction algorithm is optimized for tracks with p_T above ~ 70 MeV/c in the TPC volume, we do not give cross-sections from tracks with p_T below this value. Because of the absorption of slow protons in the material between the vertex and the TPC gas, and with a view to keeping the correction for absorption losses below 30%, cross-sections from protons are limited to $p > 450$ MeV/c at the interaction vertex. Proton cross-sections are also not given if a 10% error on the proton energy loss in materials between the interaction vertex and the TPC volume leads to a momentum change larger than 2%. Since the proton energy loss is large in the copper target, particularly at polar angles close to 90 degrees, the latter condition imposes significant restrictions. Pion cross-sections are not given if pions are separated from protons by less than twice the time-of-flight resolution.

The large errors and/or absence of results from the +15 GeV/c pion beams are caused by scarce statistics because the beam composition was dominated by protons.

We present in Figs. 1 to 7 what we consider salient features of our cross-sections.

Figure 1 shows the inclusive cross-sections of the production of protons, π^+ 's, and π^- 's,

⁴⁾In less than 0.5% of the number of good events, because of apparatus malfunction, the number of TPC hits was much larger than possible for a physics event. Such events were considered unphysical and eliminated.

from incoming protons between $3 \text{ GeV}/c$ and $15 \text{ GeV}/c$ momentum, as a function of their charge-signed p_T . The data refer to the polar-angle range $20^\circ < \theta < 30^\circ$. Figures 2 and 3 show the same for incoming π^+ 's and π^- 's.

Figure 4 shows the inclusive cross-sections of the production of protons, π^+ 's, and π^- 's, from incoming protons between $3 \text{ GeV}/c$ and $15 \text{ GeV}/c$ momentum, this time as a function of their charge-signed polar angle θ . The data refer to the p_T range $0.24 < p_T < 0.30 \text{ GeV}/c$. In this p_T range pions populate nearly all polar angles, whereas protons are absorbed at large polar angle and thus escape measurement. Figures 5 and 6 show the same for incoming π^+ 's and π^- 's.

In Fig. 7, we present the inclusive cross-sections of the production of secondary π^+ 's and π^- 's, integrated over the momentum range $0.2 < p < 1.0 \text{ GeV}/c$ and the polar-angle range $30^\circ < \theta < 90^\circ$ in the forward hemisphere, as a function of the beam momentum.

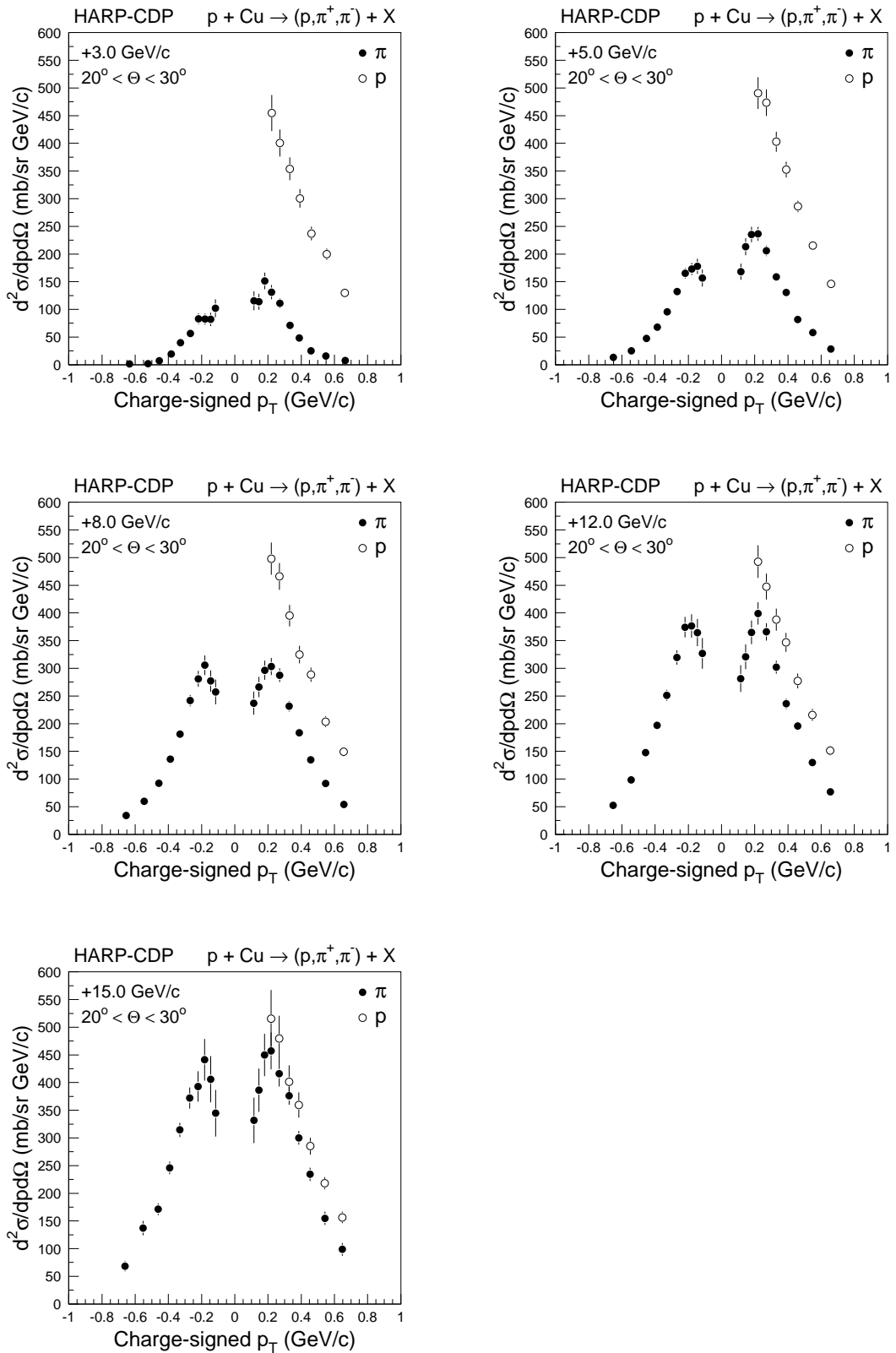


Fig. 1: Inclusive cross-sections of the production of secondary protons, π^+ 's, and π^- 's, by protons on copper nuclei, in the polar-angle range $20^\circ < \theta < 30^\circ$, for different proton beam momenta, as a function of the charge-signed p_T of the secondaries; the shown errors are total errors.

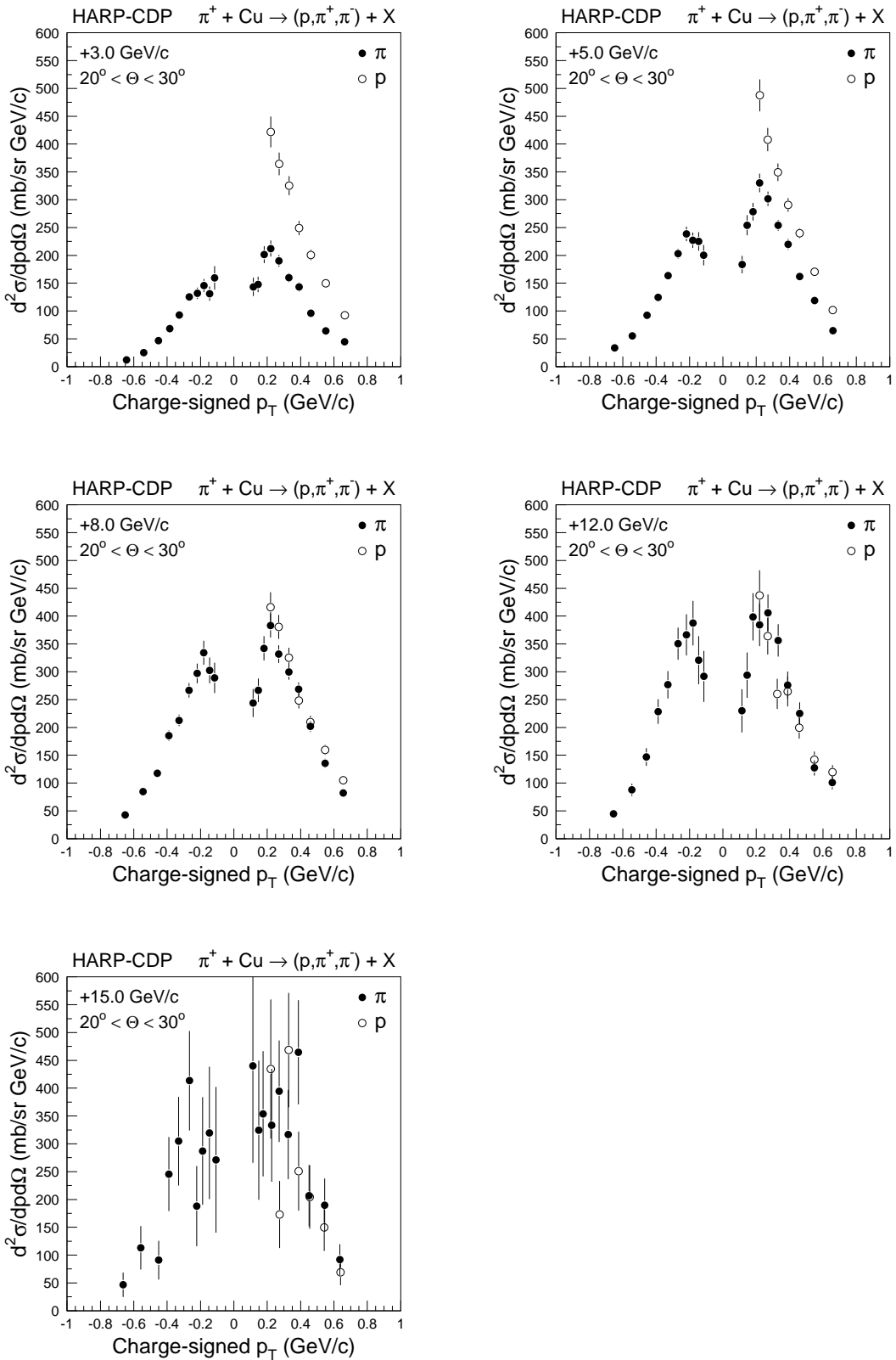


Fig. 2: Inclusive cross-sections of the production of secondary protons, π^+ 's, and π^- 's, by π^+ 's on copper nuclei, in the polar-angle range $20^\circ < \theta < 30^\circ$, for different π^+ beam momenta, as a function of the charge-signed p_T of the secondaries; the shown errors are total errors.

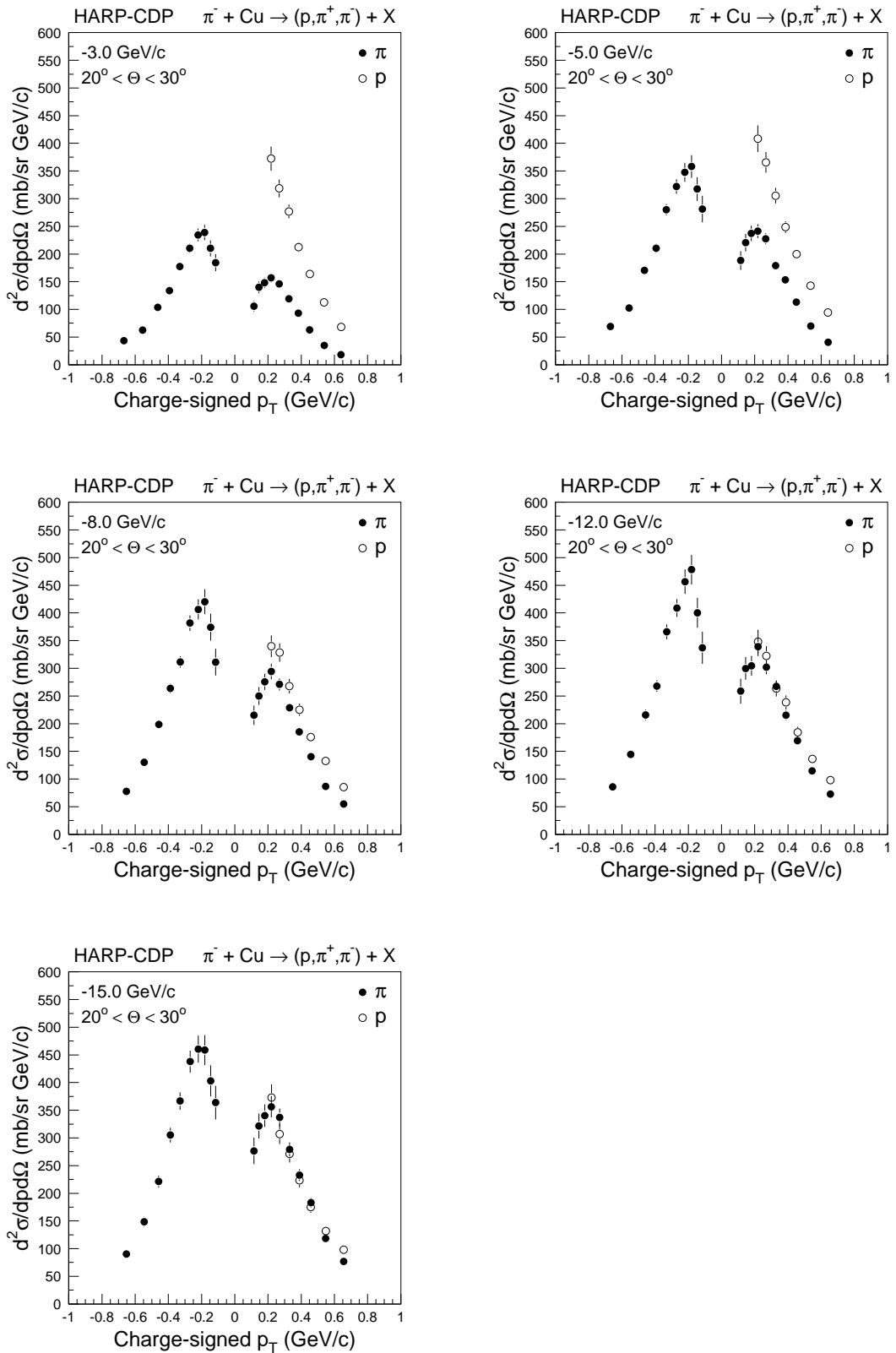


Fig. 3: Inclusive cross-sections of the production of secondary protons, π^+ 's, and π^- 's, by π^- 's on copper nuclei, in the polar-angle range $20^\circ < \theta < 30^\circ$, for different π^- beam momenta, as a function of the charge-signed p_T of the secondaries; the shown errors are total errors.

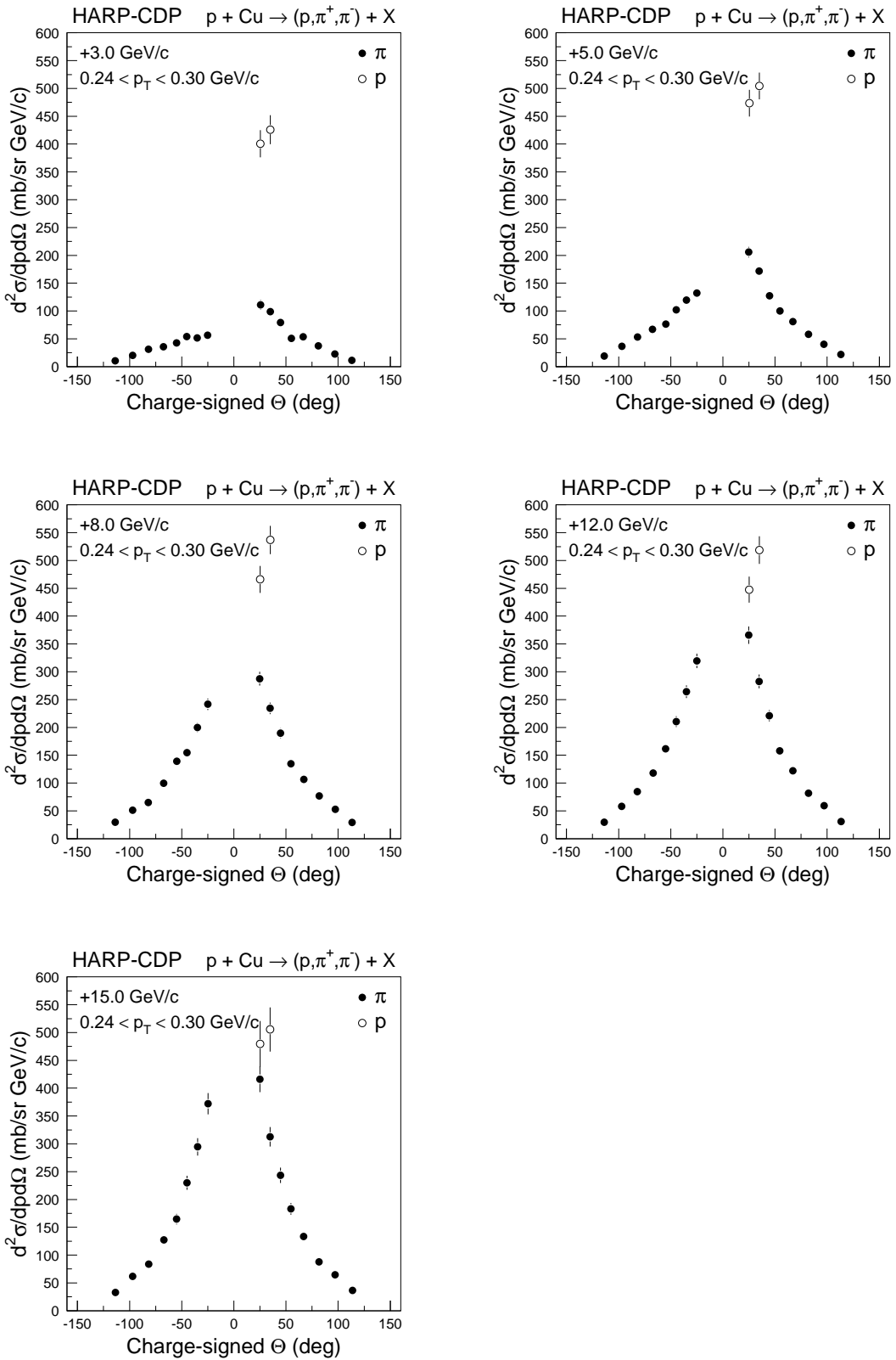


Fig. 4: Inclusive cross-sections of the production of secondary protons, π^+ 's, and π^- 's, with p_T in the range 0.24–0.30 GeV/c, by protons on copper nuclei, for different proton beam momenta, as a function of the charge-signed polar angle θ of the secondaries; the shown errors are total errors.

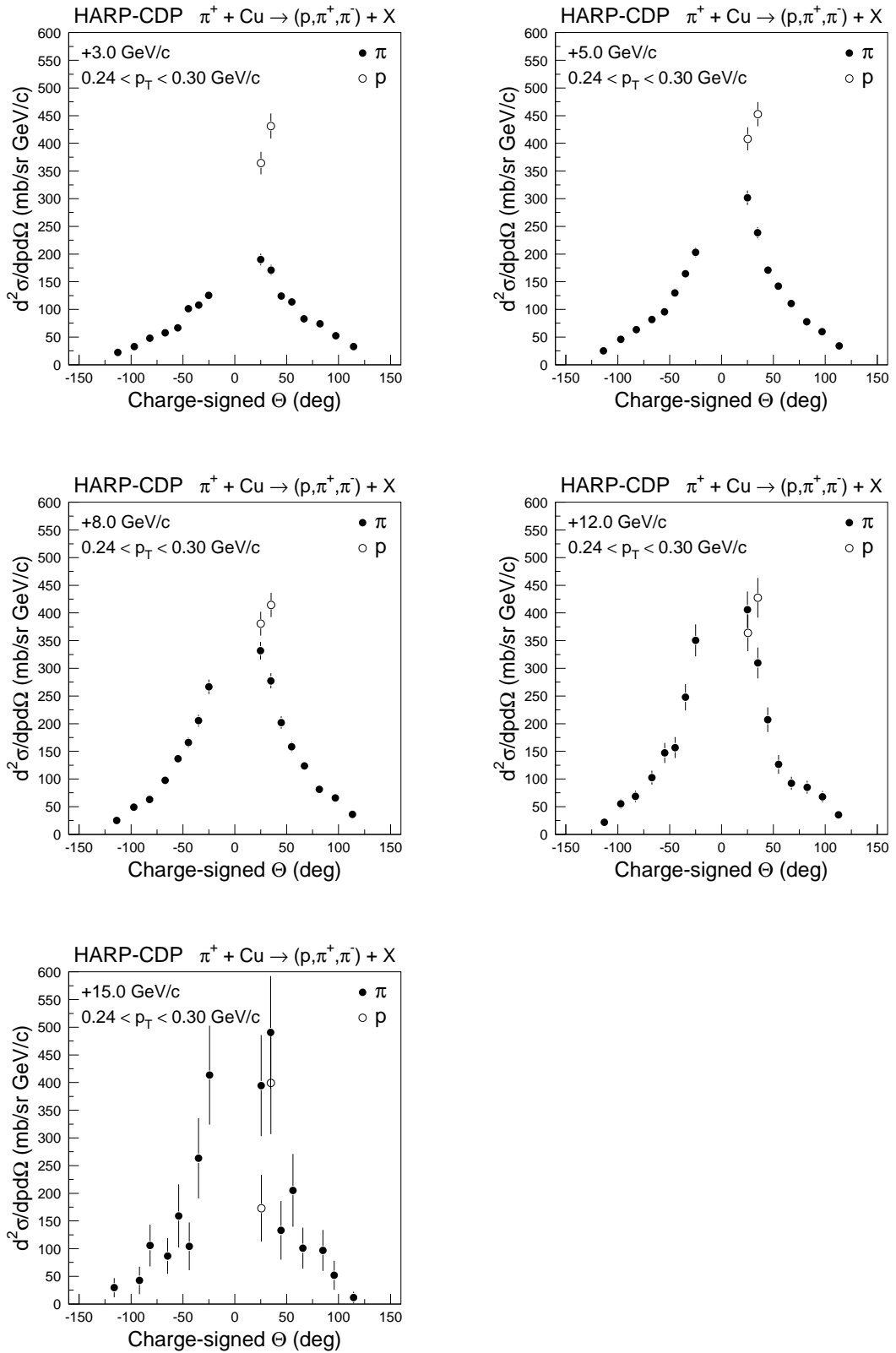


Fig. 5: Inclusive cross-sections of the production of secondary protons, π^+ 's, and π^- 's, with p_T in the range 0.24–0.30 GeV/c , by π^+ 's on copper nuclei, for different π^+ beam momenta, as a function of the charge-signed polar angle θ of the secondaries; the shown errors are total errors.

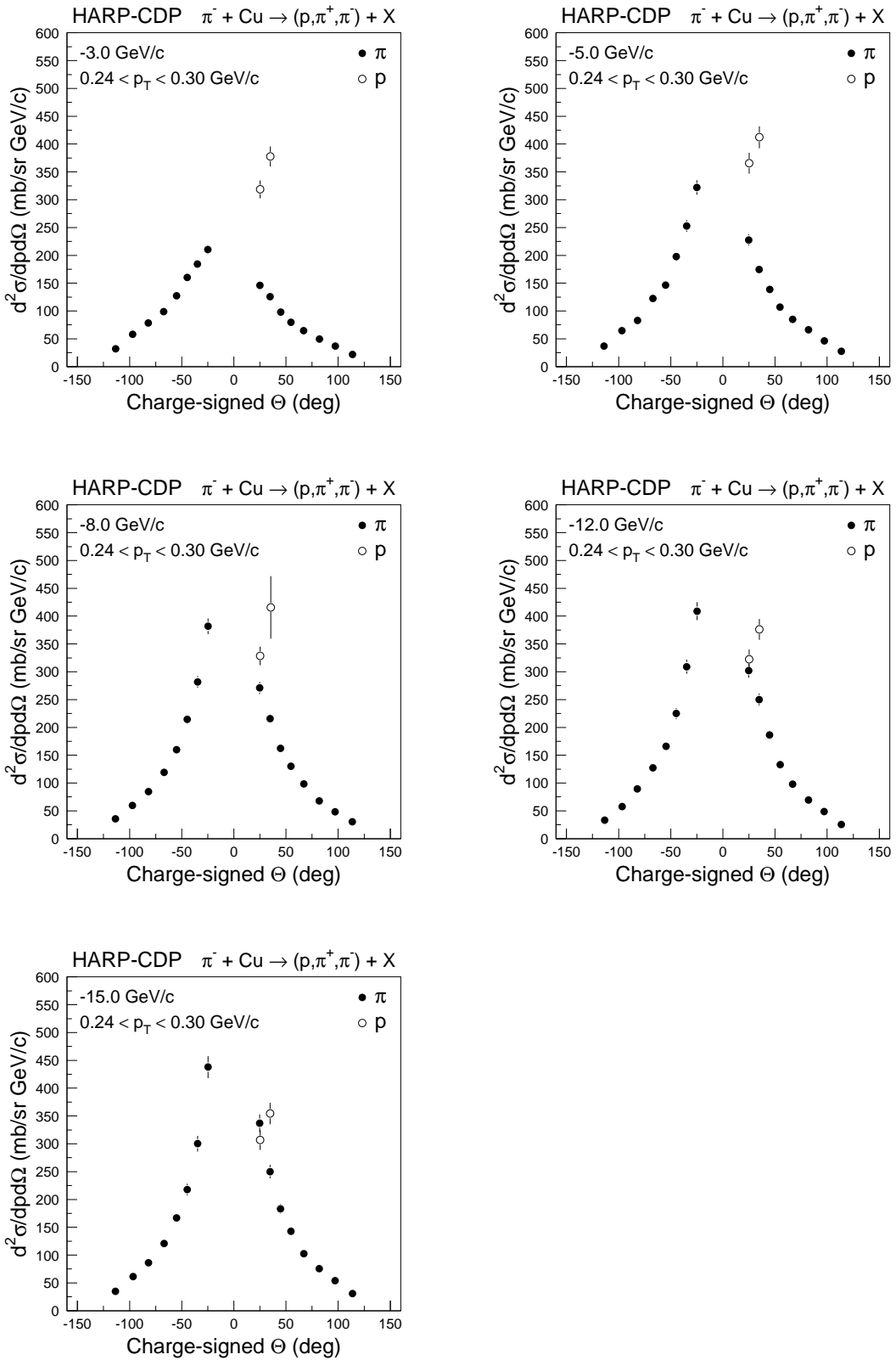


Fig. 6: Inclusive cross-sections of the production of secondary protons, π^+ 's, and π^- 's, with p_T in the range 0.24–0.30 GeV/c, by π^- 's on copper nuclei, for different π^- beam momenta, as a function of the charge-signed polar angle θ of the secondaries; the shown errors are total errors.

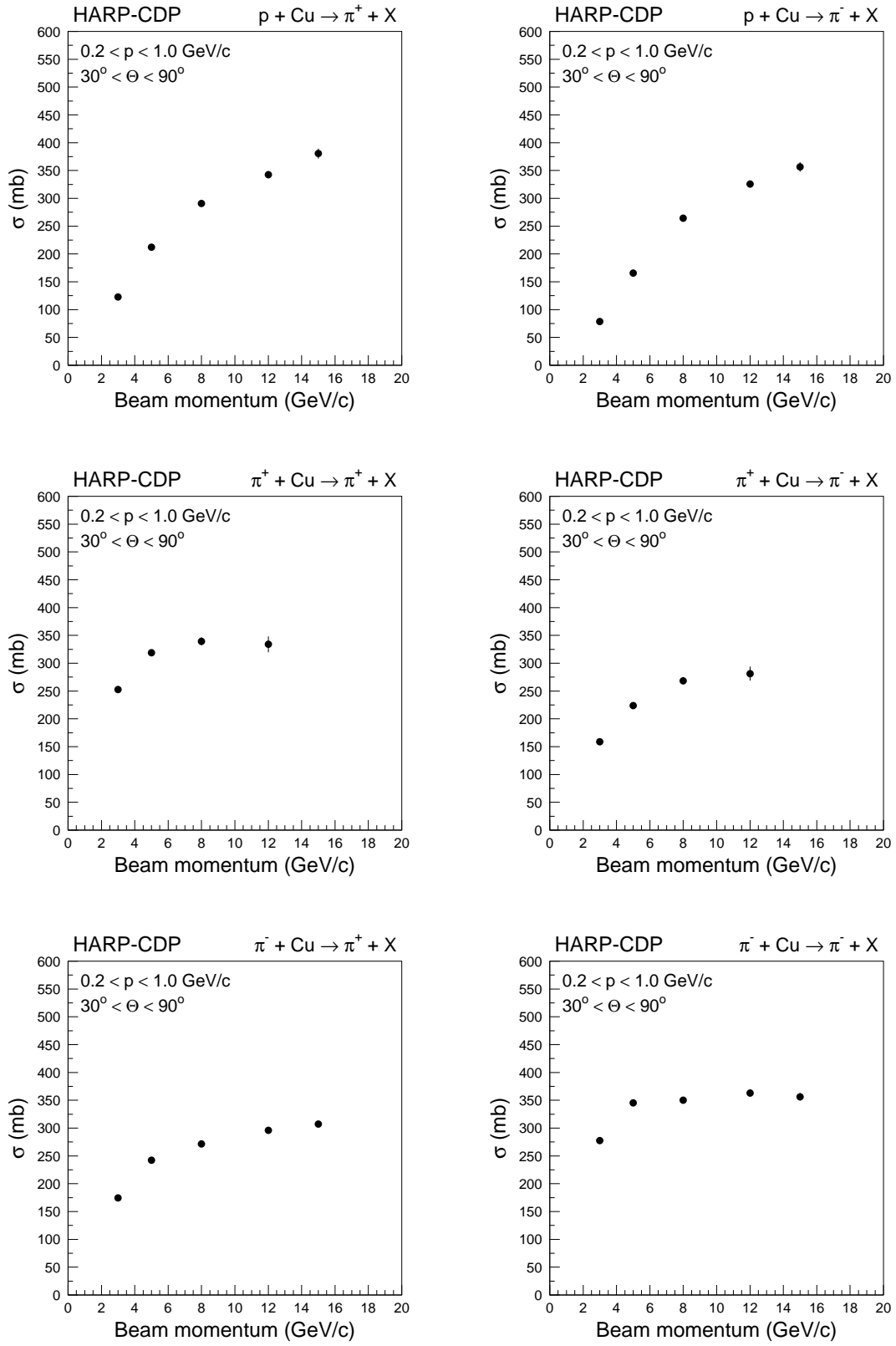


Fig. 7: Inclusive cross-sections of the production of secondary π^+ 's and π^- 's, integrated over the momentum range $0.2 < p < 1.0 \text{ GeV}/c$ and the polar-angle range $30^\circ < \theta < 90^\circ$, from the interactions on copper nuclei of protons (top row), π^+ 's (middle row), and π^- 's (bottom row), as a function of the beam momentum; the shown errors are total errors and mostly smaller than the symbol size.

7 DEUTERON PRODUCTION

Besides pions and protons, also deuterons are produced in sizeable quantities on copper nuclei. Up to momenta of about $1 \text{ GeV}/c$, deuterons are easily separated from protons by dE/dx .

Table 3 gives the ratio of deuteron to proton production as a function of the momentum at the vertex, for $8 \text{ GeV}/c$ beam protons, π^+ 's, and π^- 's⁵⁾. Cross-section ratios are not given if the data are scarce and the statistical error becomes comparable with the ratio itself—which is the case for deuterons at the high-momentum end of the spectrum.

The measured deuteron to proton production ratios are illustrated in Fig. 8, and compared with the predictions of Geant4's FRITIOF model. FRITIOF's predictions are shown for the same beam particles for which measured values are plotted. There is virtually no difference between its predictions for incoming protons, π^+ 's and π^- 's. FRITIOF underestimates deuteron production.

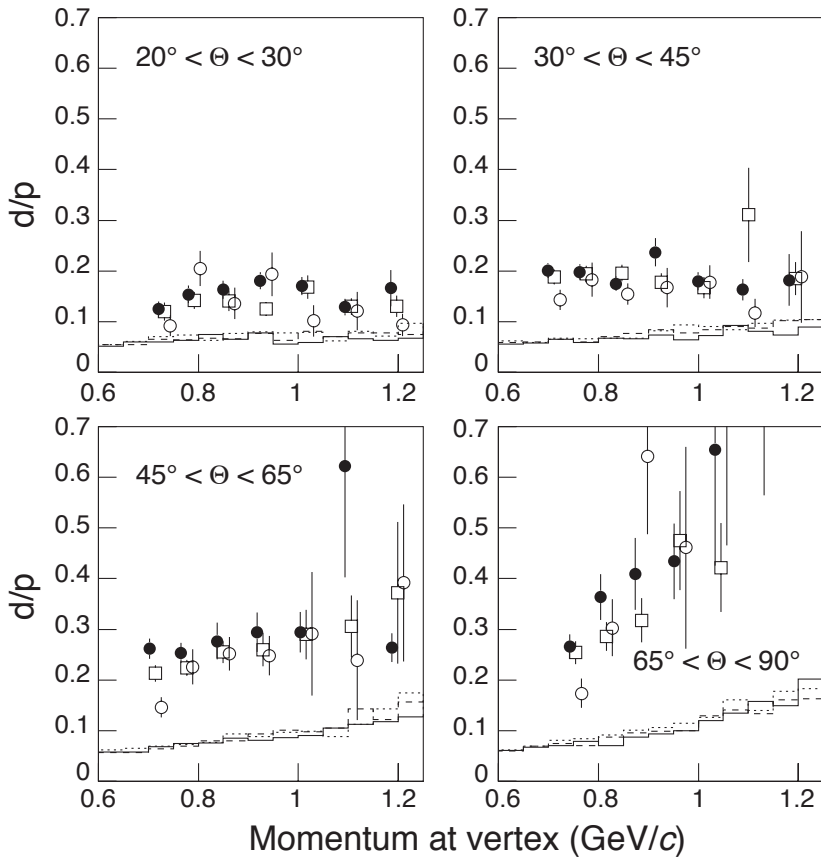


Fig. 8: Deuteron to proton ratio for $8 \text{ GeV}/c$ beam particles on copper nuclei, as a function of the momentum at the vertex, for four polar-angle regions; open squares denote beam protons, open circles beam π^+ 's, and full circles beam π^- 's; the full and broken lines denote predictions of Geant4's FRITIOF model for the three different beam particles.

⁵⁾We observe no appreciable dependence of the deuteron to proton ratio on beam momentum.

Table 3: Deuteron to proton ratio for beam protons, π^+ 's, and π^- 's of 8 GeV/c momentum, as a function of the particle momentum p [GeV/c] at the vertex, for five polar-angle regions.

Polar angle θ	p	Beam p	Beam π^+	Beam π^-
		d/p	d/p	d/p
$20^\circ - 30^\circ$	0.732	0.120 ± 0.018	0.092 ± 0.020	0.125 ± 0.015
	0.792	0.142 ± 0.017	0.205 ± 0.035	0.154 ± 0.017
	0.861	0.141 ± 0.020	0.136 ± 0.031	0.163 ± 0.018
	0.936	0.125 ± 0.014	0.193 ± 0.043	0.181 ± 0.017
	1.019	0.168 ± 0.023	0.102 ± 0.031	0.170 ± 0.018
	1.106	0.130 ± 0.016	0.121 ± 0.038	0.129 ± 0.016
	1.197	0.130 ± 0.021	0.094 ± 0.022	0.166 ± 0.036
$30^\circ - 45^\circ$	0.711	0.188 ± 0.015	0.143 ± 0.020	0.201 ± 0.014
	0.775	0.194 ± 0.016	0.183 ± 0.034	0.198 ± 0.015
	0.847	0.196 ± 0.016	0.155 ± 0.021	0.175 ± 0.014
	0.926	0.178 ± 0.018	0.167 ± 0.039	0.237 ± 0.028
	1.011	0.167 ± 0.021	0.178 ± 0.033	0.180 ± 0.018
	1.101	0.311 ± 0.093	0.117 ± 0.028	0.163 ± 0.021
	1.194	0.185 ± 0.033	0.188 ± 0.090	0.182 ± 0.051
$45^\circ - 65^\circ$	0.714	0.213 ± 0.016	0.146 ± 0.020	0.262 ± 0.020
	0.777	0.224 ± 0.016	0.226 ± 0.035	0.253 ± 0.020
	0.850	0.255 ± 0.022	0.252 ± 0.033	0.277 ± 0.036
	0.930	0.260 ± 0.033	0.248 ± 0.039	0.294 ± 0.039
	1.016	0.290 ± 0.049	0.291 ± 0.122	0.294 ± 0.040
	1.106	0.306 ± 0.061	0.239 ± 0.118	0.622 ± 0.219
	1.199	0.372 ± 0.140	0.392 ± 0.155	0.264 ± 0.028
$65^\circ - 90^\circ$	0.754	0.254 ± 0.023	0.174 ± 0.029	0.266 ± 0.024
	0.816	0.286 ± 0.028	0.303 ± 0.056	0.364 ± 0.045
	0.886	0.318 ± 0.044	0.641 ± 0.153	0.409 ± 0.071
	0.963	0.475 ± 0.098	0.461 ± 0.199	0.434 ± 0.075
	1.045	0.422 ± 0.088	0.789 ± 0.323	0.655 ± 0.229
	1.132	0.826 ± 0.262		
$90^\circ - 125^\circ$	0.743	0.316 ± 0.038	0.277 ± 0.042	0.255 ± 0.028
	0.809	0.418 ± 0.055	0.367 ± 0.077	0.399 ± 0.063
	0.883	0.788 ± 0.194	0.575 ± 0.230	0.903 ± 0.297
	0.963		0.466 ± 0.180	0.810 ± 0.250

8 COMPARISON OF CHARGED-PION PRODUCTION ON BERYLLIUM, COPPER, AND TANTALUM

Figure 9 presents a comparison between the inclusive cross-sections of π^+ and π^- production, integrated over the secondaries' momentum range $0.2 < p < 1.0 \text{ GeV}/c$ and polar-angle range $30^\circ < \theta < 90^\circ$, in the interactions of protons, π^+ and π^- , with beryllium ($A = 9.01$), copper ($A = 63.55$), and tantalum ($A = 181.0$) nuclei⁶⁾. The comparison employs the scaling variable $A^{2/3}$ where A is the atomic number of the respective nucleus. We note the approximately linear dependence on this scaling variable. At low beam momentum, the slope exhibits a strong dependence on beam particle type, which tends to disappear with higher beam momentum.

⁶⁾The beryllium data with $+8.9 \text{ GeV}/c$ beam momentum [1, 2] have been scaled, by interpolation, to a beam momentum of $8.0 \text{ GeV}/c$.

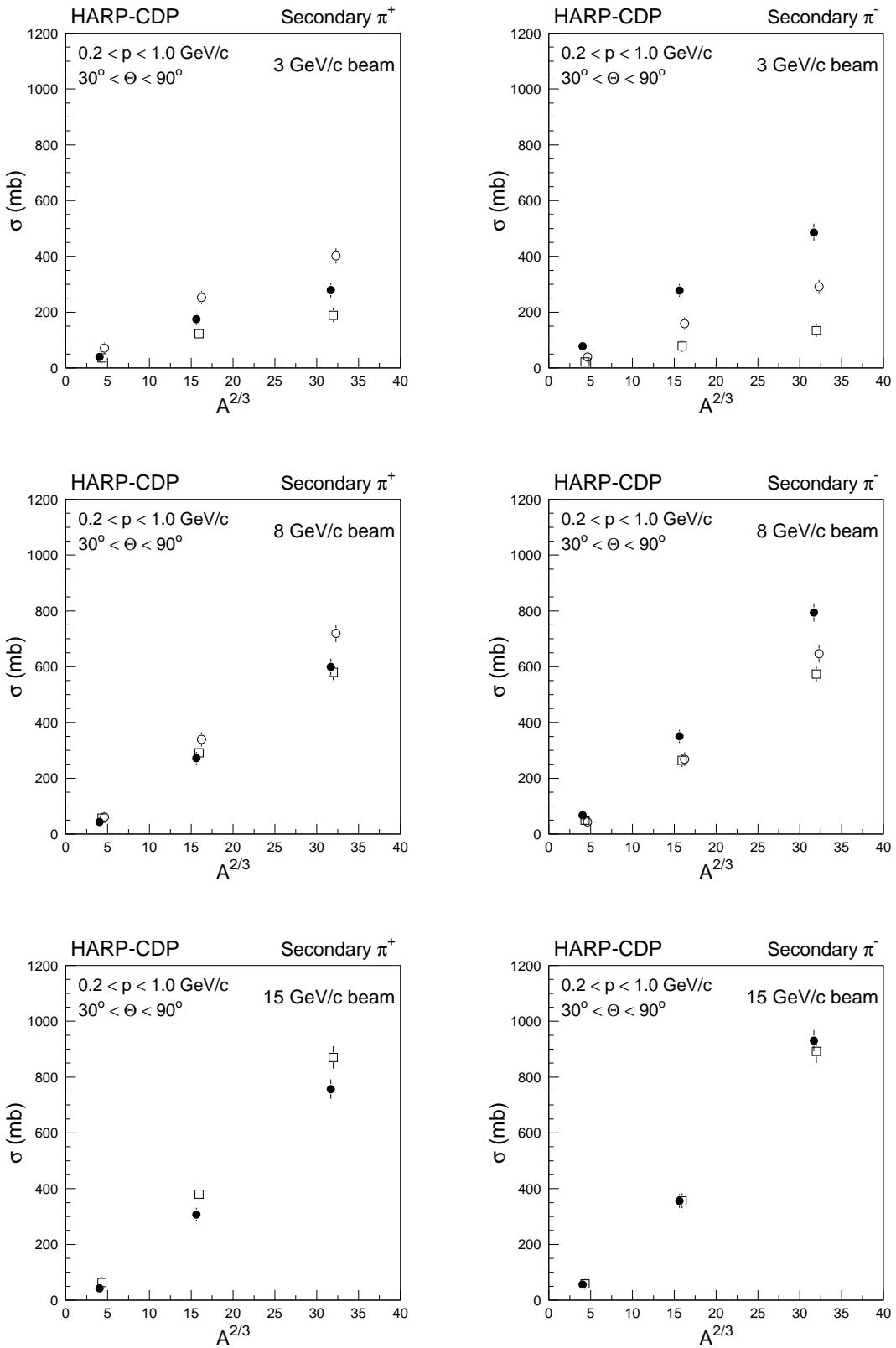


Fig. 9: Inclusive cross-sections of π^+ and π^- production by protons (open squares), π^+ 's (open circles), and π^- 's (black circles), as a function of $A^{2/3}$ for, from left to right, beryllium, copper, and tantalum nuclei; the cross-sections are integrated over the momentum range $0.2 < p < 1.0 \text{ GeV}/c$ and the polar-angle range $30^\circ < \theta < 90^\circ$; the shown errors are total errors and often smaller than the symbol size.

9 COMPARISON OF OUR RESULTS WITH RESULTS FROM OTHER EXPERIMENTS

9.1 Comparison with E802 results

Experiment E802 [11] at Brookhaven National Laboratory (BNL) measured secondary π^+ 's in the polar-angle range $5^\circ < \theta < 58^\circ$ from the interactions of $+14.6 \text{ GeV}/c$ protons with copper nuclei.

Figure 10 shows their published Lorentz-invariant cross-section of π^+ and π^- production by $+14.6 \text{ GeV}/c$ protons, in the rapidity range $1.2 < y < 1.4$, as a function of $m_T - m_\pi$, where m_T denotes the pion transverse mass. Their data are compared with our cross-sections from the interactions of $+15.0 \text{ GeV}/c$ protons with copper nuclei, expressed in the same unit as used by E802. Since E802 quoted only statistical errors, our data in Fig. 10 are also shown with their statistical errors.

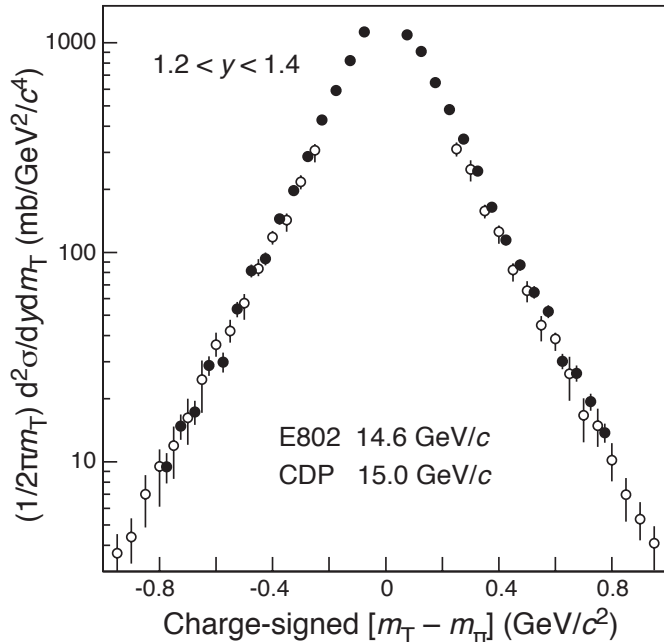


Fig. 10: Comparison of our cross-sections (black circles) of π^\pm production by $+15.0 \text{ GeV}/c$ protons off copper nuclei, with the cross-sections on copper nuclei published by the E802 Collaboration for the proton beam momentum of $+14.6 \text{ GeV}/c$ (open circles); all errors are statistical only.

The E802 π^\pm cross-sections are in good agreement with our cross-sections measured nearly at the same proton beam momentum, taking into account the normalization uncertainty of (10–15)% quoted by E802. We draw attention to the good agreement of the slopes of the cross-sections over two orders of magnitude.

9.2 Comparison with E910 results

BNL experiment E910 [12] measured secondary charged pions in the momentum range $0.1\text{--}6 \text{ GeV}/c$ from the interactions of $+12.3 \text{ GeV}/c$ protons with copper nuclei. This experiment used a TPC for the measurement of secondaries, with a comfortably large track length of $\sim 1.5 \text{ m}$.

This feature, together with a magnetic field strength of 0.5 T, is of particular significance, since it permits considerably better charge identification and proton–pion separation by dE/dx than is possible in the HARP detector. Figure 11 shows their published cross-section $d^2\sigma/dpd\Omega$ of π^\pm production by $+12.3 \text{ GeV}/c$ protons, in the polar-angle range $0.8 < \cos \theta < 0.9$. Since E910 quoted only statistical errors, our data in Fig. 11 from the interactions of $+12.0 \text{ GeV}/c$ protons with copper are also shown with their statistical errors. The normalization uncertainty quoted by E910 is $\leq 5\%$.

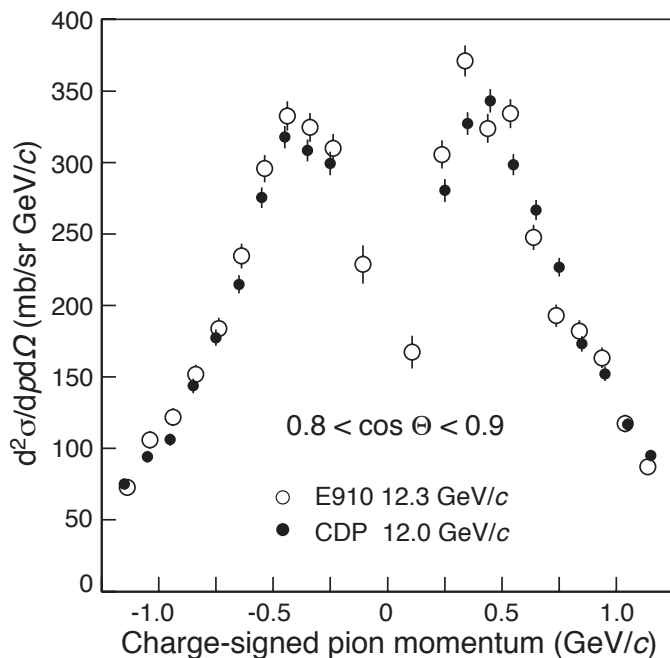


Fig. 11: Comparison of our cross-sections (black circles) of π^\pm production by $+12.0 \text{ GeV}/c$ protons off copper nuclei, with the cross-sections published by the E910 Collaboration for the proton beam momentum of $+12.3 \text{ GeV}/c$ (open circles); all errors are statistical only.

Also here, the E910 data are shown as published, and our data are expressed in the same unit as used by E910. We draw attention to the good agreement in the π^+/π^- ratio between the cross-sections from E910 and our cross-sections.

9.3 Comparison with results from the HARP Collaboration

Figure 12 (a) shows the comparison of our cross-sections of pion production by $+12.0 \text{ GeV}/c$ protons off copper nuclei with the ones published by the HARP Collaboration [13], in the polar-angle range $0.35 < \theta < 0.55 \text{ rad}$. The latter cross-sections are plotted as published, while we expressed our cross-sections in the unit used by the HARP Collaboration. Figure 12 (b) shows our ratio π^+/π^- as a function of the polar angle θ in comparison with the ratios published by the E910 Collaboration (at the slightly different proton beam momentum of $+12.3 \text{ GeV}/c$) and by the HARP Collaboration.

The discrepancy between our results and those published by the HARP Collaboration is evident. We note the difference especially of the π^+ cross-section, and the difference in the

reported momentum range. The discrepancy is even more serious as the same data set has been analysed by both groups.

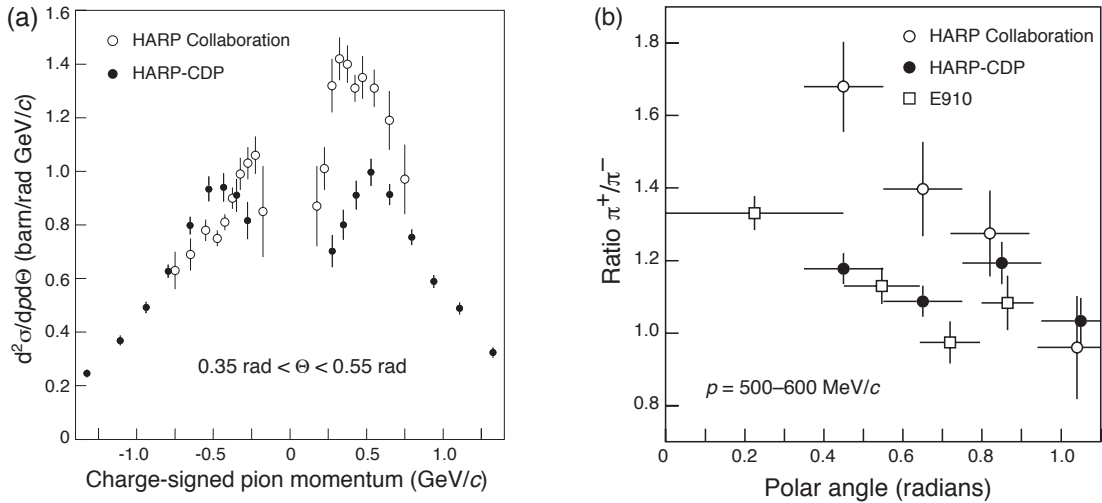


Fig. 12: (a) Comparison of our cross-sections (black circles) of π^\pm production by $+12.0 \text{ GeV}/c$ protons off copper nuclei with the cross-sections published by the HARP Collaboration (open circles); (b) Comparison of our ratio π^+/π^- at $+12.0 \text{ GeV}/c$ beam momentum as a function of the polar angle θ with the ratios published by the HARP Collaboration; also shown are the ratios π^+/π^- published by the E910 Collaboration for a $+12.3 \text{ GeV}/c$ beam momentum; in (a) total errors are shown; in (b) for the HARP Collaboration total errors are shown (only those are published), for E910 and our group, the errors are statistical only.

We hold that the discrepancy is caused by problems in the HARP Collaboration's data analysis. They result primarily, but not exclusively, from a lack of understanding TPC track distortions and RPC timing signals. These problems, together with others that affect the HARP Collaboration's data analysis, are discussed in detail in Refs [14–16] and summarized in the Appendix of Ref. [1].

10 SUMMARY

From the analysis of data from the HARP large-angle spectrometer (polar angle θ in the range $20^\circ < \theta < 125^\circ$), double-differential cross-sections $d^2\sigma/dpd\Omega$ of the production of secondary protons, π^+ 's, and π^- 's, and of deuterons, have been obtained. The incoming beam particles were protons and pions with momenta from ± 3 to $\pm 15 \text{ GeV}/c$, impinging on a $5\% \lambda_{\text{abs}}$ thick stationary copper target. Our cross-sections for π^+ and π^- production agree with results from BNL experiments E802 and E910 but disagree with the results of the HARP Collaboration that were obtained from the same raw data.

ACKNOWLEDGEMENTS

We are greatly indebted to many technical collaborators whose diligent and hard work made the HARP detector a well-functioning instrument. We thank all HARP colleagues who devoted time and effort to the design and construction of the detector, to data taking, and to setting up

the computing and software infrastructure. We express our sincere gratitude to HARP's funding agencies for their support.

REFERENCES

- [1] A. Bolshakova *et al.*, Cross-sections of large-angle hadron production in proton– and pion–nucleus interactions I: beryllium nuclei and beam momenta of $+8.9 \text{ GeV}/c$ and $-8.0 \text{ GeV}/c$, Preprint CERN–PH–EP–2008–022 [arXiv:0901.3648], accepted for publication in *Eur. Phys. J. C*
- [2] A. Bolshakova *et al.*, Cross-sections of large-angle hadron production in proton– and pion–nucleus interactions II: beryllium nuclei and beam momenta from $\pm 3 \text{ GeV}/c$ to $\pm 15 \text{ GeV}/c$, Preprint CERN–PH–EP–2008–025 [arXiv:0903.2145], accepted for publication in *Eur. Phys. J. C*
- [3] A. Bolshakova *et al.*, Cross-sections of large-angle hadron production in proton– and pion–nucleus interactions III: tantalum nuclei and beam momenta from $\pm 3 \text{ GeV}/c$ to $\pm 15 \text{ GeV}/c$, Preprint CERN–PH–EP–2009–009 [arXiv:0906.0471], to be published in *Eur. Phys. J. C*
- [4] V. Ammosov *et al.*, *Nucl. Instrum. Methods Phys. Res. A* **588** (2008) 294
- [5] V. Ammosov *et al.*, *Nucl. Instrum. Methods Phys. Res. A* **578** (2007) 119
- [6] V. Ammosov *et al.*, CERN–HARP–CDP–2008–001 (HARP Memo 08–101)
- [7] V. Ammosov *et al.*, CERN–HARP–CDP–2008–002 (HARP Memo 08–102)
- [8] S. Agostinelli *et al.*, *Nucl. Instrum. Methods Phys. Res. A* **506** (2003) 250; J. Allison *et al.*, *IEEE Trans. Nucl. Sci.* **53** (2006) 270
- [9] A. Bolshakova *et al.*, *Eur. Phys. J. C* **56** (2008) 323
- [10] A. Bolshakova *et al.*, Tables of cross-sections of large-angle hadron production in proton– and pion–nucleus interactions IV: copper nuclei and beam momenta from $\pm 3 \text{ GeV}/c$ to $\pm 15 \text{ GeV}/c$, CERN–HARP–CDP–2009–004
- [11] T. Abbott *et al.*, *Phys. Rev. D* **45** (1992) 3906
- [12] I. Chemakin *et al.*, *Phys. Rev. C* **65** (2002) 024904
- [13] M.G. Catanesi *et al.*, *Phys. Rev. C* **77** (2008) 055207
- [14] V. Ammosov *et al.*, *J. Instrum.* **3** (2008) P01002
- [15] V. Ammosov *et al.*, *Eur. Phys. J. C* **54** (2008) 169
- [16] V. Ammosov *et al.*, CERN–HARP–CDP–2006–003 (HARP Memo 06–101); CERN–HARP–CDP–2006–007 (HARP Memo 06–105); CERN–HARP–CDP–2007–001 (HARP Memo 07–101)

APPENDIX A: CROSS-SECTION TABLES

Table A.1: Double-differential inclusive cross-section $d^2\sigma/dpd\Omega$ [mb/(GeV/c sr)] of the production of protons in $p + \text{Cu} \rightarrow p + X$ interactions with +3.0 GeV/c beam momentum; the first error is statistical, the second systematic; p_T in GeV/c, polar angle θ in degrees.

p_T	20 < θ < 30						30 < θ < 40							
	$\langle p_T \rangle$	$\langle \theta \rangle$	$d^2\sigma/dpd\Omega$				$\langle p_T \rangle$	$\langle \theta \rangle$	$d^2\sigma/dpd\Omega$					
			454.76	\pm	20.41	\pm	25.27	425.92	\pm	17.82	\pm	19.16		
0.20–0.24	0.222	25.1	454.76	\pm	20.41	\pm	25.27	0.271	35.0	425.92	\pm	17.82	\pm	19.16
0.24–0.30	0.271	25.4	400.56	\pm	14.75	\pm	19.36	0.331	35.0	396.34	\pm	14.24	\pm	15.27
0.30–0.36	0.331	25.1	353.84	\pm	14.06	\pm	14.96	0.393	34.7	349.89	\pm	13.67	\pm	11.68
0.36–0.42	0.393	25.1	300.58	\pm	12.77	\pm	11.05	0.461	25.1	236.99	\pm	9.69	\pm	7.73
0.42–0.50	0.461	25.1	236.99	\pm	9.69	\pm	7.73	0.553	25.3	199.75	\pm	8.09	\pm	6.61
0.50–0.60	0.553	25.3	199.75	\pm	8.09	\pm	6.61	0.663	24.9	129.62	\pm	5.98	\pm	5.58
0.60–0.72	0.663	24.9	129.62	\pm	5.98	\pm	5.58	0.813	35.0	136.19	\pm	6.08	\pm	5.37
0.72–0.90	0.813	35.0	78.77	\pm	3.82	\pm	4.63							
p_T	40 < θ < 50						50 < θ < 60							
	$\langle p_T \rangle$	$\langle \theta \rangle$	$d^2\sigma/dpd\Omega$				$\langle p_T \rangle$	$\langle \theta \rangle$	$d^2\sigma/dpd\Omega$					
			438.14	\pm	15.06	\pm	14.48	0.392	55.2	351.61	\pm	13.18	\pm	10.43
0.30–0.36	0.332	45.2	438.14	\pm	15.06	\pm	14.48	0.462	54.9	296.53	\pm	10.63	\pm	8.49
0.36–0.42	0.393	45.1	393.90	\pm	14.55	\pm	11.68	0.555	54.8	214.64	\pm	8.22	\pm	7.32
0.42–0.50	0.462	45.2	301.96	\pm	10.82	\pm	8.44	0.665	54.9	147.16	\pm	6.31	\pm	6.60
0.50–0.60	0.555	45.0	247.12	\pm	8.91	\pm	7.64	0.809	54.9	74.15	\pm	3.71	\pm	4.71
0.60–0.72	0.665	44.7	171.23	\pm	6.87	\pm	7.14	1.053	44.7	23.80	\pm	1.33	\pm	2.31
0.72–0.90	0.809	45.2	84.43	\pm	3.92	\pm	4.89	1.056	54.8	17.83	\pm	1.14	\pm	1.84
p_T	60 < θ < 75						75 < θ < 90							
	$\langle p_T \rangle$	$\langle \theta \rangle$	$d^2\sigma/dpd\Omega$				$\langle p_T \rangle$	$\langle \theta \rangle$	$d^2\sigma/dpd\Omega$					
			209.81	\pm	6.43	\pm	7.75	0.655	81.4	72.60	\pm	3.38	\pm	5.28
0.50–0.60	0.549	67.5	120.95	\pm	4.54	\pm	6.56	0.795	81.2	25.25	\pm	1.66	\pm	2.53
0.60–0.72	0.657	67.1	59.23	\pm	2.61	\pm	4.83	1.032	81.9	4.72	\pm	0.46	\pm	0.76
p_T	90 < θ < 105						105 < θ < 125							
	$\langle p_T \rangle$	$\langle \theta \rangle$	$d^2\sigma/dpd\Omega$				$\langle p_T \rangle$	$\langle \theta \rangle$	$d^2\sigma/dpd\Omega$					
			31.28	\pm	2.22	\pm	2.85	0.654	112.6	82.33	\pm	3.83	\pm	4.74
0.42–0.50	0.651	97.1	10.89	\pm	1.07	\pm	1.30	0.794	111.2	112.0	\pm	2.10	\pm	3.14
0.50–0.60	0.797	96.2	1.32	\pm	0.23	\pm	0.26	1.059	115.1	0.11	\pm	0.34	\pm	0.36
0.60–0.72	1.013	94.6	0.457	\pm	0.04	\pm	0.05							
0.72–0.90														
0.90–1.25														

Table A.2: Double-differential inclusive cross-section $d^2\sigma/dpd\Omega$ [mb/(GeV/c sr)] of the production of π^+ 's in $p + \text{Cu} \rightarrow \pi^+ + \text{X}$ interactions with +3.0 GeV/c beam momentum; the first error is statistical, the second systematic; p_T in GeV/c, polar angle θ in degrees.

p_T	20 < θ < 30				30 < θ < 40					
	$\langle p_T \rangle$	$\langle \theta \rangle$	$d^2\sigma/dpd\Omega$		$\langle p_T \rangle$	$\langle \theta \rangle$	$d^2\sigma/dpd\Omega$			
0.10–0.13	0.116	25.2	115.62	\pm 13.74	10.13	0.115	35.1	112.03	\pm 13.00	\pm 9.14
0.13–0.16	0.145	25.3	113.77	\pm 12.16	7.91	0.144	35.1	121.45	\pm 12.24	\pm 8.73
0.16–0.20	0.180	25.1	151.41	\pm 12.15	9.05	0.180	35.0	102.01	\pm 9.31	\pm 5.97
0.20–0.24	0.221	24.9	131.06	\pm 10.88	6.84	0.223	34.5	120.40	\pm 10.02	\pm 6.17
0.24–0.30	0.271	25.6	111.15	\pm 7.97	4.64	0.270	35.0	98.69	\pm 7.33	\pm 4.19
0.30–0.36	0.332	24.7	71.19	\pm 6.14	2.89	0.329	34.5	78.67	\pm 6.53	\pm 3.19
0.36–0.42	0.389	24.7	48.40	\pm 5.15	2.30	0.393	35.3	57.71	\pm 5.49	\pm 2.53
0.42–0.50	0.458	25.3	25.20	\pm 3.09	1.27	0.464	34.8	25.58	\pm 3.14	\pm 1.22
0.50–0.60	0.548	24.9	15.68	\pm 1.99	1.05	0.549	35.1	18.10	\pm 2.26	\pm 1.12
0.60–0.72	0.665	24.4	7.71	\pm 1.19	0.72	0.658	34.7	8.21	\pm 1.26	\pm 0.72
0.72–0.90						0.785	36.0	3.29	\pm 0.66	\pm 0.46
p_T	40 < θ < 50				50 < θ < 60					
	$\langle p_T \rangle$	$\langle \theta \rangle$	$d^2\sigma/dpd\Omega$		$\langle p_T \rangle$	$\langle \theta \rangle$	$d^2\sigma/dpd\Omega$			
0.10–0.13	0.115	44.6	112.47	\pm 13.00	9.25	0.146	54.6	85.37	\pm 10.32	\pm 5.91
0.13–0.16	0.144	44.9	77.04	\pm 9.42	5.46	0.180	54.7	90.95	\pm 8.94	\pm 5.43
0.16–0.20	0.182	45.0	106.71	\pm 9.49	6.37	0.221	54.7	79.07	\pm 8.29	\pm 4.47
0.20–0.24	0.221	45.2	101.91	\pm 9.27	5.53	0.271	55.1	50.77	\pm 5.22	\pm 2.34
0.24–0.30	0.267	44.7	79.17	\pm 6.65	3.53	0.331	54.4	38.98	\pm 4.59	\pm 1.72
0.30–0.36	0.328	44.6	54.84	\pm 5.52	2.35	0.393	55.3	39.68	\pm 4.73	\pm 1.93
0.36–0.42	0.391	44.6	49.56	\pm 5.14	2.27	0.462	54.6	18.69	\pm 2.75	\pm 0.99
0.42–0.50	0.455	44.7	27.22	\pm 3.31	1.34	0.543	54.6	14.37	\pm 2.13	\pm 0.97
0.50–0.60	0.543	44.2	16.69	\pm 2.23	1.05	0.660	54.8	7.34	\pm 1.35	\pm 0.67
0.60–0.72	0.663	45.0	8.48	\pm 1.35	0.72	0.812	55.0	1.97	\pm 0.55	\pm 0.25
0.72–0.90	0.795	44.7	4.04	\pm 0.75	0.51	1.028	52.9	0.94	\pm 0.23	\pm 0.21
p_T	60 < θ < 75				75 < θ < 90					
	$\langle p_T \rangle$	$\langle \theta \rangle$	$d^2\sigma/dpd\Omega$		$\langle p_T \rangle$	$\langle \theta \rangle$	$d^2\sigma/dpd\Omega$			
0.13–0.16	0.146	67.3	94.26	\pm 9.66	6.49	0.149	81.7	73.25	\pm 10.56	\pm 8.47
0.16–0.20	0.181	67.3	86.73	\pm 7.11	4.78	0.181	82.3	67.42	\pm 6.48	\pm 3.61
0.20–0.24	0.220	67.0	70.73	\pm 6.40	3.73	0.221	82.5	58.65	\pm 5.76	\pm 2.96
0.24–0.30	0.268	66.6	53.54	\pm 4.45	2.41	0.269	81.1	37.52	\pm 3.87	\pm 1.93
0.30–0.36	0.328	67.4	30.31	\pm 3.28	1.30	0.329	82.0	25.99	\pm 3.14	\pm 1.36
0.36–0.42	0.389	66.8	25.85	\pm 3.18	1.35	0.391	82.2	17.33	\pm 2.62	\pm 1.13
0.42–0.50	0.456	66.8	18.38	\pm 2.26	1.05	0.463	81.4	9.19	\pm 1.60	\pm 0.67
0.50–0.60	0.538	66.8	7.77	\pm 1.30	0.59	0.548	79.5	6.11	\pm 1.20	\pm 0.61
0.60–0.72	0.656	66.2	3.98	\pm 0.79	0.41	0.660	80.2	3.31	\pm 0.78	\pm 0.46
0.72–0.90	0.781	67.4	1.63	\pm 0.40	0.24	0.770	84.1	0.78	\pm 0.29	\pm 0.18
0.90–1.25	1.054	68.4	0.36	\pm 0.11	0.10					
p_T	90 < θ < 105				105 < θ < 125					
	$\langle p_T \rangle$	$\langle \theta \rangle$	$d^2\sigma/dpd\Omega$		$\langle p_T \rangle$	$\langle \theta \rangle$	$d^2\sigma/dpd\Omega$			
0.13–0.16	0.146	98.4	112.19	\pm 13.63	12.61	0.145	114.4	71.16	\pm 7.10	\pm 4.18
0.16–0.20	0.178	97.7	61.01	\pm 6.36	3.18	0.178	113.9	59.25	\pm 5.31	\pm 2.80
0.20–0.24	0.218	97.3	51.06	\pm 5.63	2.84	0.220	113.8	30.50	\pm 3.57	\pm 1.62
0.24–0.30	0.270	96.8	22.52	\pm 2.89	1.11	0.265	113.2	11.34	\pm 1.83	\pm 0.69
0.30–0.36	0.327	96.2	18.45	\pm 2.68	1.22	0.328	113.9	4.92	\pm 1.17	\pm 0.41
0.36–0.42	0.386	98.4	8.78	\pm 1.81	0.72	0.387	112.5	3.30	\pm 0.96	\pm 0.38
0.42–0.50	0.457	96.7	5.88	\pm 1.30	0.61	0.471	113.7	1.85	\pm 0.62	\pm 0.28
0.50–0.60	0.543	96.5	1.58	\pm 0.59	0.23					
0.60–0.72	0.627	97.2	0.36	\pm 0.25	0.10					

Table A.3: Double-differential inclusive cross-section $d^2\sigma/dpd\Omega$ [mb/(GeV/c sr)] of the production of π^- 's in $p + \text{Cu} \rightarrow \pi^- + X$ interactions with +3.0 GeV/c beam momentum; the first error is statistical, the second systematic; p_T in GeV/c, polar angle θ in degrees.

p_T	20 < θ < 30				30 < θ < 40			
	$\langle p_T \rangle$	$\langle \theta \rangle$	$d^2\sigma/dpd\Omega$		$\langle p_T \rangle$	$\langle \theta \rangle$	$d^2\sigma/dpd\Omega$	
			$d^2\sigma/dpd\Omega$	$d^2\sigma/dpd\Omega$			$d^2\sigma/dpd\Omega$	$d^2\sigma/dpd\Omega$
0.10–0.13	0.117	24.5	102.15 \pm 12.97 \pm 9.74		0.115	34.2	94.31 \pm 11.53 \pm 8.13	
0.13–0.16	0.145	25.6	81.94 \pm 10.38 \pm 6.12		0.144	34.8	71.57 \pm 9.16 \pm 5.57	
0.16–0.20	0.179	25.0	82.63 \pm 8.74 \pm 5.25		0.176	34.8	71.03 \pm 7.48 \pm 4.72	
0.20–0.24	0.219	25.1	82.87 \pm 8.47 \pm 4.75		0.220	34.4	77.33 \pm 8.22 \pm 4.69	
0.24–0.30	0.268	25.3	56.50 \pm 5.68 \pm 2.80		0.264	35.2	51.48 \pm 5.35 \pm 2.51	
0.30–0.36	0.327	24.9	39.58 \pm 4.68 \pm 2.17		0.328	34.7	37.06 \pm 4.47 \pm 1.90	
0.36–0.42	0.383	25.0	19.39 \pm 3.28 \pm 1.27		0.385	34.4	23.52 \pm 3.59 \pm 1.39	
0.42–0.50	0.454	25.7	7.24 \pm 1.76 \pm 0.61		0.457	34.8	13.11 \pm 2.28 \pm 0.92	
0.50–0.60	0.522	23.7	1.98 \pm 0.81 \pm 0.26		0.530	34.7	5.47 \pm 1.32 \pm 0.52	
0.60–0.72	0.634	25.8	1.37 \pm 0.73 \pm 0.38		0.649	34.5	2.91 \pm 0.92 \pm 0.41	
0.72–0.90					0.752	36.9	0.52 \pm 0.37 \pm 0.14	
p_T	40 < θ < 50				50 < θ < 60			
	$\langle p_T \rangle$	$\langle \theta \rangle$	$d^2\sigma/dpd\Omega$		$\langle p_T \rangle$	$\langle \theta \rangle$	$d^2\sigma/dpd\Omega$	
			$d^2\sigma/dpd\Omega$	$d^2\sigma/dpd\Omega$			$d^2\sigma/dpd\Omega$	$d^2\sigma/dpd\Omega$
0.10–0.13	0.116	45.1	75.09 \pm 10.69 \pm 6.45		0.144	54.2	67.34 \pm 9.19 \pm 5.04	
0.13–0.16	0.144	45.0	69.81 \pm 9.13 \pm 5.26		0.179	55.0	74.82 \pm 8.09 \pm 4.87	
0.16–0.20	0.178	44.9	64.03 \pm 7.33 \pm 4.37		0.221	55.1	52.35 \pm 6.42 \pm 3.28	
0.20–0.24	0.219	45.3	62.37 \pm 7.35 \pm 3.90		0.270	55.0	42.47 \pm 4.75 \pm 2.23	
0.24–0.30	0.265	45.1	53.90 \pm 5.55 \pm 2.71		0.325	55.2	28.48 \pm 3.96 \pm 1.44	
0.30–0.36	0.326	45.4	33.38 \pm 4.40 \pm 1.74		0.387	55.8	23.98 \pm 3.66 \pm 1.37	
0.36–0.42	0.382	45.4	25.50 \pm 3.71 \pm 1.47		0.449	54.1	16.26 \pm 2.55 \pm 1.07	
0.42–0.50	0.451	44.4	13.03 \pm 2.30 \pm 0.86		0.542	55.4	6.30 \pm 1.49 \pm 0.55	
0.50–0.60	0.532	44.9	13.34 \pm 2.17 \pm 1.18		0.645	55.2	3.46 \pm 0.96 \pm 0.45	
0.60–0.72	0.626	46.2	3.35 \pm 0.94 \pm 0.44		0.789	51.6	1.08 \pm 0.44 \pm 0.23	
0.72–0.90	0.765	45.3	0.95 \pm 0.42 \pm 0.20					
p_T	60 < θ < 75				75 < θ < 90			
	$\langle p_T \rangle$	$\langle \theta \rangle$	$d^2\sigma/dpd\Omega$		$\langle p_T \rangle$	$\langle \theta \rangle$	$d^2\sigma/dpd\Omega$	
			$d^2\sigma/dpd\Omega$	$d^2\sigma/dpd\Omega$			$d^2\sigma/dpd\Omega$	$d^2\sigma/dpd\Omega$
0.13–0.16	0.145	67.3	86.06 \pm 9.20 \pm 5.90		0.148	82.1	62.92 \pm 10.65 \pm 6.77	
0.16–0.20	0.181	67.6	65.36 \pm 6.11 \pm 3.71		0.178	82.7	60.30 \pm 6.22 \pm 3.47	
0.20–0.24	0.221	68.0	43.33 \pm 5.02 \pm 2.50		0.218	82.2	41.98 \pm 4.80 \pm 2.26	
0.24–0.30	0.269	67.6	35.50 \pm 3.65 \pm 1.73		0.268	81.9	31.06 \pm 3.44 \pm 1.66	
0.30–0.36	0.328	66.4	26.03 \pm 3.11 \pm 1.27		0.323	80.8	17.47 \pm 2.62 \pm 1.08	
0.36–0.42	0.386	66.9	17.11 \pm 2.54 \pm 0.97		0.382	82.6	15.12 \pm 2.42 \pm 1.10	
0.42–0.50	0.453	66.9	12.22 \pm 1.87 \pm 0.82		0.452	82.1	5.16 \pm 1.19 \pm 0.45	
0.50–0.60	0.537	65.9	4.45 \pm 1.00 \pm 0.40		0.535	82.3	2.72 \pm 0.79 \pm 0.34	
0.60–0.72	0.648	67.2	0.79 \pm 0.39 \pm 0.11		0.655	82.0	1.72 \pm 0.57 \pm 0.38	
0.72–0.90	0.822	69.7	0.62 \pm 0.28 \pm 0.15		0.745	84.6	1.08 \pm 0.48 \pm 0.59	
p_T	90 < θ < 105				105 < θ < 125			
	$\langle p_T \rangle$	$\langle \theta \rangle$	$d^2\sigma/dpd\Omega$		$\langle p_T \rangle$	$\langle \theta \rangle$	$d^2\sigma/dpd\Omega$	
			$d^2\sigma/dpd\Omega$	$d^2\sigma/dpd\Omega$			$d^2\sigma/dpd\Omega$	$d^2\sigma/dpd\Omega$
0.13–0.16	0.178	97.2	50.38 \pm 5.75 \pm 2.92		0.144	114.8	54.21 \pm 6.48 \pm 3.45	
0.16–0.20	0.219	97.3	30.40 \pm 4.13 \pm 1.73		0.178	114.7	37.86 \pm 4.20 \pm 2.00	
0.20–0.24	0.267	97.0	20.38 \pm 2.81 \pm 1.25		0.216	113.1	21.13 \pm 3.00 \pm 1.36	
0.24–0.30	0.324	96.8	10.54 \pm 1.99 \pm 0.83		0.265	113.8	10.46 \pm 1.72 \pm 0.80	
0.30–0.36	0.384	98.0	4.12 \pm 1.25 \pm 0.43		0.335	113.8	2.53 \pm 0.84 \pm 0.28	
0.36–0.42	0.449	95.1	1.72 \pm 0.70 \pm 0.23		0.396	113.9	1.72 \pm 0.70 \pm 0.27	
0.42–0.50	0.558	94.9	1.29 \pm 0.53 \pm 0.29		0.440	114.2	1.62 \pm 0.54 \pm 0.38	

Table A.4: Double-differential inclusive cross-section $d^2\sigma/dpd\Omega$ [mb/(GeV/c sr)] of the production of protons in $\pi^+ + \text{Cu} \rightarrow p + X$ interactions with $+3.0 \text{ GeV}/c$ beam momentum; the first error is statistical, the second systematic; p_T in GeV/c , polar angle θ in degrees.

p_T	20 < θ < 30			30 < θ < 40		
	$\langle p_T \rangle$	$\langle \theta \rangle$	$d^2\sigma/dpd\Omega$	$\langle p_T \rangle$	$\langle \theta \rangle$	$d^2\sigma/dpd\Omega$
0.20–0.24	0.221	25.3	421.79 \pm 14.72 \pm 23.52			
0.24–0.30	0.271	25.2	364.28 \pm 10.24 \pm 17.75	0.272	34.8	431.30 \pm 11.49 \pm 19.50
0.30–0.36	0.331	25.3	325.25 \pm 9.91 \pm 13.88	0.332	35.1	374.11 \pm 10.14 \pm 14.53
0.36–0.42	0.391	25.3	249.09 \pm 8.50 \pm 9.41	0.391	35.1	303.36 \pm 9.36 \pm 10.27
0.42–0.50	0.462	25.4	200.66 \pm 6.50 \pm 6.80	0.463	35.1	244.71 \pm 7.19 \pm 7.36
0.50–0.60	0.552	25.4	149.71 \pm 5.05 \pm 5.13	0.552	35.3	190.54 \pm 5.69 \pm 5.89
0.60–0.72	0.664	25.3	92.11 \pm 3.57 \pm 4.04	0.663	35.2	120.94 \pm 4.12 \pm 4.84
0.72–0.90				0.812	35.1	64.51 \pm 2.45 \pm 3.82
p_T	40 < θ < 50			50 < θ < 60		
	$\langle p_T \rangle$	$\langle \theta \rangle$	$d^2\sigma/dpd\Omega$	$\langle p_T \rangle$	$\langle \theta \rangle$	$d^2\sigma/dpd\Omega$
0.30–0.36	0.331	45.1	403.88 \pm 10.57 \pm 13.48			
0.36–0.42	0.392	45.1	357.46 \pm 10.17 \pm 10.74	0.392	55.1	348.76 \pm 9.61 \pm 10.66
0.42–0.50	0.462	45.1	287.69 \pm 7.74 \pm 8.18	0.463	55.1	298.97 \pm 7.84 \pm 8.70
0.50–0.60	0.554	45.2	208.42 \pm 5.99 \pm 6.56	0.553	55.0	211.26 \pm 5.99 \pm 7.30
0.60–0.72	0.664	45.0	144.07 \pm 4.60 \pm 6.05	0.663	54.8	132.03 \pm 4.37 \pm 5.97
0.72–0.90	0.817	45.1	78.38 \pm 2.72 \pm 4.57	0.810	55.1	70.82 \pm 2.63 \pm 4.52
0.90–1.25	1.053	44.7	19.06 \pm 0.85 \pm 1.86	1.049	55.0	17.12 \pm 0.81 \pm 1.77
p_T	60 < θ < 75			75 < θ < 90		
	$\langle p_T \rangle$	$\langle \theta \rangle$	$d^2\sigma/dpd\Omega$	$\langle p_T \rangle$	$\langle \theta \rangle$	$d^2\sigma/dpd\Omega$
0.50–0.60	0.549	67.7	201.54 \pm 4.63 \pm 7.49			
0.60–0.72	0.658	67.1	121.15 \pm 3.33 \pm 6.60	0.656	81.9	83.87 \pm 2.68 \pm 6.06
0.72–0.90	0.802	67.1	53.99 \pm 1.82 \pm 4.41	0.800	81.7	34.02 \pm 1.41 \pm 3.40
0.90–1.25	1.034	66.8	13.39 \pm 0.60 \pm 1.81	1.032	81.3	6.40 \pm 0.39 \pm 1.03
p_T	90 < θ < 105			105 < θ < 125		
	$\langle p_T \rangle$	$\langle \theta \rangle$	$d^2\sigma/dpd\Omega$	$\langle p_T \rangle$	$\langle \theta \rangle$	$d^2\sigma/dpd\Omega$
0.42–0.50				0.458	113.2	114.79 \pm 3.36 \pm 6.35
0.50–0.60				0.544	112.9	48.37 \pm 1.88 \pm 4.57
0.60–0.72	0.655	97.3	46.36 \pm 1.99 \pm 4.19	0.651	112.1	16.35 \pm 1.02 \pm 2.32
0.72–0.90	0.798	96.1	16.01 \pm 0.95 \pm 1.88	0.794	111.9	3.53 \pm 0.36 \pm 0.77
0.90–1.25	1.031	95.5	2.13 \pm 0.21 \pm 0.40	1.030	111.3	0.31 \pm 0.05 \pm 0.12

Table A.7: Double-differential inclusive cross-section $d^2\sigma/dpd\Omega$ [mb/(GeV/c sr)] of the production of protons in $\pi^- + \text{Cu} \rightarrow p + X$ interactions with -3.0 GeV/c beam momentum; the first error is statistical, the second systematic; p_T in GeV/c, polar angle θ in degrees.

p_T	20 < θ < 30				30 < θ < 40			
	$\langle p_T \rangle$	$\langle \theta \rangle$	$d^2\sigma/dpd\Omega$		$\langle p_T \rangle$	$\langle \theta \rangle$	$d^2\sigma/dpd\Omega$	
			$d^2\sigma/dpd\Omega$	$d^2\sigma/dpd\Omega$			$d^2\sigma/dpd\Omega$	$d^2\sigma/dpd\Omega$
0.20–0.24	0.219	25.2	372.39 \pm 7.97 \pm 20.22		0.269	35.0	377.71 \pm 6.36 \pm 16.73	
0.24–0.30	0.267	25.3	318.53 \pm 5.72 \pm 15.16		0.326	35.1	343.56 \pm 5.83 \pm 12.92	
0.30–0.36	0.326	25.3	276.93 \pm 5.34 \pm 11.32		0.385	35.1	260.18 \pm 5.03 \pm 8.41	
0.36–0.42	0.384	25.2	212.26 \pm 4.59 \pm 7.61		0.451	35.2	219.72 \pm 4.05 \pm 6.24	
0.42–0.50	0.452	25.3	164.01 \pm 3.50 \pm 5.26		0.537	35.2	151.30 \pm 2.97 \pm 4.42	
0.50–0.60	0.538	25.4	112.87 \pm 2.55 \pm 3.67		0.642	35.3	95.74 \pm 2.19 \pm 3.73	
0.60–0.72	0.641	25.4	68.44 \pm 1.84 \pm 2.87		0.778	35.3	49.01 \pm 1.25 \pm 2.77	
0.72–0.90								
40 < θ < 50								
p_T	$\langle p_T \rangle$	$\langle \theta \rangle$	$d^2\sigma/dpd\Omega$		$\langle p_T \rangle$	$\langle \theta \rangle$	$d^2\sigma/dpd\Omega$	
			$d^2\sigma/dpd\Omega$	$d^2\sigma/dpd\Omega$			$d^2\sigma/dpd\Omega$	$d^2\sigma/dpd\Omega$
0.30–0.36	0.327	45.1	351.58 \pm 5.81 \pm 11.44		0.386	55.1	309.80 \pm 5.35 \pm 8.99	
0.36–0.42	0.386	45.1	300.18 \pm 5.39 \pm 8.58		0.454	55.0	247.15 \pm 4.21 \pm 6.87	
0.42–0.50	0.454	45.1	243.08 \pm 4.24 \pm 6.55		0.541	55.1	186.11 \pm 3.32 \pm 6.20	
0.50–0.60	0.541	45.1	175.84 \pm 3.24 \pm 5.27		0.645	55.1	115.01 \pm 2.40 \pm 5.07	
0.60–0.72	0.647	45.1	112.94 \pm 2.38 \pm 4.45		0.785	55.0	62.33 \pm 1.45 \pm 3.87	
0.72–0.90	0.787	45.1	59.28 \pm 1.40 \pm 3.37		1.013	55.1	16.74 \pm 0.49 \pm 1.65	
0.90–1.25	1.011	45.1	15.77 \pm 0.47 \pm 1.47					
60 < θ < 75								
p_T	$\langle p_T \rangle$	$\langle \theta \rangle$	$d^2\sigma/dpd\Omega$		$\langle p_T \rangle$	$\langle \theta \rangle$	$d^2\sigma/dpd\Omega$	
			$d^2\sigma/dpd\Omega$	$d^2\sigma/dpd\Omega$			$d^2\sigma/dpd\Omega$	$d^2\sigma/dpd\Omega$
0.50–0.60	0.540	67.5	174.34 \pm 2.54 \pm 6.35		0.644	81.9	73.30 \pm 1.49 \pm 5.19	
0.60–0.72	0.645	67.3	104.21 \pm 1.83 \pm 5.60		0.784	81.7	31.40 \pm 0.81 \pm 3.10	
0.72–0.90	0.783	67.2	51.14 \pm 1.04 \pm 4.14		1.004	81.4	6.79 \pm 0.24 \pm 1.06	
0.90–1.25	1.010	67.0	12.75 \pm 0.34 \pm 1.72					
90 < θ < 105								
p_T	$\langle p_T \rangle$	$\langle \theta \rangle$	$d^2\sigma/dpd\Omega$		$\langle p_T \rangle$	$\langle \theta \rangle$	$d^2\sigma/dpd\Omega$	
			$d^2\sigma/dpd\Omega$	$d^2\sigma/dpd\Omega$			$d^2\sigma/dpd\Omega$	$d^2\sigma/dpd\Omega$
0.42–0.50					0.454	112.6	129.81 \pm 30.62 \pm 6.97	
0.50–0.60					0.536	113.0	44.76 \pm 1.07 \pm 4.17	
0.60–0.72	0.643	97.1	44.38 \pm 1.14 \pm 3.97		0.639	112.7	17.75 \pm 0.61 \pm 2.50	
0.72–0.90	0.781	96.8	16.93 \pm 0.58 \pm 1.94		0.772	112.4	4.98 \pm 0.26 \pm 1.05	
0.90–1.25	0.995	95.8	2.65 \pm 0.14 \pm 0.47		1.005	111.7	0.54 \pm 0.05 \pm 0.19	

Table A.8: Double-differential inclusive cross-section $d^2\sigma/dpd\Omega$ [mb/(GeV/c sr)] of the production of π^+ 's in $\pi^- + \text{Cu} \rightarrow \pi^+ + \text{X}$ interactions with -3.0 GeV/c beam momentum; the first error is statistical, the second systematic; p_T in GeV/c, polar angle θ in degrees.

p_T	20 < θ < 30			30 < θ < 40		
	$\langle p_T \rangle$	$\langle \theta \rangle$	$d^2\sigma/dpd\Omega$	$\langle p_T \rangle$	$\langle \theta \rangle$	$d^2\sigma/dpd\Omega$
0.10–0.13	0.115	25.1	105.80 ± 5.24 ± 7.84	0.115	35.0	106.42 ± 5.05 ± 8.09
0.13–0.16	0.145	24.8	140.10 ± 5.75 ± 8.95	0.145	35.0	123.12 ± 5.18 ± 7.51
0.16–0.20	0.179	25.0	148.23 ± 4.96 ± 7.91	0.179	34.9	129.96 ± 4.42 ± 6.59
0.20–0.24	0.219	25.1	157.18 ± 4.95 ± 6.94	0.219	34.7	141.06 ± 4.65 ± 6.28
0.24–0.30	0.268	25.0	146.13 ± 3.88 ± 5.32	0.268	34.8	125.60 ± 3.56 ± 4.50
0.30–0.36	0.326	25.2	119.20 ± 3.53 ± 4.07	0.325	34.8	113.31 ± 3.39 ± 3.62
0.36–0.42	0.383	25.0	93.15 ± 3.04 ± 3.02	0.384	34.8	80.79 ± 2.82 ± 2.55
0.42–0.50	0.451	25.2	63.08 ± 2.17 ± 2.57	0.452	34.9	59.91 ± 2.12 ± 2.24
0.50–0.60	0.539	25.2	35.05 ± 1.36 ± 1.90	0.538	35.1	36.54 ± 1.43 ± 1.79
0.60–0.72	0.639	25.3	18.21 ± 0.85 ± 1.46	0.643	34.9	21.46 ± 0.95 ± 1.56
0.72–0.90				0.778	34.8	9.95 ± 0.50 ± 1.14
p_T	40 < θ < 50			50 < θ < 60		
	$\langle p_T \rangle$	$\langle \theta \rangle$	$d^2\sigma/dpd\Omega$	$\langle p_T \rangle$	$\langle \theta \rangle$	$d^2\sigma/dpd\Omega$
0.10–0.13	0.115	44.8	96.41 ± 5.08 ± 7.46	0.145	55.3	104.00 ± 4.93 ± 6.51
0.13–0.16	0.145	45.0	103.25 ± 4.63 ± 6.27	0.179	54.7	99.98 ± 3.82 ± 5.06
0.16–0.20	0.179	44.8	110.53 ± 4.11 ± 5.76	0.218	54.9	90.36 ± 3.63 ± 3.99
0.20–0.24	0.218	44.9	104.71 ± 3.90 ± 4.65	0.268	54.7	79.72 ± 2.80 ± 2.91
0.24–0.30	0.268	45.0	97.87 ± 3.12 ± 3.55	0.327	54.7	61.67 ± 2.45 ± 2.01
0.30–0.36	0.327	44.9	84.84 ± 2.91 ± 2.73	0.387	54.7	61.15 ± 2.56 ± 2.52
0.36–0.42	0.386	44.7	65.54 ± 2.59 ± 2.20	0.454	54.6	42.25 ± 1.81 ± 1.74
0.42–0.50	0.454	44.7	49.65 ± 1.94 ± 1.85	0.538	54.8	26.59 ± 1.26 ± 1.38
0.50–0.60	0.540	44.9	35.95 ± 1.47 ± 1.79	0.645	54.8	15.22 ± 0.87 ± 1.13
0.60–0.72	0.649	44.6	17.56 ± 0.89 ± 1.19	0.780	55.0	6.39 ± 0.42 ± 0.66
0.72–0.90	0.784	44.3	7.00 ± 0.42 ± 0.72	1.012	54.6	1.40 ± 0.11 ± 0.25
p_T	60 < θ < 75			75 < θ < 90		
	$\langle p_T \rangle$	$\langle \theta \rangle$	$d^2\sigma/dpd\Omega$	$\langle p_T \rangle$	$\langle \theta \rangle$	$d^2\sigma/dpd\Omega$
0.13–0.16	0.145	67.5	98.99 ± 4.24 ± 6.42	0.146	81.7	94.91 ± 9.41 ± 14.59
0.16–0.20	0.179	67.6	92.98 ± 3.11 ± 4.60	0.179	82.3	82.17 ± 3.13 ± 4.37
0.20–0.24	0.219	67.2	78.45 ± 2.77 ± 3.29	0.218	82.2	62.24 ± 2.50 ± 2.54
0.24–0.30	0.267	67.0	64.43 ± 2.09 ± 2.42	0.267	82.2	49.44 ± 1.86 ± 1.94
0.30–0.36	0.327	66.8	52.80 ± 1.92 ± 1.97	0.327	81.8	36.23 ± 1.62 ± 1.63
0.36–0.42	0.385	67.1	43.43 ± 1.78 ± 1.96	0.384	82.0	27.81 ± 1.43 ± 1.44
0.42–0.50	0.453	66.9	28.76 ± 1.22 ± 1.35	0.454	81.8	20.30 ± 1.04 ± 1.19
0.50–0.60	0.540	66.8	21.29 ± 0.94 ± 1.33	0.539	81.9	12.25 ± 0.70 ± 0.93
0.60–0.72	0.646	66.9	11.17 ± 0.61 ± 0.96	0.645	81.8	6.05 ± 0.45 ± 0.63
0.72–0.90	0.784	66.5	4.49 ± 0.30 ± 0.54	0.778	81.7	2.57 ± 0.21 ± 0.38
0.90–1.25	1.013	66.7	0.80 ± 0.07 ± 0.16	1.002	81.7	0.26 ± 0.03 ± 0.07
p_T	90 < θ < 105			105 < θ < 125		
	$\langle p_T \rangle$	$\langle \theta \rangle$	$d^2\sigma/dpd\Omega$	$\langle p_T \rangle$	$\langle \theta \rangle$	$d^2\sigma/dpd\Omega$
0.13–0.16	0.146	97.4	87.19 ± 5.80 ± 10.33	0.145	114.5	73.43 ± 3.19 ± 3.84
0.16–0.20	0.178	97.5	73.19 ± 2.96 ± 3.50	0.178	114.2	56.60 ± 2.12 ± 2.18
0.20–0.24	0.219	97.2	57.59 ± 2.53 ± 2.62	0.218	114.2	37.01 ± 1.71 ± 1.41
0.24–0.30	0.267	97.2	37.02 ± 1.60 ± 1.38	0.265	113.8	21.91 ± 1.08 ± 1.02
0.30–0.36	0.326	97.2	23.28 ± 1.29 ± 1.17	0.325	113.8	14.09 ± 0.85 ± 0.89
0.36–0.42	0.385	96.8	17.43 ± 1.12 ± 1.10	0.387	114.5	9.80 ± 0.73 ± 0.84
0.42–0.50	0.454	96.9	14.02 ± 0.85 ± 1.12	0.454	114.2	4.46 ± 0.41 ± 0.48
0.50–0.60	0.542	97.1	7.10 ± 0.55 ± 0.77	0.542	112.4	2.74 ± 0.28 ± 0.40
0.60–0.72	0.643	96.5	2.40 ± 0.25 ± 0.36	0.650	112.4	0.71 ± 0.12 ± 0.15
0.72–0.90	0.776	95.3	0.67 ± 0.10 ± 0.14	0.765	110.6	0.09 ± 0.02 ± 0.03
0.90–1.25	0.995	96.0	0.06 ± 0.02 ± 0.02			

Table A.10: Double-differential inclusive cross-section $d^2\sigma/dpd\Omega$ [mb/(GeV/c sr)] of the production of protons in $p + \text{Cu} \rightarrow p + X$ interactions with $+5.0$ GeV/c beam momentum; the first error is statistical, the second systematic; p_T in GeV/c, polar angle θ in degrees.

p_T	20 < θ < 30			30 < θ < 40		
	$\langle p_T \rangle$	$\langle \theta \rangle$	$d^2\sigma/dpd\Omega$	$\langle p_T \rangle$	$\langle \theta \rangle$	$d^2\sigma/dpd\Omega$
0.20–0.24	0.220	25.1	490.74 \pm 10.91 \pm 26.52			
0.24–0.30	0.270	25.3	473.49 \pm 8.32 \pm 22.37	0.271	34.9	504.43 \pm 8.78 \pm 22.18
0.30–0.36	0.330	25.2	402.84 \pm 7.59 \pm 16.31	0.331	35.0	448.88 \pm 7.95 \pm 16.70
0.36–0.42	0.390	25.2	352.60 \pm 7.19 \pm 12.41	0.391	35.1	399.77 \pm 7.52 \pm 12.73
0.42–0.50	0.461	25.2	285.95 \pm 5.48 \pm 8.92	0.461	35.1	312.22 \pm 5.69 \pm 8.69
0.50–0.60	0.550	25.2	215.47 \pm 4.24 \pm 6.75	0.551	35.1	237.47 \pm 4.45 \pm 6.78
0.60–0.72	0.660	25.1	146.15 \pm 3.12 \pm 5.74	0.661	35.1	171.37 \pm 3.49 \pm 6.42
0.72–0.90				0.807	35.0	95.40 \pm 2.11 \pm 5.31
p_T	40 < θ < 50			50 < θ < 60		
	$\langle p_T \rangle$	$\langle \theta \rangle$	$d^2\sigma/dpd\Omega$	$\langle p_T \rangle$	$\langle \theta \rangle$	$d^2\sigma/dpd\Omega$
0.30–0.36	0.330	45.2	501.22 \pm 8.42 \pm 15.84			
0.36–0.42	0.391	45.2	430.50 \pm 7.76 \pm 12.08	0.390	55.2	434.74 \pm 7.56 \pm 13.03
0.42–0.50	0.461	45.1	342.99 \pm 6.00 \pm 9.06	0.460	55.1	352.50 \pm 6.02 \pm 9.60
0.50–0.60	0.551	45.1	253.87 \pm 4.61 \pm 7.49	0.549	55.0	253.05 \pm 4.62 \pm 8.33
0.60–0.72	0.660	45.1	178.75 \pm 3.59 \pm 6.95	0.658	54.9	167.22 \pm 3.48 \pm 7.32
0.72–0.90	0.805	44.9	97.23 \pm 2.16 \pm 5.48	0.806	55.0	86.96 \pm 2.04 \pm 5.33
0.90–1.25	1.044	44.7	34.56 \pm 0.90 \pm 3.12	1.035	54.9	24.14 \pm 0.75 \pm 2.30
p_T	60 < θ < 75			75 < θ < 90		
	$\langle p_T \rangle$	$\langle \theta \rangle$	$d^2\sigma/dpd\Omega$	$\langle p_T \rangle$	$\langle \theta \rangle$	$d^2\sigma/dpd\Omega$
0.50–0.60	0.549	67.4	231.42 \pm 3.47 \pm 8.73			
0.60–0.72	0.658	67.1	140.47 \pm 2.54 \pm 7.52	0.655	81.7	83.57 \pm 1.89 \pm 5.99
0.72–0.90	0.802	66.9	68.25 \pm 1.46 \pm 5.51	0.799	81.6	38.02 \pm 1.07 \pm 3.76
0.90–1.25	1.038	66.9	15.65 \pm 0.47 \pm 2.07	1.022	81.6	7.30 \pm 0.32 \pm 1.12
p_T	90 < θ < 105			105 < θ < 125		
	$\langle p_T \rangle$	$\langle \theta \rangle$	$d^2\sigma/dpd\Omega$	$\langle p_T \rangle$	$\langle \theta \rangle$	$d^2\sigma/dpd\Omega$
0.42–0.50				0.459	113.3	103.14 \pm 2.22 \pm 5.81
0.50–0.60				0.544	112.7	45.24 \pm 1.29 \pm 4.24
0.60–0.72	0.656	96.8	45.98 \pm 1.38 \pm 4.17	0.655	112.3	14.57 \pm 0.67 \pm 2.07
0.72–0.90	0.796	96.4	15.97 \pm 0.68 \pm 1.84	0.790	111.9	3.99 \pm 0.27 \pm 0.85
0.90–1.25	1.020	96.0	2.47 \pm 0.17 \pm 0.43	1.032	112.1	0.32 \pm 0.04 \pm 0.12

Table A.11: Double-differential inclusive cross-section $d^2\sigma/dpd\Omega$ [mb/(GeV/c sr)] of the production of π^+ 's in $p + \text{Cu} \rightarrow \pi^+ + X$ interactions with +5.0 GeV/c beam momentum; the first error is statistical, the second systematic; p_T in GeV/c, polar angle θ in degrees.

p_T	20 < θ < 30			30 < θ < 40		
	$\langle p_T \rangle$	$\langle \theta \rangle$	$d^2\sigma/dpd\Omega$	$\langle p_T \rangle$	$\langle \theta \rangle$	$d^2\sigma/dpd\Omega$
0.10–0.13	0.116	24.9	168.02 ± 8.06 ± 12.38	0.116	34.7	154.11 ± 7.72 ± 11.60
0.13–0.16	0.145	24.8	213.31 ± 8.53 ± 13.01	0.145	34.9	155.03 ± 6.89 ± 9.31
0.16–0.20	0.180	24.9	235.27 ± 7.38 ± 11.72	0.181	34.6	175.62 ± 6.24 ± 8.78
0.20–0.24	0.220	24.9	236.54 ± 7.31 ± 10.27	0.221	34.6	182.94 ± 6.29 ± 7.88
0.24–0.30	0.270	24.8	205.89 ± 5.59 ± 7.78	0.270	34.7	171.78 ± 5.00 ± 6.11
0.30–0.36	0.331	25.0	158.63 ± 4.75 ± 5.09	0.330	34.8	132.77 ± 4.38 ± 4.19
0.36–0.42	0.389	24.8	130.63 ± 4.37 ± 4.83	0.390	34.8	102.95 ± 3.83 ± 3.24
0.42–0.50	0.459	24.8	81.83 ± 2.84 ± 3.07	0.460	34.8	78.47 ± 2.94 ± 3.09
0.50–0.60	0.549	25.0	58.04 ± 2.08 ± 3.14	0.549	34.9	45.56 ± 1.83 ± 2.25
0.60–0.72	0.659	25.0	28.54 ± 1.19 ± 2.27	0.657	34.9	28.40 ± 1.26 ± 2.07
0.72–0.90	0.800	25.0		0.800	34.8	12.61 ± 0.62 ± 1.42
p_T	40 < θ < 50			50 < θ < 60		
	$\langle p_T \rangle$	$\langle \theta \rangle$	$d^2\sigma/dpd\Omega$	$\langle p_T \rangle$	$\langle \theta \rangle$	$d^2\sigma/dpd\Omega$
0.10–0.13	0.115	44.9	142.31 ± 7.64 ± 10.92	0.145	55.1	135.24 ± 6.75 ± 8.41
0.13–0.16	0.146	45.0	157.21 ± 7.24 ± 9.53	0.179	54.8	130.27 ± 5.46 ± 6.63
0.16–0.20	0.180	44.9	145.79 ± 5.68 ± 7.44	0.220	54.9	103.40 ± 4.71 ± 4.61
0.20–0.24	0.221	45.0	132.37 ± 5.38 ± 5.86	0.270	54.6	100.18 ± 3.78 ± 3.64
0.24–0.30	0.270	44.8	127.43 ± 4.30 ± 4.59	0.331	54.7	80.22 ± 3.47 ± 2.84
0.30–0.36	0.330	45.0	94.37 ± 3.64 ± 3.02	0.390	54.7	72.35 ± 3.30 ± 2.65
0.36–0.42	0.389	44.7	82.49 ± 3.49 ± 2.68	0.461	54.7	48.12 ± 2.30 ± 1.95
0.42–0.50	0.459	44.7	61.33 ± 2.63 ± 2.39	0.547	54.8	30.76 ± 1.62 ± 1.64
0.50–0.60	0.548	44.6	37.58 ± 1.72 ± 1.82	0.663	54.7	17.15 ± 1.07 ± 1.27
0.60–0.72	0.658	44.5	22.20 ± 1.16 ± 1.51	0.797	54.7	9.26 ± 0.63 ± 0.99
0.72–0.90	0.803	44.6	11.58 ± 0.66 ± 1.20	1.029	54.5	2.55 ± 0.20 ± 0.42
p_T	60 < θ < 75			75 < θ < 90		
	$\langle p_T \rangle$	$\langle \theta \rangle$	$d^2\sigma/dpd\Omega$	$\langle p_T \rangle$	$\langle \theta \rangle$	$d^2\sigma/dpd\Omega$
0.13–0.16	0.146	67.4	125.83 ± 5.86 ± 8.32	0.146	82.1	107.90 ± 7.87 ± 10.69
0.16–0.20	0.179	67.3	111.66 ± 4.09 ± 5.53	0.180	82.1	103.54 ± 4.22 ± 5.15
0.20–0.24	0.221	67.3	100.87 ± 3.93 ± 4.61	0.218	82.0	83.94 ± 3.63 ± 3.67
0.24–0.30	0.269	67.0	80.90 ± 2.80 ± 2.81	0.268	82.0	57.99 ± 2.43 ± 2.31
0.30–0.36	0.329	66.7	57.37 ± 2.43 ± 2.17	0.330	81.3	39.50 ± 2.03 ± 1.77
0.36–0.42	0.391	66.8	46.63 ± 2.15 ± 1.75	0.388	81.9	24.98 ± 1.54 ± 1.13
0.42–0.50	0.461	66.8	32.27 ± 1.55 ± 1.53	0.458	81.7	19.95 ± 1.23 ± 1.18
0.50–0.60	0.549	66.4	21.10 ± 1.08 ± 1.31	0.548	81.5	12.35 ± 0.88 ± 0.99
0.60–0.72	0.659	66.1	10.59 ± 0.69 ± 0.91	0.662	81.8	6.13 ± 0.55 ± 0.65
0.72–0.90	0.805	66.3	4.95 ± 0.37 ± 0.60	0.794	81.1	2.31 ± 0.25 ± 0.34
0.90–1.25	1.050	66.0	0.96 ± 0.09 ± 0.18	1.038	81.7	0.26 ± 0.05 ± 0.06
p_T	90 < θ < 105			105 < θ < 125		
	$\langle p_T \rangle$	$\langle \theta \rangle$	$d^2\sigma/dpd\Omega$	$\langle p_T \rangle$	$\langle \theta \rangle$	$d^2\sigma/dpd\Omega$
0.13–0.16	0.148	98.1	114.96 ± 7.63 ± 10.19	0.143	112.6	134.23 ± 29.57 ± 7.91
0.16–0.20	0.179	97.3	99.94 ± 4.22 ± 4.69	0.180	113.9	67.10 ± 2.84 ± 2.62
0.20–0.24	0.219	97.2	66.67 ± 3.21 ± 2.56	0.219	113.9	46.85 ± 2.33 ± 1.90
0.24–0.30	0.267	96.8	40.12 ± 2.01 ± 1.53	0.267	113.2	21.81 ± 1.28 ± 1.04
0.30–0.36	0.329	97.7	26.36 ± 1.66 ± 1.37	0.329	114.0	12.46 ± 0.97 ± 0.81
0.36–0.42	0.389	97.0	14.47 ± 1.21 ± 0.92	0.390	113.6	9.19 ± 0.84 ± 0.80
0.42–0.50	0.460	96.6	13.01 ± 1.03 ± 1.12	0.453	113.3	3.57 ± 0.43 ± 0.41
0.50–0.60	0.545	96.9	5.83 ± 0.59 ± 0.64	0.552	113.4	1.34 ± 0.23 ± 0.22
0.60–0.72	0.659	96.4	1.87 ± 0.28 ± 0.28	0.650	110.6	0.55 ± 0.13 ± 0.14
0.72–0.90	0.790	96.3	0.60 ± 0.12 ± 0.13			
0.90–1.25	1.031	94.6	0.04 ± 0.02 ± 0.02			

Table A.12: Double-differential inclusive cross-section $d^2\sigma/dpd\Omega$ [mb/(GeV/c sr)] of the production of π^- 's in $p + \text{Cu} \rightarrow \pi^- + \text{X}$ interactions with $+5.0$ GeV/c beam momentum; the first error is statistical, the second systematic; p_T in GeV/c, polar angle θ in degrees.

p_T	20 < θ < 30				30 < θ < 40			
	$\langle p_T \rangle$	$\langle \theta \rangle$	$d^2\sigma/dpd\Omega$		$\langle p_T \rangle$	$\langle \theta \rangle$	$d^2\sigma/dpd\Omega$	
0.10–0.13	0.115	25.2	156.73	\pm 8.05	13.14	0.115	35.1	135.97 \pm 6.96 \pm 10.65
0.13–0.16	0.145	25.0	177.63	\pm 7.80	11.44	0.145	35.0	167.15 \pm 7.25 \pm 10.65
0.16–0.20	0.180	25.0	172.82	\pm 6.35	8.92	0.179	34.8	138.91 \pm 5.52 \pm 7.28
0.20–0.24	0.219	24.9	165.03	\pm 6.18	7.46	0.219	35.0	159.01 \pm 5.96 \pm 7.07
0.24–0.30	0.268	24.9	132.03	\pm 4.42	4.76	0.268	35.0	119.79 \pm 4.14 \pm 4.33
0.30–0.36	0.327	25.0	95.54	\pm 3.77	3.18	0.327	34.8	103.32 \pm 3.90 \pm 3.43
0.36–0.42	0.387	25.1	67.89	\pm 3.15	2.39	0.388	35.1	67.31 \pm 3.10 \pm 2.32
0.42–0.50	0.453	25.3	47.57	\pm 2.36	2.16	0.454	34.8	44.71 \pm 2.21 \pm 1.81
0.50–0.60	0.544	25.7	25.16	\pm 1.47	1.45	0.542	35.1	26.99 \pm 1.56 \pm 1.49
0.60–0.72	0.652	25.7	13.37	\pm 1.00	1.06	0.649	35.1	15.84 \pm 1.06 \pm 1.22
0.72–0.90	0.791	34.6				0.791	34.6	6.27 \pm 0.55 \pm 0.67
p_T	40 < θ < 50				50 < θ < 60			
	$\langle p_T \rangle$	$\langle \theta \rangle$	$d^2\sigma/dpd\Omega$		$\langle p_T \rangle$	$\langle \theta \rangle$	$d^2\sigma/dpd\Omega$	
0.10–0.13	0.115	45.1	135.22	\pm 7.14	10.78	0.145	55.1	119.67 \pm 6.24 \pm 7.68
0.13–0.16	0.145	45.0	126.53	\pm 6.25	8.04	0.178	55.0	116.92 \pm 5.16 \pm 6.19
0.16–0.20	0.179	45.0	120.34	\pm 5.16	6.45	0.218	55.0	94.42 \pm 4.39 \pm 4.42
0.20–0.24	0.219	45.0	118.67	\pm 5.14	5.62	0.267	54.6	76.34 \pm 3.25 \pm 2.88
0.24–0.30	0.269	44.8	102.18	\pm 3.92	3.91	0.327	54.8	67.56 \pm 3.20 \pm 2.46
0.30–0.36	0.327	44.9	79.22	\pm 3.37	2.62	0.388	54.6	46.03 \pm 2.61 \pm 1.75
0.36–0.42	0.388	44.9	63.75	\pm 3.10	2.34	0.457	55.0	34.42 \pm 1.96 \pm 1.54
0.42–0.50	0.454	44.9	43.82	\pm 2.18	1.84	0.543	54.7	24.50 \pm 1.50 \pm 1.54
0.50–0.60	0.543	44.8	24.61	\pm 1.48	1.42	0.650	54.7	9.99 \pm 0.84 \pm 0.84
0.60–0.72	0.647	44.5	12.03	\pm 0.92	0.97	0.786	54.7	4.68 \pm 0.48 \pm 0.54
0.72–0.90	0.788	44.9	6.53	\pm 0.60	0.76	0.995	54.4	1.09 \pm 0.17 \pm 0.20
0.90–1.25								
p_T	60 < θ < 75				75 < θ < 90			
	$\langle p_T \rangle$	$\langle \theta \rangle$	$d^2\sigma/dpd\Omega$		$\langle p_T \rangle$	$\langle \theta \rangle$	$d^2\sigma/dpd\Omega$	
0.13–0.16	0.145	67.3	124.03	\pm 5.52	7.54	0.147	82.3	126.38 \pm 7.51 \pm 16.04
0.16–0.20	0.178	67.1	103.49	\pm 3.94	4.99	0.178	82.1	97.39 \pm 4.10 \pm 4.67
0.20–0.24	0.220	67.4	78.09	\pm 3.24	3.31	0.219	81.8	73.23 \pm 3.33 \pm 3.06
0.24–0.30	0.267	67.5	67.22	\pm 2.59	2.57	0.267	81.9	53.41 \pm 2.31 \pm 2.06
0.30–0.36	0.327	67.0	46.82	\pm 2.18	1.76	0.328	81.8	34.57 \pm 1.89 \pm 1.54
0.36–0.42	0.387	66.5	36.70	\pm 1.87	1.46	0.384	81.5	21.87 \pm 1.52 \pm 1.19
0.42–0.50	0.455	66.7	26.62	\pm 1.43	1.38	0.454	81.3	14.48 \pm 1.06 \pm 0.95
0.50–0.60	0.544	66.8	13.48	\pm 0.89	0.91	0.541	81.6	7.62 \pm 0.69 \pm 0.67
0.60–0.72	0.649	66.8	7.98	\pm 0.63	0.73	0.649	81.9	3.56 \pm 0.42 \pm 0.42
0.72–0.90	0.778	67.6	3.09	\pm 0.33	0.40	0.787	81.3	1.05 \pm 0.19 \pm 0.17
0.90–1.25	1.015	66.5	0.46	\pm 0.08	0.09	1.054	81.8	0.19 \pm 0.04 \pm 0.07
p_T	90 < θ < 105				105 < θ < 125			
	$\langle p_T \rangle$	$\langle \theta \rangle$	$d^2\sigma/dpd\Omega$		$\langle p_T \rangle$	$\langle \theta \rangle$	$d^2\sigma/dpd\Omega$	
0.13–0.16	0.146	98.0	132.88	\pm 8.42	20.58	0.144	114.2	89.78 \pm 4.24 \pm 4.64
0.16–0.20	0.179	97.5	84.66	\pm 3.88	4.02	0.178	114.0	62.34 \pm 2.77 \pm 2.47
0.20–0.24	0.218	97.0	57.85	\pm 3.01	2.36	0.218	113.0	34.29 \pm 1.96 \pm 1.49
0.24–0.30	0.266	96.9	36.45	\pm 1.99	1.75	0.266	113.7	19.20 \pm 1.22 \pm 1.03
0.30–0.36	0.327	96.3	20.16	\pm 1.44	1.10	0.326	113.8	11.84 \pm 0.95 \pm 0.89
0.36–0.42	0.389	97.4	14.00	\pm 1.17	0.98	0.385	112.7	6.47 \pm 0.70 \pm 0.65
0.42–0.50	0.454	96.7	9.11	\pm 0.86	0.85	0.451	113.5	3.19 \pm 0.43 \pm 0.42
0.50–0.60	0.541	96.5	4.24	\pm 0.51	0.53	0.536	111.7	0.88 \pm 0.20 \pm 0.17
0.60–0.72	0.646	95.6	1.40	\pm 0.26	0.25	0.644	111.9	0.36 \pm 0.10 \pm 0.12
0.72–0.90	0.788	94.4	0.38	\pm 0.10	0.11			
0.90–1.25	0.962	94.8	0.08	\pm 0.03	0.06			

Table A.13: Double-differential inclusive cross-section $d^2\sigma/dpd\Omega$ [mb/(GeV/c sr)] of the production of protons in $\pi^+ + \text{Cu} \rightarrow p + X$ interactions with +5.0 GeV/c beam momentum; the first error is statistical, the second systematic; p_T in GeV/c, polar angle θ in degrees.

p_T	20 < θ < 30					30 < θ < 40								
	$\langle p_T \rangle$	$\langle \theta \rangle$	$d^2\sigma/dpd\Omega$			$\langle p_T \rangle$	$\langle \theta \rangle$	$d^2\sigma/dpd\Omega$						
			487.58	\pm	9.85	\pm	26.98	452.54	\pm	7.48	\pm	20.35		
0.20–0.24	0.221	25.3	487.58	\pm	9.85	\pm	26.98	452.54	\pm	7.48	\pm	20.35		
0.24–0.30	0.269	25.2	408.01	\pm	6.90	\pm	19.72	0.271	35.0	402.65	\pm	6.75	\pm	15.50
0.30–0.36	0.330	25.2	349.24	\pm	6.31	\pm	14.63	0.330	35.1	339.08	\pm	6.19	\pm	11.40
0.36–0.42	0.390	25.3	290.63	\pm	5.83	\pm	10.77	0.390	35.0	274.23	\pm	4.77	\pm	8.19
0.42–0.50	0.460	25.2	239.68	\pm	4.44	\pm	7.99	0.460	35.1	201.59	\pm	3.65	\pm	6.21
0.50–0.60	0.550	25.3	170.53	\pm	3.31	\pm	5.77	0.550	35.1	140.18	\pm	2.78	\pm	5.56
0.60–0.72	0.659	25.3	101.62	\pm	2.25	\pm	4.26	0.659	35.0	75.00	\pm	1.63	\pm	4.30
0.72–0.90								0.803	35.0					
p_T	40 < θ < 50					50 < θ < 60								
	$\langle p_T \rangle$	$\langle \theta \rangle$	$d^2\sigma/dpd\Omega$			$\langle p_T \rangle$	$\langle \theta \rangle$	$d^2\sigma/dpd\Omega$						
			445.65	\pm	7.09	\pm	14.71	396.39	\pm	6.49	\pm	12.38		
0.30–0.36	0.330	45.2	380.59	\pm	6.55	\pm	11.38	0.391	55.1	310.04	\pm	5.07	\pm	8.96
0.36–0.42	0.390	45.1	287.71	\pm	4.93	\pm	8.14	0.460	55.1	225.21	\pm	3.91	\pm	7.78
0.42–0.50	0.460	45.1	224.30	\pm	3.88	\pm	7.04	0.549	55.0	152.44	\pm	2.90	\pm	6.58
0.50–0.60	0.551	45.1	152.44	\pm	2.95	\pm	6.19	0.659	55.0	85.67	\pm	1.72	\pm	4.51
0.60–0.72	0.659	45.0	85.03	\pm	1.79	\pm	4.91	0.803	55.0	34.74	\pm	0.92	\pm	3.47
0.72–0.90	0.806	45.0	14.07	\pm	0.40	\pm	1.87	1.037	66.8	7.14	\pm	0.28	\pm	1.11
0.90–1.25								0.459	113.4	118.08	\pm	2.16	\pm	6.58
p_T	60 < θ < 75					75 < θ < 90								
	$\langle p_T \rangle$	$\langle \theta \rangle$	$d^2\sigma/dpd\Omega$			$\langle p_T \rangle$	$\langle \theta \rangle$	$d^2\sigma/dpd\Omega$						
			207.55	\pm	2.95	\pm	8.06	0.657	81.8	85.67	\pm	1.72	\pm	6.21
0.50–0.60	0.549	67.4	123.97	\pm	2.14	\pm	6.75	0.801	81.7	34.74	\pm	0.92	\pm	3.47
0.60–0.72	0.658	67.3	58.63	\pm	1.21	\pm	4.78	1.032	81.8	7.14	\pm	0.28	\pm	1.11
0.72–0.90	0.804	67.1												
0.90–1.25	1.037	66.8												
p_T	90 < θ < 105					105 < θ < 125								
	$\langle p_T \rangle$	$\langle \theta \rangle$	$d^2\sigma/dpd\Omega$			$\langle p_T \rangle$	$\langle \theta \rangle$	$d^2\sigma/dpd\Omega$						
			49.07	\pm	1.28	\pm	4.50	0.459	113.4	112.5	\pm	0.71	\pm	2.87
0.42–0.50	0.654	96.8	18.15	\pm	0.65	\pm	2.12	0.796	112.3	5.42	\pm	0.29	\pm	1.16
0.50–0.60	0.801	96.9	2.91	\pm	0.16	\pm	0.52	1.025	111.3	0.42	\pm	0.04	\pm	0.16
0.60–0.72														
0.72–0.90														
0.90–1.25														

Table A.14: Double-differential inclusive cross-section $d^2\sigma/dpd\Omega$ [mb/(GeV/c sr)] of the production of π^+ 's in $\pi^+ + \text{Cu} \rightarrow \pi^+ + \text{X}$ interactions with +5.0 GeV/c beam momentum; the first error is statistical, the second systematic; p_T in GeV/c, polar angle θ in degrees.

p_T	20 < θ < 30			30 < θ < 40		
	$\langle p_T \rangle$	$\langle \theta \rangle$	$d^2\sigma/dpd\Omega$	$\langle p_T \rangle$	$\langle \theta \rangle$	$d^2\sigma/dpd\Omega$
0.10–0.13	0.116	24.7	183.45 ± 7.39 ± 13.86	0.116	35.1	200.03 ± 7.79 ± 15.35
0.13–0.16	0.146	24.8	254.15 ± 8.26 ± 16.05	0.145	34.8	187.99 ± 6.75 ± 11.70
0.16–0.20	0.181	24.7	278.40 ± 7.09 ± 14.21	0.181	34.7	236.11 ± 6.48 ± 12.20
0.20–0.24	0.220	24.8	330.01 ± 7.68 ± 14.77	0.220	34.7	240.76 ± 6.43 ± 10.72
0.24–0.30	0.271	24.9	301.66 ± 6.04 ± 11.68	0.270	34.8	238.51 ± 5.26 ± 8.73
0.30–0.36	0.331	24.7	253.97 ± 5.38 ± 8.34	0.330	34.8	205.73 ± 4.89 ± 6.71
0.36–0.42	0.391	24.8	219.70 ± 5.15 ± 8.33	0.391	34.8	171.46 ± 4.44 ± 5.54
0.42–0.50	0.460	24.8	162.14 ± 3.66 ± 6.15	0.460	34.9	141.22 ± 3.57 ± 5.66
0.50–0.60	0.550	24.9	118.77 ± 2.75 ± 6.42	0.550	34.8	91.79 ± 2.38 ± 4.54
0.60–0.72	0.659	24.9	64.48 ± 1.74 ± 5.10	0.659	34.8	53.17 ± 1.59 ± 3.86
0.72–0.90				0.804	34.6	27.75 ± 0.89 ± 3.12
p_T	40 < θ < 50			50 < θ < 60		
	$\langle p_T \rangle$	$\langle \theta \rangle$	$d^2\sigma/dpd\Omega$	$\langle p_T \rangle$	$\langle \theta \rangle$	$d^2\sigma/dpd\Omega$
0.10–0.13	0.116	45.0	167.14 ± 7.34 ± 13.22	0.146	55.1	158.40 ± 6.53 ± 10.19
0.13–0.16	0.145	45.1	199.44 ± 7.29 ± 12.56	0.180	54.9	164.81 ± 5.48 ± 8.73
0.16–0.20	0.181	44.9	188.80 ± 5.74 ± 10.00	0.220	54.9	157.38 ± 5.20 ± 7.41
0.20–0.24	0.220	44.9	182.39 ± 5.62 ± 8.43	0.270	54.8	141.91 ± 4.03 ± 5.41
0.24–0.30	0.269	44.8	170.96 ± 4.45 ± 6.39	0.331	54.9	124.80 ± 3.90 ± 4.61
0.30–0.36	0.331	44.7	151.40 ± 4.12 ± 5.05	0.390	54.7	107.98 ± 3.62 ± 4.09
0.36–0.42	0.391	44.8	134.05 ± 3.99 ± 4.50	0.460	54.7	85.65 ± 2.76 ± 3.54
0.42–0.50	0.460	44.8	110.91 ± 3.18 ± 4.38	0.549	54.8	53.19 ± 1.93 ± 2.87
0.50–0.60	0.551	44.9	67.57 ± 2.10 ± 3.29	0.657	54.6	34.72 ± 1.40 ± 2.57
0.60–0.72	0.659	44.6	40.84 ± 1.44 ± 2.79	0.802	54.5	15.49 ± 0.76 ± 1.65
0.72–0.90	0.803	44.6	22.76 ± 0.86 ± 2.35	1.027	54.3	4.00 ± 0.23 ± 0.65
p_T	60 < θ < 75			75 < θ < 90		
	$\langle p_T \rangle$	$\langle \theta \rangle$	$d^2\sigma/dpd\Omega$	$\langle p_T \rangle$	$\langle \theta \rangle$	$d^2\sigma/dpd\Omega$
0.13–0.16	0.145	67.5	163.71 ± 6.08 ± 11.43	0.148	82.1	111.04 ± 5.85 ± 9.45
0.16–0.20	0.181	67.2	139.77 ± 4.08 ± 7.14	0.180	81.8	130.74 ± 4.25 ± 6.75
0.20–0.24	0.220	67.0	131.39 ± 4.00 ± 6.25	0.219	82.3	107.99 ± 3.68 ± 5.00
0.24–0.30	0.269	67.1	110.47 ± 2.92 ± 4.04	0.269	82.1	77.70 ± 2.52 ± 3.28
0.30–0.36	0.329	66.9	86.06 ± 2.67 ± 3.41	0.329	81.8	57.15 ± 2.19 ± 2.69
0.36–0.42	0.390	66.9	68.00 ± 2.33 ± 2.67	0.389	81.9	38.50 ± 1.72 ± 1.81
0.42–0.50	0.458	66.8	55.19 ± 1.83 ± 2.68	0.460	81.6	31.75 ± 1.39 ± 1.91
0.50–0.60	0.550	66.8	34.27 ± 1.24 ± 2.15	0.549	81.4	21.97 ± 1.06 ± 1.78
0.60–0.72	0.658	66.7	21.17 ± 0.89 ± 1.83	0.654	81.6	11.98 ± 0.70 ± 1.28
0.72–0.90	0.804	66.5	9.58 ± 0.48 ± 1.16	0.797	82.0	4.09 ± 0.31 ± 0.60
0.90–1.25	1.029	66.3	1.77 ± 0.12 ± 0.34	1.024	80.5	0.53 ± 0.06 ± 0.13
p_T	90 < θ < 105			105 < θ < 125		
	$\langle p_T \rangle$	$\langle \theta \rangle$	$d^2\sigma/dpd\Omega$	$\langle p_T \rangle$	$\langle \theta \rangle$	$d^2\sigma/dpd\Omega$
0.13–0.16	0.144	97.5	217.04 ± 69.59 ± 17.04	0.145	114.8	124.99 ± 4.62 ± 7.53
0.16–0.20	0.179	97.6	117.25 ± 4.11 ± 5.83	0.179	113.9	82.50 ± 2.86 ± 3.46
0.20–0.24	0.219	97.3	88.61 ± 3.33 ± 3.71	0.219	114.0	58.24 ± 2.33 ± 2.57
0.24–0.30	0.267	96.9	59.88 ± 2.20 ± 2.46	0.268	113.5	34.14 ± 1.44 ± 1.69
0.30–0.36	0.331	97.0	39.47 ± 1.82 ± 2.13	0.330	113.3	23.40 ± 1.19 ± 1.54
0.36–0.42	0.390	97.1	26.30 ± 1.47 ± 1.70	0.389	113.8	14.44 ± 0.94 ± 1.26
0.42–0.50	0.459	97.3	22.67 ± 1.22 ± 1.96	0.456	113.0	8.95 ± 0.61 ± 1.02
0.50–0.60	0.547	96.9	12.06 ± 0.76 ± 1.33	0.542	112.6	2.87 ± 0.30 ± 0.46
0.60–0.72	0.656	96.5	3.95 ± 0.37 ± 0.60	0.652	112.8	1.03 ± 0.15 ± 0.26
0.72–0.90	0.796	96.1	1.17 ± 0.15 ± 0.27	0.781	110.6	0.08 ± 0.02 ± 0.05
0.90–1.25	0.998	96.7	0.15 ± 0.03 ± 0.07			

Table A.16: Double-differential inclusive cross-section $d^2\sigma/dpd\Omega$ [mb/(GeV/c sr)] of the production of protons in $\pi^- + \text{Cu} \rightarrow p + X$ interactions with $-5.0 \text{ GeV}/c$ beam momentum; the first error is statistical, the second systematic; p_T in GeV/c , polar angle θ in degrees.

p_T	20 < θ < 30				30 < θ < 40			
	$\langle p_T \rangle$	$\langle \theta \rangle$	$d^2\sigma/dpd\Omega$		$\langle p_T \rangle$	$\langle \theta \rangle$	$d^2\sigma/dpd\Omega$	
0.20–0.24	0.219	25.2	408.33	\pm 9.83	\pm 22.13			
0.24–0.30	0.267	25.2	365.49	\pm 7.25	\pm 17.35	0.269	34.9	412.34 \pm 7.74 \pm 18.21
0.30–0.36	0.326	25.2	305.38	\pm 6.58	\pm 12.42	0.326	35.2	356.95 \pm 7.03 \pm 13.37
0.36–0.42	0.385	25.2	248.79	\pm 5.85	\pm 8.81	0.385	35.0	292.51 \pm 6.31 \pm 9.40
0.42–0.50	0.452	25.4	199.83	\pm 4.54	\pm 6.29	0.451	35.2	232.23 \pm 4.84 \pm 6.54
0.50–0.60	0.536	25.3	142.76	\pm 3.40	\pm 4.53	0.537	35.0	180.82 \pm 3.86 \pm 5.23
0.60–0.72	0.641	25.4	94.14	\pm 2.44	\pm 3.75	0.642	35.1	123.10 \pm 2.87 \pm 4.66
0.72–0.90						0.780	35.1	67.44 \pm 1.75 \pm 3.82
<hr/>								
40 < θ < 50								
p_T	$\langle p_T \rangle$	$\langle \theta \rangle$	$d^2\sigma/dpd\Omega$		$\langle p_T \rangle$	$\langle \theta \rangle$	$d^2\sigma/dpd\Omega$	
0.30–0.36	0.327	45.1	391.51	\pm 7.29	\pm 12.50	0.384	55.1	339.78 \pm 6.53 \pm 11.22
0.36–0.42	0.384	45.0	323.08	\pm 6.63	\pm 9.17	0.451	55.0	279.66 \pm 5.27 \pm 7.72
0.42–0.50	0.451	45.0	260.34	\pm 5.12	\pm 6.97	0.538	55.0	201.53 \pm 4.04 \pm 6.69
0.50–0.60	0.538	45.0	190.74	\pm 3.95	\pm 5.69	0.641	55.1	126.61 \pm 2.96 \pm 5.56
0.60–0.72	0.641	44.9	133.84	\pm 3.05	\pm 5.24	0.779	54.9	72.82 \pm 1.87 \pm 4.52
0.72–0.90	0.781	45.0	75.84	\pm 1.88	\pm 4.30	0.999	55.0	19.95 \pm 0.65 \pm 1.90
0.90–1.25	0.997	45.0	22.64	\pm 0.71	\pm 2.05			
<hr/>								
60 < θ < 75								
p_T	$\langle p_T \rangle$	$\langle \theta \rangle$	$d^2\sigma/dpd\Omega$		$\langle p_T \rangle$	$\langle \theta \rangle$	$d^2\sigma/dpd\Omega$	
0.50–0.60	0.547	67.6	186.71	\pm 3.10	\pm 6.94	0.654	81.9	80.09 \pm 1.85 \pm 5.67
0.60–0.72	0.654	67.4	119.47	\pm 2.30	\pm 6.41	0.796	81.7	34.09 \pm 0.98 \pm 3.38
0.72–0.90	0.796	67.2	57.74	\pm 1.32	\pm 4.66	1.021	81.7	8.86 \pm 0.35 \pm 1.34
0.90–1.25	1.031	67.1	15.81	\pm 0.48	\pm 2.08			
<hr/>								
90 < θ < 105								
p_T	$\langle p_T \rangle$	$\langle \theta \rangle$	$d^2\sigma/dpd\Omega$		$\langle p_T \rangle$	$\langle \theta \rangle$	$d^2\sigma/dpd\Omega$	
0.42–0.50					0.457	113.4	101.23 \pm 2.33 \pm 5.48	
0.50–0.60					0.544	112.8	50.10 \pm 1.36 \pm 4.62	
0.60–0.72	0.650	97.1	47.09	\pm 1.39	\pm 4.24	0.650	113.0	20.02 \pm 0.78 \pm 2.80
0.72–0.90	0.794	96.5	18.37	\pm 0.72	\pm 2.10	0.788	112.0	5.93 \pm 0.33 \pm 1.26
0.90–1.25	1.028	96.0	3.21	\pm 0.19	\pm 0.55	1.018	112.5	0.46 \pm 0.05 \pm 0.16

Table A.17: Double-differential inclusive cross-section $d^2\sigma/dpd\Omega$ [mb/(GeV/c sr)] of the production of π^+ 's in $\pi^- + \text{Cu} \rightarrow \pi^+ + \text{X}$ interactions with $-5.0 \text{ GeV}/c$ beam momentum; the first error is statistical, the second systematic; p_T in GeV/c , polar angle θ in degrees.

		20 < θ < 30					30 < θ < 40				
p_T	$\langle p_T \rangle$	$\langle \theta \rangle$	$d^2\sigma/dpd\Omega$			$\langle p_T \rangle$	$\langle \theta \rangle$	$d^2\sigma/dpd\Omega$			
0.10–0.13	0.115	24.8	188.30	± 8.56	± 14.69	0.115	35.0	151.51	± 7.33	± 11.23	
0.13–0.16	0.145	25.0	220.45	± 8.50	± 13.48	0.144	34.8	166.26	± 6.96	± 9.81	
0.16–0.20	0.179	24.9	237.40	± 7.26	± 11.84	0.178	34.7	185.43	± 6.30	± 9.14	
0.20–0.24	0.219	24.8	241.44	± 7.17	± 10.29	0.218	34.8	196.53	± 6.53	± 8.53	
0.24–0.30	0.267	24.8	227.58	± 5.69	± 8.14	0.267	34.7	174.77	± 4.98	± 6.16	
0.30–0.36	0.326	24.8	178.95	± 5.00	± 5.56	0.325	34.8	159.38	± 4.71	± 4.84	
0.36–0.42	0.384	24.8	153.40	± 4.64	± 4.97	0.384	34.9	121.47	± 4.11	± 3.60	
0.42–0.50	0.451	24.8	112.88	± 3.40	± 4.31	0.452	34.7	99.55	± 3.28	± 3.83	
0.50–0.60	0.537	24.8	69.96	± 2.29	± 3.63	0.539	34.8	59.99	± 2.14	± 2.84	
0.60–0.72	0.641	25.2	40.66	± 1.52	± 3.17	0.645	34.8	36.67	± 1.49	± 2.63	
0.72–0.90						0.773	35.0	15.88	± 0.73	± 1.77	
		40 < θ < 50					50 < θ < 60				
p_T	$\langle p_T \rangle$	$\langle \theta \rangle$	$d^2\sigma/dpd\Omega$			$\langle p_T \rangle$	$\langle \theta \rangle$	$d^2\sigma/dpd\Omega$			
0.10–0.13	0.115	45.2	126.67	± 6.99	± 9.63	0.145	55.1	134.75	± 6.49	± 8.26	
0.13–0.16	0.144	45.1	150.65	± 6.75	± 8.92	0.179	54.8	131.88	± 5.24	± 6.53	
0.16–0.20	0.179	44.8	164.42	± 5.97	± 8.20	0.218	54.9	121.45	± 5.02	± 5.18	
0.20–0.24	0.218	44.9	148.80	± 5.61	± 6.40	0.218	54.8	107.01	± 3.88	± 3.76	
0.24–0.30	0.267	44.9	138.76	± 4.35	± 4.89	0.268	54.8	94.37	± 3.66	± 2.97	
0.30–0.36	0.327	44.8	118.95	± 4.10	± 3.64	0.327	54.9	78.38	± 3.38	± 2.69	
0.36–0.42	0.385	44.7	105.95	± 3.93	± 3.50	0.384	54.8	59.06	± 2.51	± 2.22	
0.42–0.50	0.451	44.7	72.01	± 2.76	± 2.46	0.452	54.8	39.58	± 1.86	± 2.08	
0.50–0.60	0.538	44.7	48.46	± 2.01	± 2.27	0.537	54.6	22.99	± 1.24	± 1.63	
0.60–0.72	0.644	44.5	28.09	± 1.32	± 1.86	0.643	54.6	9.21	± 0.60	± 0.94	
0.72–0.90	0.778	44.3	13.22	± 0.70	± 1.33	0.777	54.6	2.55	± 0.20	± 0.42	
0.90–1.25						0.996	54.9				
		60 < θ < 75					75 < θ < 90				
p_T	$\langle p_T \rangle$	$\langle \theta \rangle$	$d^2\sigma/dpd\Omega$			$\langle p_T \rangle$	$\langle \theta \rangle$	$d^2\sigma/dpd\Omega$			
0.13–0.16	0.145	67.0	119.88	± 5.57	± 7.62	0.149	82.0	91.20	± 6.32	± 7.99	
0.16–0.20	0.180	67.1	124.06	± 4.24	± 6.06	0.180	82.1	105.58	± 4.11	± 5.06	
0.20–0.24	0.219	67.2	97.55	± 3.63	± 4.00	0.220	81.9	88.79	± 3.63	± 3.78	
0.24–0.30	0.269	66.9	84.96	± 2.83	± 2.95	0.267	82.1	66.27	± 2.58	± 2.64	
0.30–0.36	0.330	67.2	68.47	± 2.64	± 2.72	0.328	81.8	43.14	± 2.08	± 1.78	
0.36–0.42	0.389	67.0	49.23	± 2.16	± 1.70	0.390	81.8	32.58	± 1.78	± 1.43	
0.42–0.50	0.458	66.7	38.65	± 1.68	± 1.75	0.458	81.9	25.95	± 1.39	± 1.46	
0.50–0.60	0.546	66.7	29.88	± 1.32	± 1.83	0.544	81.9	15.62	± 0.96	± 1.18	
0.60–0.72	0.653	66.3	13.49	± 0.78	± 1.13	0.655	81.5	8.28	± 0.63	± 0.85	
0.72–0.90	0.792	66.3	5.70	± 0.40	± 0.68	0.794	81.1	2.96	± 0.27	± 0.43	
0.90–1.25	1.018	66.7	1.08	± 0.10	± 0.21	1.014	80.9	0.44	± 0.06	± 0.11	
		90 < θ < 105					105 < θ < 125				
p_T	$\langle p_T \rangle$	$\langle \theta \rangle$	$d^2\sigma/dpd\Omega$			$\langle p_T \rangle$	$\langle \theta \rangle$	$d^2\sigma/dpd\Omega$			
0.13–0.16	0.144	99.1	126.63	± 27.62	± 13.47	0.145	114.7	93.22	± 4.21	± 4.79	
0.16–0.20	0.179	97.3	93.54	± 4.02	± 4.47	0.179	114.1	64.93	± 2.77	± 2.46	
0.20–0.24	0.219	97.2	70.81	± 3.28	± 2.70	0.219	114.1	47.37	± 2.28	± 1.77	
0.24–0.30	0.265	97.2	46.39	± 2.12	± 1.63	0.267	113.6	27.75	± 1.44	± 1.20	
0.30–0.36	0.327	96.7	30.57	± 1.76	± 1.44	0.328	113.4	17.84	± 1.13	± 1.08	
0.36–0.42	0.389	97.2	23.96	± 1.57	± 1.50	0.388	113.3	11.25	± 0.91	± 0.91	
0.42–0.50	0.459	97.1	14.33	± 1.01	± 1.11	0.460	112.9	6.47	± 0.60	± 0.69	
0.50–0.60	0.545	96.1	7.90	± 0.69	± 0.85	0.545	111.6	2.47	± 0.29	± 0.38	
0.60–0.72	0.648	96.3	3.35	± 0.37	± 0.49	0.644	112.1	0.72	± 0.13	± 0.16	
0.72–0.90	0.803	95.9	0.78	± 0.13	± 0.17	0.795	114.4	0.08	± 0.02	± 0.03	
0.90–1.25	1.044	94.3	0.12	± 0.03	± 0.05						

Table A.19: Double-differential inclusive cross-section $d^2\sigma/dpd\Omega$ [mb/(GeV/c sr)] of the production of protons in $p + \text{Cu} \rightarrow p + X$ interactions with $+8.0$ GeV/c beam momentum; the first error is statistical, the second systematic; p_T in GeV/c, polar angle θ in degrees.

p_T	20 < θ < 30						30 < θ < 40					
	$\langle p_T \rangle$	$\langle \theta \rangle$	$d^2\sigma/dpd\Omega$				$\langle p_T \rangle$	$\langle \theta \rangle$	$d^2\sigma/dpd\Omega$			
			498.06	\pm 11.13	\pm 27.02	536.91	\pm 9.51	\pm 23.67	462.94	\pm 8.27	\pm 17.47	
0.20–0.24	0.221	25.0	498.06	\pm 11.13	\pm 27.02	536.91	\pm 9.51	\pm 23.67	462.94	\pm 8.27	\pm 17.47	
0.24–0.30	0.269	25.1	465.98	\pm 8.62	\pm 22.48	390.95	\pm 7.91	\pm 14.33	301.76	\pm 6.15	\pm 12.28	
0.30–0.36	0.329	25.1	395.20	\pm 8.00	\pm 17.68	229.10	\pm 4.80	\pm 9.91	242.71	\pm 4.79	\pm 9.50	
0.36–0.42	0.389	25.2	324.77	\pm 7.24	\pm 14.03	157.83	\pm 3.69	\pm 8.63	153.68	\pm 3.67	\pm 9.21	
0.42–0.50	0.458	25.1	288.49	\pm 5.98	\pm 11.38	0.800	\pm 2.27	\pm 6.58	82.99	\pm 2.28	\pm 6.87	
0.50–0.60	0.548	25.2	203.61	\pm 4.44	\pm 9.01	0.655	\pm 35.1	\pm 8.63	0.547	\pm 35.0	\pm 9.91	
0.60–0.72	0.655	25.1	149.29	\pm 3.45	\pm 7.60	0.389	\pm 35.2	\pm 14.33	0.458	\pm 35.0	\pm 12.28	
0.72–0.90	0.800	35.0	90.53	\pm 2.27	\pm 6.58	0.329	\pm 35.0	\pm 17.47	0.655	\pm 35.1	\pm 8.63	
p_T	40 < θ < 50						50 < θ < 60					
	$\langle p_T \rangle$	$\langle \theta \rangle$	$d^2\sigma/dpd\Omega$				$\langle p_T \rangle$	$\langle \theta \rangle$	$d^2\sigma/dpd\Omega$			
			493.97	\pm 8.41	\pm 15.74	426.30	\pm 10.76	\pm 12.35	426.30	\pm 10.76	\pm 12.35	
0.30–0.36	0.329	45.1	427.85	\pm 8.00	\pm 12.40	344.27	\pm 6.11	\pm 9.66	344.27	\pm 6.11	\pm 9.66	
0.36–0.42	0.389	45.1	336.03	\pm 6.22	\pm 10.76	242.71	\pm 4.79	\pm 9.50	242.71	\pm 4.79	\pm 9.50	
0.42–0.50	0.458	45.0	245.16	\pm 4.95	\pm 10.54	153.68	\pm 3.67	\pm 9.21	153.68	\pm 3.67	\pm 9.21	
0.50–0.60	0.547	45.0	162.78	\pm 3.82	\pm 9.38	0.800	\pm 2.28	\pm 6.87	0.655	\pm 2.28	\pm 6.87	
0.60–0.72	0.655	45.0	91.60	\pm 2.36	\pm 7.02	0.389	\pm 0.85	\pm 2.85	0.799	\pm 0.85	\pm 2.85	
0.72–0.90	0.799	45.0	25.29	\pm 0.89	\pm 3.01	1.036	\pm 0.85	\pm 2.85	0.655	\pm 0.85	\pm 2.85	
0.90–1.25	1.035	45.0	0.800	\pm 0.85	\pm 2.85	0.389	\pm 0.85	\pm 2.85	0.389	\pm 0.85	\pm 2.85	
p_T	60 < θ < 75						75 < θ < 90					
	$\langle p_T \rangle$	$\langle \theta \rangle$	$d^2\sigma/dpd\Omega$				$\langle p_T \rangle$	$\langle \theta \rangle$	$d^2\sigma/dpd\Omega$			
			233.04	\pm 3.62	\pm 8.82	98.62	\pm 2.16	\pm 6.98	81.6	\pm 2.16	\pm 6.98	
0.50–0.60	0.547	67.4	137.23	\pm 2.70	\pm 8.15	38.31	\pm 1.23	\pm 4.16	81.5	\pm 1.23	\pm 4.16	
0.60–0.72	0.654	67.0	63.50	\pm 1.62	\pm 6.11	7.31	\pm 0.42	\pm 1.30	0.653	\pm 0.42	\pm 1.30	
0.72–0.90	0.797	66.9	15.98	\pm 0.60	\pm 2.49	1.022	\pm 0.42	\pm 1.30	0.794	\pm 0.42	\pm 1.30	
0.90–1.25	1.034	66.3	0.653	\pm 0.60	\pm 2.49	0.389	\pm 0.42	\pm 1.30	0.653	\pm 0.42	\pm 1.30	
p_T	90 < θ < 105						105 < θ < 125					
	$\langle p_T \rangle$	$\langle \theta \rangle$	$d^2\sigma/dpd\Omega$				$\langle p_T \rangle$	$\langle \theta \rangle$	$d^2\sigma/dpd\Omega$			
			52.60	\pm 1.57	\pm 4.68	108.24	\pm 2.29	\pm 6.39	113.3	\pm 2.29	\pm 6.39	
0.42–0.50	0.652	96.9	18.58	\pm 0.88	\pm 2.33	52.41	\pm 1.48	\pm 4.88	112.9	\pm 1.48	\pm 4.88	
0.50–0.60	0.792	96.8	3.18	\pm 0.28	\pm 0.61	19.16	\pm 0.89	\pm 2.76	112.7	\pm 0.89	\pm 2.76	
0.60–0.72	1.023	96.2	0.651	\pm 0.28	\pm 0.61	4.28	\pm 0.39	\pm 0.96	113.0	\pm 0.39	\pm 0.96	
0.72–0.90	0.792	96.8	0.787	\pm 0.28	\pm 0.61	112.7	\pm 0.39	\pm 0.96	113.3	\pm 0.39	\pm 0.96	
0.90–1.25	1.023	96.2	0.651	\pm 0.28	\pm 0.61	0.651	\pm 0.39	\pm 0.96	112.9	\pm 0.39	\pm 0.96	

Table A.20: Double-differential inclusive cross-section $d^2\sigma/dpd\Omega$ [mb/(GeV/c sr)] of the production of π^+ 's in $p + \text{Cu} \rightarrow \pi^+ + \text{X}$ interactions with $+8.0$ GeV/c beam momentum; the first error is statistical, the second systematic; p_T in GeV/c, polar angle θ in degrees.

p_T	20 < θ < 30			30 < θ < 40		
	$\langle p_T \rangle$	$\langle \theta \rangle$	$d^2\sigma/dpd\Omega$	$\langle p_T \rangle$	$\langle \theta \rangle$	$d^2\sigma/dpd\Omega$
0.10–0.13	0.115	25.0	237.06 ± 10.27 ± 18.35	0.115	35.0	209.12 ± 9.05 ± 15.45
0.13–0.16	0.146	24.8	266.29 ± 9.61 ± 15.72	0.145	34.9	227.97 ± 8.87 ± 13.37
0.16–0.20	0.180	24.8	296.43 ± 8.54 ± 14.97	0.181	34.8	246.20 ± 7.76 ± 12.23
0.20–0.24	0.220	24.8	303.16 ± 8.45 ± 13.09	0.219	34.8	253.77 ± 7.72 ± 10.90
0.24–0.30	0.270	24.8	287.57 ± 6.70 ± 10.51	0.270	34.8	234.25 ± 6.05 ± 8.35
0.30–0.36	0.328	24.7	231.39 ± 5.88 ± 7.31	0.329	34.9	192.12 ± 5.48 ± 5.99
0.36–0.42	0.389	24.9	183.54 ± 5.19 ± 5.73	0.388	34.6	155.44 ± 4.84 ± 4.83
0.42–0.50	0.457	24.8	134.56 ± 3.77 ± 5.00	0.458	34.8	112.21 ± 3.54 ± 3.97
0.50–0.60	0.547	24.8	91.71 ± 2.68 ± 4.84	0.547	34.6	71.23 ± 2.40 ± 3.49
0.60–0.72	0.657	24.8	54.23 ± 1.77 ± 4.26	0.655	34.5	41.78 ± 1.61 ± 3.02
0.72–0.90				0.795	34.7	19.10 ± 0.78 ± 2.15
p_T	40 < θ < 50			50 < θ < 60		
	$\langle p_T \rangle$	$\langle \theta \rangle$	$d^2\sigma/dpd\Omega$	$\langle p_T \rangle$	$\langle \theta \rangle$	$d^2\sigma/dpd\Omega$
0.10–0.13	0.116	45.0	186.79 ± 9.04 ± 14.53	0.145	55.0	154.95 ± 7.22 ± 9.63
0.13–0.16	0.145	45.0	197.16 ± 8.04 ± 11.69	0.180	54.8	178.34 ± 6.36 ± 8.88
0.16–0.20	0.180	44.9	198.16 ± 6.81 ± 9.89	0.220	54.9	155.95 ± 6.00 ± 6.69
0.20–0.24	0.220	44.8	194.90 ± 6.81 ± 8.56	0.269	54.8	134.55 ± 4.64 ± 4.94
0.24–0.30	0.269	44.8	189.75 ± 5.53 ± 7.14	0.329	54.8	105.87 ± 4.03 ± 3.42
0.30–0.36	0.329	44.9	136.36 ± 4.56 ± 4.30	0.388	54.6	87.77 ± 3.76 ± 3.15
0.36–0.42	0.389	44.7	113.01 ± 4.22 ± 3.73	0.457	54.7	61.98 ± 2.65 ± 2.47
0.42–0.50	0.457	44.5	86.87 ± 3.16 ± 3.20	0.546	55.0	42.50 ± 1.95 ± 2.23
0.50–0.60	0.547	44.6	58.68 ± 2.22 ± 2.82	0.652	54.4	22.78 ± 1.24 ± 1.69
0.60–0.72	0.656	44.7	34.71 ± 1.55 ± 2.38	0.798	54.7	10.29 ± 0.64 ± 1.08
0.72–0.90	0.791	44.7	14.73 ± 0.72 ± 1.55	1.025	54.1	2.67 ± 0.18 ± 0.46
p_T	60 < θ < 75			75 < θ < 90		
	$\langle p_T \rangle$	$\langle \theta \rangle$	$d^2\sigma/dpd\Omega$	$\langle p_T \rangle$	$\langle \theta \rangle$	$d^2\sigma/dpd\Omega$
0.13–0.16	0.146	67.0	138.52 ± 5.99 ± 8.71	0.148	82.0	108.21 ± 6.60 ± 10.39
0.16–0.20	0.180	67.6	129.58 ± 4.43 ± 6.40	0.180	82.1	113.01 ± 4.18 ± 5.41
0.20–0.24	0.218	67.1	126.27 ± 4.35 ± 5.23	0.219	82.2	108.13 ± 4.07 ± 4.27
0.24–0.30	0.268	67.2	106.52 ± 3.41 ± 4.23	0.268	81.8	76.77 ± 2.86 ± 2.93
0.30–0.36	0.329	67.1	71.68 ± 2.75 ± 2.33	0.328	82.0	53.40 ± 2.41 ± 2.11
0.36–0.42	0.389	66.9	62.19 ± 2.60 ± 2.45	0.387	81.6	35.15 ± 1.93 ± 1.61
0.42–0.50	0.459	67.0	44.79 ± 1.87 ± 2.03	0.458	81.7	27.08 ± 1.48 ± 1.62
0.50–0.60	0.547	66.8	27.59 ± 1.29 ± 1.72	0.548	81.6	14.88 ± 0.94 ± 1.18
0.60–0.72	0.654	66.6	15.39 ± 0.88 ± 1.33	0.658	81.1	6.77 ± 0.59 ± 0.73
0.72–0.90	0.794	66.1	5.37 ± 0.37 ± 0.66	0.792	80.8	2.15 ± 0.24 ± 0.33
0.90–1.25	1.019	65.9	1.17 ± 0.10 ± 0.23	1.017	80.9	0.53 ± 0.08 ± 0.12
p_T	90 < θ < 105			105 < θ < 125		
	$\langle p_T \rangle$	$\langle \theta \rangle$	$d^2\sigma/dpd\Omega$	$\langle p_T \rangle$	$\langle \theta \rangle$	$d^2\sigma/dpd\Omega$
0.13–0.16	0.148	97.8	106.28 ± 6.79 ± 9.97	0.144	114.8	92.59 ± 4.00 ± 5.17
0.16–0.20	0.180	97.4	97.87 ± 3.91 ± 4.44	0.179	114.4	67.80 ± 2.68 ± 3.07
0.20–0.24	0.219	97.3	76.11 ± 3.33 ± 2.87	0.218	113.6	48.19 ± 2.38 ± 1.85
0.24–0.30	0.268	97.3	52.77 ± 2.39 ± 2.07	0.267	113.3	29.13 ± 1.56 ± 1.36
0.30–0.36	0.328	96.6	31.85 ± 1.89 ± 1.61	0.327	113.9	15.25 ± 1.11 ± 0.99
0.36–0.42	0.390	96.5	21.77 ± 1.53 ± 1.40	0.386	113.6	11.57 ± 0.97 ± 1.01
0.42–0.50	0.453	96.9	12.21 ± 0.98 ± 1.01	0.453	114.1	5.49 ± 0.55 ± 0.63
0.50–0.60	0.543	96.1	7.22 ± 0.66 ± 0.81	0.536	111.3	2.51 ± 0.32 ± 0.38
0.60–0.72	0.649	96.3	3.44 ± 0.40 ± 0.53	0.646	111.1	0.87 ± 0.19 ± 0.18
0.72–0.90	0.798	96.3	0.81 ± 0.15 ± 0.16	0.777	111.0	0.18 ± 0.05 ± 0.05
0.90–1.25	1.014	97.2	0.16 ± 0.04 ± 0.05	1.091	112.8	0.04 ± 0.02 ± 0.02

Table A.21: Double-differential inclusive cross-section $d^2\sigma/dpd\Omega$ [mb/(GeV/c sr)] of the production of π^- 's in $p + Cu \rightarrow \pi^- + X$ interactions with $+8.0$ GeV/c beam momentum; the first error is statistical, the second systematic; p_T in GeV/c, polar angle θ in degrees.

p_T	20 < θ < 30			30 < θ < 40		
	$\langle p_T \rangle$	$\langle \theta \rangle$	$d^2\sigma/dpd\Omega$	$\langle p_T \rangle$	$\langle \theta \rangle$	$d^2\sigma/dpd\Omega$
0.10–0.13	0.115	24.9	257.38 ± 10.30 ± 19.92	0.116	34.9	220.14 ± 9.23 ± 16.98
0.13–0.16	0.145	25.0	277.00 ± 9.65 ± 16.60	0.145	34.8	240.77 ± 8.92 ± 14.54
0.16–0.20	0.180	24.9	305.58 ± 8.54 ± 15.60	0.180	34.7	242.05 ± 7.50 ± 12.15
0.20–0.24	0.220	24.8	281.02 ± 8.06 ± 12.19	0.220	34.8	225.27 ± 7.08 ± 9.61
0.24–0.30	0.269	25.0	241.69 ± 6.04 ± 8.36	0.269	34.9	199.75 ± 5.47 ± 6.93
0.30–0.36	0.329	24.9	181.16 ± 5.20 ± 5.44	0.328	34.9	165.46 ± 5.01 ± 5.00
0.36–0.42	0.389	25.0	136.01 ± 4.53 ± 4.31	0.388	34.9	127.47 ± 4.29 ± 4.04
0.42–0.50	0.457	24.9	92.28 ± 3.18 ± 3.55	0.457	35.0	92.15 ± 3.19 ± 3.48
0.50–0.60	0.546	25.0	59.55 ± 2.27 ± 3.16	0.547	34.9	52.66 ± 2.12 ± 2.73
0.60–0.72	0.654	25.2	33.99 ± 1.59 ± 2.52	0.656	35.1	28.52 ± 1.41 ± 2.06
0.72–0.90				0.794	34.9	15.54 ± 0.85 ± 1.58
p_T	40 < θ < 50			50 < θ < 60		
	$\langle p_T \rangle$	$\langle \theta \rangle$	$d^2\sigma/dpd\Omega$	$\langle p_T \rangle$	$\langle \theta \rangle$	$d^2\sigma/dpd\Omega$
0.10–0.13	0.115	45.0	206.30 ± 9.20 ± 16.26	0.146	55.0	170.13 ± 7.45 ± 10.79
0.13–0.16	0.145	45.2	218.91 ± 8.56 ± 13.43	0.180	54.9	164.47 ± 6.06 ± 8.34
0.16–0.20	0.180	44.9	190.37 ± 6.50 ± 9.65	0.219	54.8	155.81 ± 6.04 ± 6.89
0.20–0.24	0.220	44.9	202.87 ± 6.85 ± 8.79	0.269	54.7	139.10 ± 4.65 ± 5.14
0.24–0.30	0.269	44.9	154.58 ± 4.83 ± 5.40	0.329	54.8	101.40 ± 3.89 ± 3.26
0.30–0.36	0.329	44.7	135.36 ± 4.57 ± 4.33	0.389	54.9	78.32 ± 3.54 ± 3.09
0.36–0.42	0.389	44.7	105.74 ± 3.93 ± 3.49	0.460	54.9	55.61 ± 2.46 ± 2.38
0.42–0.50	0.458	44.8	77.24 ± 2.94 ± 3.09	0.545	54.7	29.23 ± 1.54 ± 1.72
0.50–0.60	0.546	44.9	47.22 ± 2.02 ± 2.60	0.651	54.9	17.80 ± 1.14 ± 1.43
0.60–0.72	0.654	44.8	23.42 ± 1.22 ± 1.89	0.794	54.6	8.23 ± 0.61 ± 0.92
0.72–0.90	0.795	44.7	10.67 ± 0.70 ± 1.16	1.016	54.7	1.84 ± 0.20 ± 0.32
p_T	60 < θ < 75			75 < θ < 90		
	$\langle p_T \rangle$	$\langle \theta \rangle$	$d^2\sigma/dpd\Omega$	$\langle p_T \rangle$	$\langle \theta \rangle$	$d^2\sigma/dpd\Omega$
0.13–0.16	0.145	67.2	149.06 ± 6.08 ± 9.04	0.147	81.7	124.75 ± 7.96 ± 9.67
0.16–0.20	0.179	67.4	140.77 ± 4.65 ± 6.67	0.180	81.8	116.52 ± 4.31 ± 5.39
0.20–0.24	0.221	67.2	122.47 ± 4.29 ± 4.87	0.219	82.2	99.30 ± 3.93 ± 3.92
0.24–0.30	0.267	67.3	99.45 ± 3.22 ± 3.52	0.268	82.0	65.13 ± 2.60 ± 2.33
0.30–0.36	0.328	67.2	74.86 ± 2.82 ± 2.76	0.327	82.2	49.87 ± 2.32 ± 2.20
0.36–0.42	0.389	67.1	55.64 ± 2.39 ± 2.12	0.389	81.7	34.34 ± 1.90 ± 1.74
0.42–0.50	0.457	66.8	37.69 ± 1.66 ± 1.81	0.458	81.6	21.62 ± 1.28 ± 1.37
0.50–0.60	0.543	66.6	23.56 ± 1.16 ± 1.54	0.542	81.4	11.88 ± 0.82 ± 1.02
0.60–0.72	0.654	67.2	12.77 ± 0.76 ± 1.15	0.656	82.1	5.19 ± 0.48 ± 0.60
0.72–0.90	0.795	67.1	4.66 ± 0.37 ± 0.58	0.796	80.9	2.48 ± 0.27 ± 0.39
0.90–1.25	1.032	66.4	0.89 ± 0.11 ± 0.17	1.005	81.6	0.37 ± 0.07 ± 0.09
p_T	90 < θ < 105			105 < θ < 125		
	$\langle p_T \rangle$	$\langle \theta \rangle$	$d^2\sigma/dpd\Omega$	$\langle p_T \rangle$	$\langle \theta \rangle$	$d^2\sigma/dpd\Omega$
0.13–0.16	0.146	97.8	112.30 ± 7.96 ± 7.25	0.144	113.7	100.81 ± 4.42 ± 5.41
0.16–0.20	0.179	97.5	95.84 ± 3.87 ± 4.35	0.178	113.7	69.97 ± 2.78 ± 2.92
0.20–0.24	0.219	97.2	73.53 ± 3.30 ± 2.85	0.218	114.2	45.00 ± 2.30 ± 1.84
0.24–0.30	0.267	97.2	51.23 ± 2.36 ± 2.15	0.268	113.9	29.74 ± 1.53 ± 1.50
0.30–0.36	0.327	97.3	30.79 ± 1.79 ± 1.53	0.328	113.8	16.19 ± 1.14 ± 1.19
0.36–0.42	0.387	96.9	21.93 ± 1.52 ± 1.52	0.387	113.1	7.71 ± 0.75 ± 0.76
0.42–0.50	0.457	96.7	13.29 ± 1.01 ± 1.21	0.459	111.6	5.05 ± 0.54 ± 0.65
0.50–0.60	0.543	95.9	6.38 ± 0.62 ± 0.79	0.544	112.1	1.92 ± 0.29 ± 0.33
0.60–0.72	0.649	97.3	2.07 ± 0.31 ± 0.35	0.642	110.4	0.49 ± 0.14 ± 0.11
0.72–0.90	0.787	96.3	0.54 ± 0.12 ± 0.12	0.775	114.1	0.11 ± 0.05 ± 0.04
0.90–1.25	1.033	95.3	0.15 ± 0.04 ± 0.05			

Table A.22: Double-differential inclusive cross-section $d^2\sigma/dpd\Omega$ [mb/(GeV/c sr)] of the production of protons in $\pi^+ + \text{Cu} \rightarrow p + X$ interactions with +8.0 GeV/c beam momentum; the first error is statistical, the second systematic; p_T in GeV/c, polar angle θ in degrees.

p_T	20 < θ < 30				30 < θ < 40					
	$\langle p_T \rangle$	$\langle \theta \rangle$	$d^2\sigma/dpd\Omega$		$\langle p_T \rangle$	$\langle \theta \rangle$	$d^2\sigma/dpd\Omega$			
			$\langle p_T \rangle$	$\langle \theta \rangle$			$\langle p_T \rangle$	$\langle \theta \rangle$		
0.20–0.24	0.220	25.1	416.01	\pm 14.70	\pm 22.76	0.271	35.0	414.40	\pm 11.65	\pm 18.50
0.24–0.30	0.269	25.0	380.56	\pm 11.26	\pm 18.56	0.329	35.1	376.78	\pm 10.81	\pm 14.48
0.30–0.36	0.330	25.3	325.06	\pm 10.52	\pm 14.76	0.389	35.2	295.13	\pm 9.95	\pm 11.08
0.36–0.42	0.389	25.2	248.43	\pm 9.09	\pm 10.94	0.458	35.1	237.82	\pm 7.89	\pm 9.90
0.42–0.50	0.459	25.0	209.70	\pm 7.29	\pm 8.39	0.546	35.0	180.66	\pm 6.13	\pm 7.97
0.50–0.60	0.547	25.0	159.53	\pm 5.59	\pm 7.19	0.656	35.1	115.55	\pm 4.49	\pm 6.40
0.60–0.72	0.656	25.1	104.91	\pm 4.07	\pm 5.42	0.800	34.9	64.04	\pm 2.71	\pm 4.70
0.72–0.90										
p_T	40 < θ < 50				50 < θ < 60					
	$\langle p_T \rangle$	$\langle \theta \rangle$	$d^2\sigma/dpd\Omega$		$\langle p_T \rangle$	$\langle \theta \rangle$	$d^2\sigma/dpd\Omega$			
			$\langle p_T \rangle$	$\langle \theta \rangle$			$\langle p_T \rangle$	$\langle \theta \rangle$		
0.30–0.36	0.329	45.0	421.26	\pm 11.22	\pm 13.74	0.388	55.2	357.49	\pm 10.07	\pm 10.95
0.36–0.42	0.388	45.0	342.80	\pm 10.35	\pm 10.23	0.457	55.0	275.27	\pm 7.90	\pm 7.96
0.42–0.50	0.459	45.1	268.14	\pm 8.05	\pm 8.84	0.547	55.0	197.73	\pm 6.27	\pm 7.92
0.50–0.60	0.547	45.1	182.78	\pm 6.17	\pm 8.03	0.656	54.9	116.45	\pm 4.62	\pm 7.08
0.60–0.72	0.656	45.1	121.35	\pm 4.75	\pm 7.07	0.798	55.0	62.85	\pm 2.86	\pm 5.24
0.72–0.90	0.800	45.1	65.99	\pm 2.88	\pm 5.09	1.031	55.0	17.88	\pm 1.10	\pm 2.32
0.90–1.25	1.035	45.1	18.63	\pm 1.09	\pm 2.23					
p_T	60 < θ < 75				75 < θ < 90					
	$\langle p_T \rangle$	$\langle \theta \rangle$	$d^2\sigma/dpd\Omega$		$\langle p_T \rangle$	$\langle \theta \rangle$	$d^2\sigma/dpd\Omega$			
			$\langle p_T \rangle$	$\langle \theta \rangle$			$\langle p_T \rangle$	$\langle \theta \rangle$		
0.50–0.60	0.547	67.5	194.89	\pm 4.79	\pm 7.53	0.652	81.7	82.15	\pm 2.85	\pm 5.84
0.60–0.72	0.653	67.2	110.16	\pm 3.50	\pm 6.61	0.797	82.0	31.84	\pm 1.62	\pm 3.48
0.72–0.90	0.796	67.2	51.24	\pm 2.11	\pm 4.97	1.014	81.9	6.94	\pm 0.59	\pm 1.24
0.90–1.25	1.031	66.4	12.91	\pm 0.78	\pm 2.02					
p_T	90 < θ < 105				105 < θ < 125					
	$\langle p_T \rangle$	$\langle \theta \rangle$	$d^2\sigma/dpd\Omega$		$\langle p_T \rangle$	$\langle \theta \rangle$	$d^2\sigma/dpd\Omega$			
			$\langle p_T \rangle$	$\langle \theta \rangle$			$\langle p_T \rangle$	$\langle \theta \rangle$		
0.42–0.50					0.459	113.5	101.89	\pm 3.25	\pm 5.87	
0.50–0.60					0.541	112.9	51.57	\pm 2.13	\pm 4.79	
0.60–0.72	0.650	97.1	49.14	\pm 2.19	\pm 4.39	0.649	112.8	20.28	\pm 1.33	\pm 2.91
0.72–0.90	0.791	96.6	16.16	\pm 1.17	\pm 2.02	0.792	112.7	4.88	\pm 0.59	\pm 1.08
0.90–1.25	1.015	96.1	2.73	\pm 0.37	\pm 0.53					

Table A.25: Double-differential inclusive cross-section $d^2\sigma/dpd\Omega$ [mb/(GeV/c sr)] of the production of protons in $\pi^- + \text{Cu} \rightarrow p + X$ interactions with -8.0 GeV/c beam momentum; the first error is statistical, the second systematic; p_T in GeV/c, polar angle θ in degrees.

p_T	20 < θ < 30				30 < θ < 40			
	$\langle p_T \rangle$	$\langle \theta \rangle$	$d^2\sigma/dpd\Omega$		$\langle p_T \rangle$	$\langle \theta \rangle$	$d^2\sigma/dpd\Omega$	
			$d^2\sigma/dpd\Omega$	$d^2\sigma/dpd\Omega$			$d^2\sigma/dpd\Omega$	$d^2\sigma/dpd\Omega$
0.20–0.24	0.220	25.3	339.98 \pm 6.99	\pm 18.36				
0.24–0.30	0.270	25.2	328.63 \pm 5.48	\pm 15.84	0.267	35.3	415.67 \pm 53.20	\pm 18.36
0.30–0.36	0.329	25.3	267.73 \pm 4.97	\pm 12.12	0.329	35.1	321.00 \pm 5.22	\pm 12.20
0.36–0.42	0.390	25.2	225.01 \pm 4.61	\pm 10.03	0.389	35.1	259.09 \pm 4.84	\pm 9.69
0.42–0.50	0.458	25.2	175.83 \pm 3.49	\pm 7.54	0.458	35.1	198.95 \pm 3.77	\pm 8.29
0.50–0.60	0.547	25.2	132.81 \pm 2.69	\pm 5.90	0.547	35.0	149.55 \pm 2.94	\pm 6.95
0.60–0.72	0.656	25.2	85.20 \pm 1.93	\pm 4.26	0.655	35.2	96.04 \pm 2.17	\pm 5.74
0.72–0.90					0.799	35.1	52.85 \pm 1.30	\pm 3.99
40 < θ < 50								
p_T	$\langle p_T \rangle$	$\langle \theta \rangle$	$d^2\sigma/dpd\Omega$		$\langle p_T \rangle$	$\langle \theta \rangle$	$d^2\sigma/dpd\Omega$	
			$d^2\sigma/dpd\Omega$	$d^2\sigma/dpd\Omega$			$d^2\sigma/dpd\Omega$	$d^2\sigma/dpd\Omega$
0.30–0.36	0.329	45.1	349.65 \pm 5.42	\pm 11.15	0.389	55.1	296.41 \pm 4.74	\pm 9.40
0.36–0.42	0.389	45.2	281.84 \pm 4.85	\pm 8.12	0.458	55.0	242.54 \pm 3.87	\pm 6.86
0.42–0.50	0.458	45.1	218.90 \pm 3.81	\pm 7.19	0.547	54.9	160.73 \pm 2.96	\pm 6.48
0.50–0.60	0.548	45.1	159.84 \pm 3.06	\pm 7.28	0.654	55.0	99.16 \pm 2.25	\pm 5.94
0.60–0.72	0.655	45.0	101.43 \pm 2.27	\pm 6.19	0.797	54.9	49.19 \pm 1.33	\pm 4.11
0.72–0.90	0.799	44.9	52.08 \pm 1.35	\pm 4.28	1.035	54.9	12.60 \pm 0.48	\pm 1.70
0.90–1.25	1.032	44.9	14.99 \pm 0.51	\pm 1.83				
60 < θ < 75								
p_T	$\langle p_T \rangle$	$\langle \theta \rangle$	$d^2\sigma/dpd\Omega$		$\langle p_T \rangle$	$\langle \theta \rangle$	$d^2\sigma/dpd\Omega$	
			$d^2\sigma/dpd\Omega$	$d^2\sigma/dpd\Omega$			$d^2\sigma/dpd\Omega$	$d^2\sigma/dpd\Omega$
0.50–0.60	0.546	67.5	157.32 \pm 2.24	\pm 6.14	0.654	81.8	67.69 \pm 1.34	\pm 4.82
0.60–0.72	0.653	67.3	93.69 \pm 1.68	\pm 5.51	0.796	81.6	26.15 \pm 0.78	\pm 2.89
0.72–0.90	0.798	67.1	40.46 \pm 0.98	\pm 3.96	1.029	81.5	5.33 \pm 0.27	\pm 0.95
0.90–1.25	1.033	66.9	10.70 \pm 0.37	\pm 1.66				
90 < θ < 105								
p_T	$\langle p_T \rangle$	$\langle \theta \rangle$	$d^2\sigma/dpd\Omega$		$\langle p_T \rangle$	$\langle \theta \rangle$	$d^2\sigma/dpd\Omega$	
			$d^2\sigma/dpd\Omega$	$d^2\sigma/dpd\Omega$			$d^2\sigma/dpd\Omega$	$d^2\sigma/dpd\Omega$
0.42–0.50					0.458	113.6	87.42 \pm 1.56	\pm 5.09
0.50–0.60					0.544	113.1	42.57 \pm 1.00	\pm 3.96
0.60–0.72	0.652	97.0	40.09 \pm 1.03	\pm 3.56	0.651	112.7	16.48 \pm 0.62	\pm 2.36
0.72–0.90	0.796	96.5	13.73 \pm 0.57	\pm 1.75	0.795	112.1	4.42 \pm 0.30	\pm 0.97
0.90–1.25	1.012	96.5	2.58 \pm 0.19	\pm 0.50	1.008	112.0	0.59 \pm 0.08	\pm 0.21
105 < θ < 125								

Table A.28: Double-differential inclusive cross-section $d^2\sigma/dpd\Omega$ [mb/(GeV/c sr)] of the production of protons in $p + \text{Cu} \rightarrow p + X$ interactions with $+12.0 \text{ GeV}/c$ beam momentum; the first error is statistical, the second systematic; p_T in GeV/c , polar angle θ in degrees.

p_T	20 < θ < 30			30 < θ < 40		
	$\langle p_T \rangle$	$\langle \theta \rangle$	$d^2\sigma/dpd\Omega$	$\langle p_T \rangle$	$\langle \theta \rangle$	$d^2\sigma/dpd\Omega$
0.20–0.24	0.220	25.2	492.70 \pm 12.36 \pm 26.78	0.271	34.9	518.58 \pm 9.82 \pm 22.89
0.24–0.30	0.270	25.2	447.61 \pm 9.21 \pm 21.57	0.329	35.1	447.35 \pm 9.00 \pm 17.05
0.30–0.36	0.329	25.2	387.95 \pm 8.81 \pm 17.86	0.390	35.0	376.91 \pm 8.58 \pm 14.26
0.36–0.42	0.389	25.2	346.93 \pm 8.37 \pm 15.02	0.458	34.9	300.59 \pm 6.75 \pm 12.62
0.42–0.50	0.459	25.1	277.22 \pm 6.32 \pm 11.93	0.546	35.0	238.18 \pm 5.48 \pm 11.81
0.50–0.60	0.547	25.2	215.87 \pm 4.97 \pm 9.63	0.657	35.1	162.49 \pm 4.07 \pm 9.07
0.60–0.72	0.655	25.1	151.55 \pm 3.78 \pm 7.77	0.801	35.1	94.11 \pm 2.53 \pm 7.01
0.72–0.90						
p_T	40 < θ < 50			50 < θ < 60		
	$\langle p_T \rangle$	$\langle \theta \rangle$	$d^2\sigma/dpd\Omega$	$\langle p_T \rangle$	$\langle \theta \rangle$	$d^2\sigma/dpd\Omega$
0.30–0.36	0.326	45.4	572.21 \pm 76.15 \pm 18.26	0.388	55.2	438.79 \pm 8.55 \pm 12.94
0.36–0.42	0.389	45.1	424.45 \pm 8.64 \pm 12.34	0.459	55.0	342.61 \pm 6.71 \pm 9.82
0.42–0.50	0.459	45.1	329.46 \pm 6.86 \pm 10.45	0.549	55.0	242.98 \pm 5.30 \pm 9.56
0.50–0.60	0.547	45.0	243.24 \pm 5.46 \pm 10.71	0.655	54.9	147.87 \pm 3.98 \pm 8.90
0.60–0.72	0.657	45.1	158.65 \pm 4.10 \pm 9.29	0.799	54.7	82.51 \pm 2.53 \pm 6.90
0.72–0.90	0.799	44.9	92.58 \pm 2.64 \pm 7.41	1.028	54.8	22.80 \pm 0.93 \pm 2.91
0.90–1.25	1.037	44.9	27.44 \pm 1.01 \pm 3.45			
p_T	60 < θ < 75			75 < θ < 90		
	$\langle p_T \rangle$	$\langle \theta \rangle$	$d^2\sigma/dpd\Omega$	$\langle p_T \rangle$	$\langle \theta \rangle$	$d^2\sigma/dpd\Omega$
0.50–0.60	0.546	67.4	228.90 \pm 3.94 \pm 9.08	0.652	81.6	101.02 \pm 2.39 \pm 7.21
0.60–0.72	0.654	67.3	140.63 \pm 3.01 \pm 8.22	0.796	81.6	40.39 \pm 1.42 \pm 4.52
0.72–0.90	0.799	67.2	66.98 \pm 1.84 \pm 6.46	1.023	81.6	9.60 \pm 0.53 \pm 1.65
0.90–1.25	1.031	66.9	16.46 \pm 0.70 \pm 2.71			
p_T	90 < θ < 105			105 < θ < 125		
	$\langle p_T \rangle$	$\langle \theta \rangle$	$d^2\sigma/dpd\Omega$	$\langle p_T \rangle$	$\langle \theta \rangle$	$d^2\sigma/dpd\Omega$
0.42–0.50				0.458	113.5	109.22 \pm 2.53 \pm 6.47
0.50–0.60				0.543	112.8	55.78 \pm 1.67 \pm 5.24
0.60–0.72	0.652	97.1	58.20 \pm 1.82 \pm 5.16	0.652	113.0	21.98 \pm 1.05 \pm 3.15
0.72–0.90	0.792	96.9	20.15 \pm 1.01 \pm 2.58	0.785	113.1	5.92 \pm 0.50 \pm 1.32
0.90–1.25	1.023	96.6	3.70 \pm 0.33 \pm 0.70	1.018	111.9	0.92 \pm 0.14 \pm 0.32

Table A.30: Double-differential inclusive cross-section $d^2\sigma/dpd\Omega$ [mb/(GeV/c sr)] of the production of π^- 's in $p + \text{Cu} \rightarrow \pi^- + \text{X}$ interactions with +12.0 GeV/c beam momentum; the first error is statistical, the second systematic; p_T in GeV/c, polar angle θ in degrees.

			20 < θ < 30						30 < θ < 40							
p_T	$\langle p_T \rangle$	$\langle \theta \rangle$	$d^2\sigma/dpd\Omega$						$\langle p_T \rangle$	$\langle \theta \rangle$	$d^2\sigma/dpd\Omega$					
0.10–0.13	0.115	25.0	326.83	±	12.68	±	24.69	0.115	34.9	292.28	±	11.78	±	22.30		
0.13–0.16	0.145	24.8	364.51	±	12.06	±	21.44	0.145	34.8	286.16	±	10.51	±	17.12		
0.16–0.20	0.180	24.7	376.49	±	10.23	±	18.53	0.180	34.9	298.02	±	9.25	±	14.91		
0.20–0.24	0.219	24.9	374.27	±	10.15	±	15.63	0.220	34.7	296.19	±	9.07	±	12.46		
0.24–0.30	0.269	24.9	319.49	±	7.56	±	10.73	0.269	34.9	264.33	±	6.96	±	8.99		
0.30–0.36	0.329	24.9	251.23	±	6.70	±	7.30	0.328	34.8	206.68	±	6.08	±	6.07		
0.36–0.42	0.389	24.9	197.17	±	5.93	±	5.97	0.388	34.8	163.96	±	5.32	±	5.00		
0.42–0.50	0.458	25.0	147.84	±	4.49	±	5.50	0.458	34.7	119.10	±	3.96	±	4.38		
0.50–0.60	0.545	25.0	98.46	±	3.25	±	5.08	0.547	34.9	84.65	±	2.99	±	4.29		
0.60–0.72	0.652	24.8	52.49	±	2.05	±	3.86	0.654	34.5	45.77	±	1.91	±	3.33		
0.72–0.90								0.794	34.6	16.78	±	0.89	±	1.79		
			40 < θ < 50						50 < θ < 60							
p_T	$\langle p_T \rangle$	$\langle \theta \rangle$	$d^2\sigma/dpd\Omega$						$\langle p_T \rangle$	$\langle \theta \rangle$	$d^2\sigma/dpd\Omega$					
0.10–0.13	0.116	45.0	239.23	±	11.23	±	19.07	0.145	54.7	202.31	±	9.04	±	12.68		
0.13–0.16	0.145	44.9	251.71	±	10.04	±	15.29	0.180	54.8	207.90	±	7.60	±	10.51		
0.16–0.20	0.180	44.7	241.55	±	8.23	±	12.22	0.220	54.8	175.49	±	6.94	±	7.48		
0.20–0.24	0.220	44.9	224.50	±	7.76	±	9.68	0.269	54.9	161.38	±	5.48	±	5.62		
0.24–0.30	0.269	44.8	210.40	±	6.27	±	7.24	0.329	54.9	120.26	±	4.72	±	3.73		
0.30–0.36	0.329	44.7	157.98	±	5.37	±	4.71	0.387	54.7	92.12	±	4.07	±	3.11		
0.36–0.42	0.389	44.7	124.03	±	4.62	±	3.96	0.456	55.0	67.06	±	2.99	±	2.79		
0.42–0.50	0.456	44.6	93.95	±	3.51	±	3.68	0.546	54.7	41.24	±	2.00	±	2.45		
0.50–0.60	0.546	44.7	57.45	±	2.38	±	3.16	0.651	54.8	24.55	±	1.48	±	1.96		
0.60–0.72	0.655	45.0	30.28	±	1.55	±	2.37	0.799	54.6	8.74	±	0.65	±	1.03		
0.72–0.90	0.802	44.6	14.17	±	0.87	±	1.55	1.039	54.2	1.76	±	0.19	±	0.32		
			60 < θ < 75						75 < θ < 90							
p_T	$\langle p_T \rangle$	$\langle \theta \rangle$	$d^2\sigma/dpd\Omega$						$\langle p_T \rangle$	$\langle \theta \rangle$	$d^2\sigma/dpd\Omega$					
0.13–0.16	0.145	67.8	180.39	±	9.03	±	10.84	0.147	83.0	124.05	±	9.88	±	8.96		
0.16–0.20	0.179	67.1	166.74	±	5.59	±	7.82	0.180	82.0	131.73	±	4.96	±	6.03		
0.20–0.24	0.219	67.1	149.15	±	5.26	±	5.88	0.219	81.6	110.61	±	4.46	±	4.20		
0.24–0.30	0.268	67.0	118.05	±	3.88	±	4.12	0.269	82.1	84.71	±	3.28	±	3.10		
0.30–0.36	0.329	66.9	83.91	±	3.21	±	2.63	0.329	81.7	59.92	±	2.84	±	2.75		
0.36–0.42	0.388	66.9	68.02	±	2.95	±	2.68	0.389	81.7	41.30	±	2.29	±	2.03		
0.42–0.50	0.459	66.6	45.59	±	2.01	±	2.16	0.456	82.0	29.03	±	1.68	±	1.88		
0.50–0.60	0.546	67.2	29.06	±	1.43	±	1.89	0.544	81.3	15.00	±	1.05	±	1.27		
0.60–0.72	0.654	66.8	13.96	±	0.88	±	1.25	0.654	81.0	6.72	±	0.59	±	0.79		
0.72–0.90	0.798	66.3	5.16	±	0.40	±	0.67	0.794	81.0	2.87	±	0.31	±	0.45		
0.90–1.25	1.036	66.8	1.29	±	0.15	±	0.24	1.016	80.5	0.29	±	0.07	±	0.07		
			90 < θ < 105						105 < θ < 125							
p_T	$\langle p_T \rangle$	$\langle \theta \rangle$	$d^2\sigma/dpd\Omega$						$\langle p_T \rangle$	$\langle \theta \rangle$	$d^2\sigma/dpd\Omega$					
0.13–0.16	0.147	97.9	150.43	±	8.58	±	10.95	0.144	114.2	105.22	±	4.62	±	6.02		
0.16–0.20	0.179	97.7	99.98	±	4.24	±	4.70	0.179	114.0	81.51	±	3.34	±	3.23		
0.20–0.24	0.219	97.5	84.55	±	4.01	±	3.21	0.218	113.9	51.06	±	2.70	±	2.05		
0.24–0.30	0.268	97.0	58.08	±	2.73	±	2.18	0.266	113.9	29.62	±	1.68	±	1.49		
0.30–0.36	0.327	96.9	33.17	±	2.06	±	1.66	0.329	113.6	18.60	±	1.33	±	1.36		
0.36–0.42	0.389	97.0	21.10	±	1.63	±	1.42	0.386	114.0	9.78	±	0.93	±	0.97		
0.42–0.50	0.458	96.7	14.96	±	1.18	±	1.35	0.461	112.5	5.09	±	0.58	±	0.65		
0.50–0.60	0.544	97.3	5.37	±	0.59	±	0.66	0.540	110.8	2.44	±	0.37	±	0.41		
0.60–0.72	0.642	97.0	2.62	±	0.39	±	0.43	0.644	109.9	0.54	±	0.14	±	0.12		
0.72–0.90	0.789	96.7	0.56	±	0.14	±	0.13	0.775	112.9	0.15	±	0.06	±	0.04		
0.90–1.25	1.013	95.8	0.15	±	0.05	±	0.05									

Table A.31: Double-differential inclusive cross-section $d^2\sigma/dpd\Omega$ [mb/(GeV/c sr)] of the production of protons in $\pi^+ + \text{Cu} \rightarrow p + X$ interactions with +12.0 GeV/c beam momentum; the first error is statistical, the second systematic; p_T in GeV/c, polar angle θ in degrees.

p_T	20 < θ < 30						30 < θ < 40							
				$d^2\sigma/dpd\Omega$						$d^2\sigma/dpd\Omega$				
	$\langle p_T \rangle$	$\langle \theta \rangle$		$d^2\sigma/dpd\Omega$			$\langle p_T \rangle$	$\langle \theta \rangle$		$d^2\sigma/dpd\Omega$				
0.20–0.24	0.220	25.3	437.21	\pm	38.51	\pm	24.01	0.270	35.0	427.50	\pm	30.30	\pm	19.21
0.24–0.30	0.269	25.4	363.91	\pm	27.78	\pm	17.84	0.330	35.0	365.49	\pm	26.84	\pm	14.25
0.30–0.36	0.326	25.3	260.19	\pm	24.03	\pm	12.33	0.387	34.9	287.49	\pm	24.90	\pm	11.26
0.36–0.42	0.388	25.5	264.55	\pm	24.08	\pm	11.77	0.460	34.7	244.14	\pm	20.20	\pm	10.61
0.42–0.50	0.457	25.1	199.36	\pm	17.63	\pm	8.76	0.548	35.3	152.57	\pm	14.55	\pm	7.72
0.50–0.60	0.548	25.0	142.09	\pm	13.19	\pm	6.47	0.651	35.7	106.63	\pm	10.85	\pm	6.04
0.60–0.72	0.658	25.3	119.47	\pm	10.95	\pm	6.21	0.804	34.6	70.57	\pm	7.12	\pm	5.30
40 < θ < 50														
p_T	$\langle p_T \rangle$	$\langle \theta \rangle$	$d^2\sigma/dpd\Omega$			$\langle p_T \rangle$	$\langle \theta \rangle$	$d^2\sigma/dpd\Omega$						
0.30–0.36	0.328	45.4	395.18	\pm	27.60	\pm	13.00	0.387	55.1	365.20	\pm	25.67	\pm	11.57
0.36–0.42	0.389	44.9	336.01	\pm	25.42	\pm	10.15	0.458	54.9	267.82	\pm	19.70	\pm	7.99
0.42–0.50	0.462	45.1	252.58	\pm	19.98	\pm	8.43	0.549	55.0	166.94	\pm	14.60	\pm	6.78
0.50–0.60	0.546	44.9	155.63	\pm	14.43	\pm	7.13	0.650	54.5	122.47	\pm	12.01	\pm	7.56
0.60–0.72	0.651	45.4	102.53	\pm	10.95	\pm	6.11	0.794	54.9	70.28	\pm	7.77	\pm	5.94
0.72–0.90	0.802	45.1	65.69	\pm	7.35	\pm	5.31	1.058	55.1	17.36	\pm	2.69	\pm	2.23
60 < θ < 75														
p_T	$\langle p_T \rangle$	$\langle \theta \rangle$	$d^2\sigma/dpd\Omega$			$\langle p_T \rangle$	$\langle \theta \rangle$	$d^2\sigma/dpd\Omega$						
0.50–0.60	0.547	67.9	195.54	\pm	12.07	\pm	8.04	0.656	81.7	79.73	\pm	7.01	\pm	5.76
0.60–0.72	0.655	67.1	113.37	\pm	8.95	\pm	6.74	0.799	81.5	31.56	\pm	4.20	\pm	3.64
0.72–0.90	0.796	66.6	42.30	\pm	4.84	\pm	4.16	1.012	81.6	8.14	\pm	1.65	\pm	1.45
90 < θ < 105														
p_T	$\langle p_T \rangle$	$\langle \theta \rangle$	$d^2\sigma/dpd\Omega$			$\langle p_T \rangle$	$\langle \theta \rangle$	$d^2\sigma/dpd\Omega$						
0.42–0.50						0.459	114.0	109.69	\pm	8.39	\pm	6.58		
0.50–0.60						0.548	113.8	48.02	\pm	5.13	\pm	4.53		
0.60–0.72	0.650	97.0	61.58	\pm	6.21	\pm	5.50	0.658	112.6	22.73	\pm	3.54	\pm	3.25
0.72–0.90	0.798	97.1	16.33	\pm	3.04	\pm	2.15	0.794	111.3	6.50	\pm	1.72	\pm	1.44
0.90–1.25	1.027	98.1	2.93	\pm	1.00	\pm	0.58	1.043	109.1	0.89	\pm	0.46	\pm	0.31
105 < θ < 125														
p_T	$\langle p_T \rangle$	$\langle \theta \rangle$	$d^2\sigma/dpd\Omega$			$\langle p_T \rangle$	$\langle \theta \rangle$	$d^2\sigma/dpd\Omega$						

Table A.32: Double-differential inclusive cross-section $d^2\sigma/dpd\Omega$ [mb/(GeV/c sr)] of the production of π^+ 's in $\pi^+ + \text{Cu} \rightarrow \pi^+ + \text{X}$ interactions with +12.0 GeV/c beam momentum; the first error is statistical, the second systematic; p_T in GeV/c, polar angle θ in degrees.

			20 < θ < 30				30 < θ < 40					
p_T	$\langle p_T \rangle$	$\langle \theta \rangle$	$d^2\sigma/dpd\Omega$				$\langle p_T \rangle$	$\langle \theta \rangle$	$d^2\sigma/dpd\Omega$			
0.10–0.13	0.115	25.5	229.78	± 35.11	± 16.40		0.115	34.5	308.80	± 39.19	± 22.59	
0.13–0.16	0.146	25.1	293.82	± 36.83	± 17.62		0.147	34.8	252.81	± 33.90	± 15.05	
0.16–0.20	0.180	24.6	398.64	± 37.08	± 20.71		0.181	35.6	270.35	± 30.33	± 13.64	
0.20–0.24	0.219	24.8	384.29	± 34.64	± 16.70		0.221	34.6	237.77	± 27.37	± 10.21	
0.24–0.30	0.270	24.9	405.96	± 29.38	± 14.99		0.269	35.0	309.70	± 25.58	± 11.14	
0.30–0.36	0.331	25.1	356.39	± 26.97	± 11.12		0.327	34.3	257.19	± 22.78	± 8.09	
0.36–0.42	0.388	24.6	276.02	± 22.78	± 8.52		0.391	34.8	165.35	± 18.09	± 5.04	
0.42–0.50	0.460	24.4	225.08	± 18.00	± 8.35		0.460	34.6	138.72	± 14.33	± 4.85	
0.50–0.60	0.548	24.9	127.16	± 11.84	± 6.62		0.549	34.9	112.82	± 11.44	± 5.44	
0.60–0.72	0.656	24.9	100.80	± 9.21	± 7.84		0.655	35.2	56.93	± 6.96	± 4.07	
0.72–0.90							0.792	34.7	33.31	± 4.02	± 3.72	
			40 < θ < 50				50 < θ < 60					
p_T	$\langle p_T \rangle$	$\langle \theta \rangle$	$d^2\sigma/dpd\Omega$				$\langle p_T \rangle$	$\langle \theta \rangle$	$d^2\sigma/dpd\Omega$			
0.10–0.13	0.112	44.5	206.02	± 34.75	± 15.53		0.145	54.8	207.55	± 31.24	± 12.97	
0.13–0.16	0.144	45.5	213.58	± 31.21	± 12.73		0.185	55.9	122.87	± 19.61	± 6.21	
0.16–0.20	0.179	45.0	241.50	± 27.73	± 12.21		0.220	55.7	159.14	± 22.20	± 6.85	
0.20–0.24	0.218	44.8	208.10	± 26.11	± 9.17		0.267	54.9	126.34	± 16.34	± 4.63	
0.24–0.30	0.268	44.6	207.12	± 21.00	± 7.45		0.329	54.3	117.78	± 15.33	± 3.74	
0.30–0.36	0.331	44.1	166.21	± 18.86	± 5.54		0.391	54.4	102.59	± 14.59	± 3.43	
0.36–0.42	0.389	44.7	160.12	± 17.88	± 5.08		0.463	54.2	84.28	± 11.30	± 3.32	
0.42–0.50	0.457	44.3	98.10	± 12.10	± 3.56		0.552	54.7	49.61	± 7.73	± 2.60	
0.50–0.60	0.551	44.7	76.09	± 9.42	± 3.69		0.653	55.1	36.65	± 5.92	± 2.68	
0.60–0.72	0.650	44.6	39.93	± 5.95	± 2.74		0.785	54.6	14.72	± 2.87	± 1.55	
0.72–0.90	0.814	44.4	21.81	± 3.37	± 2.24		1.051	53.5	2.15	± 0.53	± 0.40	
			60 < θ < 75				75 < θ < 90					
p_T	$\langle p_T \rangle$	$\langle \theta \rangle$	$d^2\sigma/dpd\Omega$				$\langle p_T \rangle$	$\langle \theta \rangle$	$d^2\sigma/dpd\Omega$			
0.13–0.16	0.146	66.9	170.62	± 24.48	± 10.74		0.147	83.2	100.45	± 21.15	± 8.00	
0.16–0.20	0.179	67.0	154.44	± 18.06	± 7.73		0.178	82.6	128.45	± 17.20	± 6.17	
0.20–0.24	0.219	67.1	149.58	± 17.52	± 6.25		0.217	82.2	124.69	± 16.22	± 4.98	
0.24–0.30	0.265	67.3	92.32	± 11.34	± 3.23		0.264	82.5	85.10	± 11.15	± 3.26	
0.30–0.36	0.331	67.0	99.89	± 12.03	± 3.48		0.333	80.7	34.16	± 7.04	± 1.30	
0.36–0.42	0.390	67.6	74.69	± 10.32	± 2.80		0.394	80.1	41.97	± 7.72	± 1.89	
0.42–0.50	0.454	67.3	45.89	± 6.89	± 2.06		0.458	82.4	25.02	± 5.05	± 1.43	
0.50–0.60	0.549	66.5	34.68	± 5.25	± 2.16		0.556	83.4	23.82	± 4.54	± 1.85	
0.60–0.72	0.649	65.3	12.68	± 2.78	± 1.10		0.655	81.1	5.14	± 1.75	± 0.56	
0.72–0.90	0.820	66.6	6.04	± 1.43	± 0.76		0.750	81.4	3.26	± 1.17	± 0.49	
0.90–1.25	1.038	64.2	1.52	± 0.42	± 0.31		1.026	80.9	0.46	± 0.24	± 0.11	
			90 < θ < 105				105 < θ < 125					
p_T	$\langle p_T \rangle$	$\langle \theta \rangle$	$d^2\sigma/dpd\Omega$				$\langle p_T \rangle$	$\langle \theta \rangle$	$d^2\sigma/dpd\Omega$			
0.13–0.16	0.148	98.0	79.76	± 18.43	± 5.02		0.146	114.7	87.75	± 14.31	± 4.70	
0.16–0.20	0.178	96.2	86.18	± 13.35	± 4.11		0.179	115.0	64.04	± 9.78	± 2.75	
0.20–0.24	0.220	96.1	87.66	± 13.35	± 3.30		0.221	113.1	56.80	± 9.54	± 2.18	
0.24–0.30	0.269	97.2	68.08	± 9.98	± 2.57		0.265	112.8	35.19	± 6.11	± 1.57	
0.30–0.36	0.330	96.6	29.88	± 6.66	± 1.45		0.326	115.2	12.52	± 3.57	± 0.79	
0.36–0.42	0.380	97.3	22.64	± 5.61	± 1.39		0.388	112.0	11.16	± 3.43	± 0.97	
0.42–0.50	0.458	96.0	15.48	± 3.95	± 1.28		0.464	111.3	4.65	± 1.82	± 0.54	
0.50–0.60	0.542	96.8	9.95	± 2.79	± 1.12		0.541	118.0	2.65	± 1.27	± 0.40	
0.60–0.72	0.656	95.9	5.12	± 1.92	± 0.78		0.654	114.0	1.48	± 0.70	± 0.31	
0.72–0.90	0.785	96.6	1.60	± 0.81	± 0.33							
0.90–1.25	0.988	96.5	0.40	± 0.23	± 0.13							

Table A.33: Double-differential inclusive cross-section $d^2\sigma/dpd\Omega$ [mb/(GeV/c sr)] of the production of π^- 's in $\pi^+ + \text{Cu} \rightarrow \pi^- + \text{X}$ interactions with +12.0 GeV/c beam momentum; the first error is statistical, the second systematic; p_T in GeV/c, polar angle θ in degrees.

20 < θ < 30				30 < θ < 40			
p_T	$\langle p_T \rangle$	$\langle \theta \rangle$	$d^2\sigma/dpd\Omega$	$\langle p_T \rangle$	$\langle \theta \rangle$	$d^2\sigma/dpd\Omega$	
0.10–0.13	0.114	24.6	291.72 ± 39.90 ± 22.44	0.116	35.4	242.70 ± 35.82 ± 18.74	
0.13–0.16	0.146	24.7	320.73 ± 38.41 ± 19.54	0.145	34.0	239.09 ± 32.01 ± 14.40	
0.16–0.20	0.179	24.8	387.54 ± 35.06 ± 19.47	0.179	35.2	242.33 ± 28.06 ± 12.50	
0.20–0.24	0.219	24.7	366.48 ± 33.55 ± 15.65	0.217	34.9	257.32 ± 28.35 ± 11.06	
0.24–0.30	0.269	24.9	350.51 ± 26.43 ± 12.02	0.268	34.8	247.73 ± 22.34 ± 8.61	
0.30–0.36	0.329	24.6	276.63 ± 23.37 ± 8.23	0.330	35.0	171.51 ± 18.51 ± 5.15	
0.36–0.42	0.388	24.7	228.34 ± 21.05 ± 7.03	0.387	34.4	132.46 ± 15.88 ± 4.10	
0.42–0.50	0.459	24.7	146.77 ± 14.81 ± 5.52	0.461	34.5	110.53 ± 12.70 ± 4.10	
0.50–0.60	0.545	24.7	87.85 ± 10.18 ± 4.55	0.536	34.5	59.19 ± 8.31 ± 3.01	
0.60–0.72	0.655	24.6	44.57 ± 6.26 ± 3.28	0.650	34.5	52.80 ± 6.83 ± 3.84	
0.72–0.90				0.778	35.6	19.16 ± 3.21 ± 2.04	
40 < θ < 50				50 < θ < 60			
p_T	$\langle p_T \rangle$	$\langle \theta \rangle$	$d^2\sigma/dpd\Omega$	$\langle p_T \rangle$	$\langle \theta \rangle$	$d^2\sigma/dpd\Omega$	
0.10–0.13	0.115	44.4	190.29 ± 32.83 ± 14.95	0.146	55.5	139.53 ± 24.89 ± 8.80	
0.13–0.16	0.143	44.5	201.31 ± 30.50 ± 12.32	0.179	54.0	181.36 ± 23.51 ± 9.32	
0.16–0.20	0.181	45.3	230.44 ± 26.94 ± 11.87	0.218	54.3	136.81 ± 20.36 ± 5.98	
0.20–0.24	0.220	45.4	186.79 ± 23.70 ± 8.22	0.266	54.8	147.15 ± 17.45 ± 5.29	
0.24–0.30	0.268	44.7	156.78 ± 17.98 ± 5.54	0.328	54.4	109.51 ± 14.99 ± 3.49	
0.30–0.36	0.329	44.5	134.79 ± 16.51 ± 4.12	0.396	54.3	79.25 ± 12.55 ± 2.73	
0.36–0.42	0.386	45.1	94.87 ± 13.40 ± 3.08	0.463	53.9	39.62 ± 7.63 ± 1.67	
0.42–0.50	0.460	45.3	102.95 ± 12.31 ± 4.07	0.547	54.8	22.54 ± 4.92 ± 1.35	
0.50–0.60	0.542	44.5	65.17 ± 8.42 ± 3.61	0.657	54.7	20.43 ± 4.47 ± 1.64	
0.60–0.72	0.650	44.4	40.18 ± 5.93 ± 3.15	0.800	53.3	8.90 ± 2.16 ± 1.05	
0.72–0.90	0.813	45.2	15.01 ± 3.00 ± 1.64	1.027	55.6	1.95 ± 0.69 ± 0.35	
60 < θ < 75				75 < θ < 90			
p_T	$\langle p_T \rangle$	$\langle \theta \rangle$	$d^2\sigma/dpd\Omega$	$\langle p_T \rangle$	$\langle \theta \rangle$	$d^2\sigma/dpd\Omega$	
0.13–0.16	0.146	67.7	111.32 ± 18.81 ± 6.77	0.147	83.0	152.61 ± 33.20 ± 26.70	
0.16–0.20	0.178	67.4	148.05 ± 17.68 ± 7.05	0.179	82.8	128.32 ± 16.47 ± 5.96	
0.20–0.24	0.223	67.5	146.72 ± 17.52 ± 5.96	0.218	82.4	103.73 ± 14.32 ± 4.02	
0.24–0.30	0.268	67.1	102.39 ± 11.99 ± 3.70	0.270	82.9	68.56 ± 9.98 ± 2.57	
0.30–0.36	0.332	67.4	69.36 ± 9.75 ± 2.24	0.329	82.2	36.96 ± 7.43 ± 1.70	
0.36–0.42	0.386	66.1	61.57 ± 9.33 ± 2.47	0.390	81.0	36.67 ± 7.20 ± 1.79	
0.42–0.50	0.457	66.7	35.91 ± 5.94 ± 1.73	0.459	83.3	26.16 ± 5.35 ± 1.68	
0.50–0.60	0.543	67.5	28.63 ± 4.71 ± 1.88	0.538	80.9	14.50 ± 3.42 ± 1.22	
0.60–0.72	0.647	66.7	17.60 ± 3.27 ± 1.59	0.634	81.0	5.15 ± 1.72 ± 0.61	
0.72–0.90	0.808	67.9	3.15 ± 1.05 ± 0.41	0.851	85.8	1.90 ± 0.85 ± 0.30	
0.90–1.25	1.023	66.6	0.74 ± 0.37 ± 0.14	1.016	79.3	0.63 ± 0.37 ± 0.15	
90 < θ < 105				105 < θ < 125			
p_T	$\langle p_T \rangle$	$\langle \theta \rangle$	$d^2\sigma/dpd\Omega$	$\langle p_T \rangle$	$\langle \theta \rangle$	$d^2\sigma/dpd\Omega$	
0.13–0.16	0.148	96.2	130.21 ± 33.97 ± 12.56	0.143	115.7	79.61 ± 13.01 ± 4.67	
0.16–0.20	0.179	97.9	121.29 ± 15.64 ± 5.92	0.178	114.9	77.89 ± 11.00 ± 3.10	
0.20–0.24	0.220	97.3	60.07 ± 11.31 ± 2.37	0.216	114.1	40.23 ± 7.90 ± 1.68	
0.24–0.30	0.269	97.2	55.09 ± 8.96 ± 2.17	0.270	112.8	21.73 ± 4.87 ± 1.11	
0.30–0.36	0.330	97.7	34.12 ± 6.99 ± 1.71	0.325	111.2	20.47 ± 4.71 ± 1.47	
0.36–0.42	0.387	97.0	37.25 ± 7.20 ± 2.46	0.385	114.9	7.80 ± 2.76 ± 0.75	
0.42–0.50	0.456	95.9	14.71 ± 3.93 ± 1.30	0.453	112.1	8.85 ± 2.55 ± 1.10	
0.50–0.60	0.553	96.9	5.62 ± 1.99 ± 0.68	0.575	115.5	1.21 ± 0.86 ± 0.19	
0.60–0.72	0.659	93.8	1.27 ± 0.90 ± 0.20				
0.72–0.90	0.768	93.2	1.55 ± 0.78 ± 0.34				

Table A.34: Double-differential inclusive cross-section $d^2\sigma/dpd\Omega$ [mb/(GeV/c sr)] of the production of protons in $\pi^- + \text{Cu} \rightarrow p + X$ interactions with $-12.0 \text{ GeV}/c$ beam momentum; the first error is statistical, the second systematic; p_T in GeV/c , polar angle θ in degrees.

p_T	20 < θ < 30				30 < θ < 40			
	$\langle p_T \rangle$	$\langle \theta \rangle$	$d^2\sigma/dpd\Omega$		$\langle p_T \rangle$	$\langle \theta \rangle$	$d^2\sigma/dpd\Omega$	
0.20–0.24	0.220	25.0	347.91	\pm	10.51	\pm	18.84	
0.24–0.30	0.270	25.2	322.20	\pm	8.07	\pm	15.63	0.271
0.30–0.36	0.329	25.3	263.39	\pm	7.36	\pm	12.14	0.329
0.36–0.42	0.389	25.3	238.35	\pm	7.12	\pm	10.60	0.389
0.42–0.50	0.459	25.2	184.34	\pm	5.39	\pm	8.44	0.458
0.50–0.60	0.548	25.2	136.24	\pm	4.04	\pm	6.42	0.548
0.60–0.72	0.655	25.0	98.10	\pm	3.07	\pm	4.94	0.654
0.72–0.90								0.799
								35.0
								56.41
								\pm 2.04
								\pm 4.55
$40 < \theta < 50$								
p_T	$\langle p_T \rangle$	$\langle \theta \rangle$	$d^2\sigma/dpd\Omega$		$\langle p_T \rangle$	$\langle \theta \rangle$	$d^2\sigma/dpd\Omega$	
0.30–0.36	0.329	45.1	344.72	\pm	7.96	\pm	11.08	
0.36–0.42	0.388	45.1	283.57	\pm	7.28	\pm	8.30	0.389
0.42–0.50	0.458	45.1	230.16	\pm	5.93	\pm	7.68	0.458
0.50–0.60	0.546	45.1	159.98	\pm	4.57	\pm	7.53	0.546
0.60–0.72	0.654	45.1	103.37	\pm	3.49	\pm	6.46	0.654
0.72–0.90	0.799	44.9	55.43	\pm	2.10	\pm	4.69	0.797
0.90–1.25	1.038	45.0	17.88	\pm	0.83	\pm	2.21	1.033
								54.9
								15.30
								\pm 0.80
								\pm 2.04
$60 < \theta < 75$								
p_T	$\langle p_T \rangle$	$\langle \theta \rangle$	$d^2\sigma/dpd\Omega$		$\langle p_T \rangle$	$\langle \theta \rangle$	$d^2\sigma/dpd\Omega$	
0.50–0.60	0.549	67.5	159.72	\pm	3.38	\pm	6.32	
0.60–0.72	0.659	67.5	98.40	\pm	2.62	\pm	5.88	0.658
0.72–0.90	0.803	67.1	45.29	\pm	1.57	\pm	4.50	0.801
0.90–1.25	1.042	67.2	12.71	\pm	0.62	\pm	2.08	1.034
								81.8
								7.05
								\pm 0.47
								\pm 1.27
$90 < \theta < 105$								
p_T	$\langle p_T \rangle$	$\langle \theta \rangle$	$d^2\sigma/dpd\Omega$		$\langle p_T \rangle$	$\langle \theta \rangle$	$d^2\sigma/dpd\Omega$	
0.42–0.50							0.460	113.5
0.50–0.60							0.547	112.9
0.60–0.72	0.655	97.1	47.69	\pm	1.69	\pm	4.23	0.656
0.72–0.90	0.800	96.7	17.27	\pm	0.96	\pm	2.20	0.796
0.90–1.25	1.030	96.8	3.02	\pm	0.31	\pm	0.59	112.4
								5.60
								\pm 0.49
								\pm 1.23
$105 < \theta < 125$								
p_T	$\langle p_T \rangle$	$\langle \theta \rangle$	$d^2\sigma/dpd\Omega$		$\langle p_T \rangle$	$\langle \theta \rangle$	$d^2\sigma/dpd\Omega$	
0.42–0.50							0.460	86.85
0.50–0.60							0.547	43.20
0.60–0.72							0.656	112.8
0.72–0.90							0.796	18.59
0.90–1.25								5.60
								\pm 0.99
								\pm 2.65
								\pm 4.02
								\pm 1.53
								\pm 1.22
								\pm 3.20
								\pm 1.27

Table A.36: Double-differential inclusive cross-section $d^2\sigma/dpd\Omega$ [mb/(GeV/c sr)] of the production of π^- 's in $\pi^- + \text{Cu} \rightarrow \pi^- + \text{X}$ interactions with -12.0 GeV/c beam momentum; the first error is statistical, the second systematic; p_T in GeV/c, polar angle θ in degrees.

p_T	20 < θ < 30				30 < θ < 40			
	$\langle p_T \rangle$	$\langle \theta \rangle$	$d^2\sigma/dpd\Omega$		$\langle p_T \rangle$	$\langle \theta \rangle$	$d^2\sigma/dpd\Omega$	
			$d^2\sigma/dpd\Omega$	$d^2\sigma/dpd\Omega$			$d^2\sigma/dpd\Omega$	$d^2\sigma/dpd\Omega$
0.10–0.13	0.116	24.7	336.97 ± 13.30	± 25.79	0.115	34.7	277.43 ± 11.66	± 20.63
0.13–0.16	0.145	24.6	400.32 ± 13.15	± 23.77	0.146	34.8	287.28 ± 10.95	± 16.81
0.16–0.20	0.180	24.6	478.17 ± 12.09	± 23.83	0.180	34.8	312.10 ± 9.67	± 15.31
0.20–0.24	0.220	24.8	456.53 ± 11.63	± 18.98	0.220	34.7	327.66 ± 9.80	± 13.39
0.24–0.30	0.269	24.7	408.90 ± 8.85	± 13.54	0.269	34.7	309.01 ± 7.71	± 10.27
0.30–0.36	0.329	24.8	365.95 ± 8.33	± 10.32	0.330	34.6	246.75 ± 6.83	± 6.95
0.36–0.42	0.389	24.7	268.01 ± 7.14	± 7.74	0.389	34.7	209.84 ± 6.29	± 5.98
0.42–0.50	0.457	24.6	215.86 ± 5.53	± 7.78	0.458	34.7	154.13 ± 4.61	± 5.39
0.50–0.60	0.547	24.6	144.51 ± 4.04	± 7.29	0.546	34.7	98.77 ± 3.34	± 4.81
0.60–0.72	0.655	24.7	85.74 ± 2.81	± 6.10	0.654	34.8	58.99 ± 2.32	± 4.05
0.72–0.90					0.795	34.6	26.58 ± 1.24	± 2.60
p_T	40 < θ < 50				50 < θ < 60			
	$\langle p_T \rangle$	$\langle \theta \rangle$	$d^2\sigma/dpd\Omega$		$\langle p_T \rangle$	$\langle \theta \rangle$	$d^2\sigma/dpd\Omega$	
			$d^2\sigma/dpd\Omega$	$d^2\sigma/dpd\Omega$			$d^2\sigma/dpd\Omega$	$d^2\sigma/dpd\Omega$
0.10–0.13	0.115	44.9	219.10 ± 10.54	± 16.70	0.145	54.7	199.84 ± 9.19	± 12.20
0.13–0.16	0.145	44.7	239.20 ± 10.06	± 14.21	0.180	54.8	195.46 ± 7.65	± 9.55
0.16–0.20	0.180	44.9	253.44 ± 8.74	± 12.48	0.219	55.0	202.45 ± 7.71	± 8.14
0.20–0.24	0.220	44.7	249.84 ± 8.57	± 10.32	0.270	54.5	165.98 ± 5.73	± 5.45
0.24–0.30	0.269	44.7	225.02 ± 6.61	± 7.47	0.329	54.7	132.01 ± 5.06	± 3.75
0.30–0.36	0.329	44.7	183.41 ± 5.98	± 5.18	0.390	54.7	115.90 ± 4.70	± 3.56
0.36–0.42	0.388	44.5	140.33 ± 5.07	± 4.14	0.458	54.9	84.40 ± 3.43	± 3.28
0.42–0.50	0.458	44.9	110.29 ± 3.96	± 4.07	0.543	54.9	45.33 ± 2.21	± 2.45
0.50–0.60	0.547	44.7	68.62 ± 2.70	± 3.56	0.646	54.8	28.45 ± 1.59	± 2.15
0.60–0.72	0.654	44.8	45.95 ± 2.04	± 3.36	0.797	54.5	11.95 ± 0.83	± 1.28
0.72–0.90	0.800	44.9	18.67 ± 1.04	± 1.94	1.037	54.8	2.57 ± 0.24	± 0.45
p_T	60 < θ < 75				75 < θ < 90			
	$\langle p_T \rangle$	$\langle \theta \rangle$	$d^2\sigma/dpd\Omega$		$\langle p_T \rangle$	$\langle \theta \rangle$	$d^2\sigma/dpd\Omega$	
			$d^2\sigma/dpd\Omega$	$d^2\sigma/dpd\Omega$			$d^2\sigma/dpd\Omega$	$d^2\sigma/dpd\Omega$
0.13–0.16	0.145	67.5	169.95 ± 7.16	± 10.00	0.147	81.8	137.41 ± 8.61	± 15.89
0.16–0.20	0.179	67.3	158.80 ± 5.61	± 7.28	0.179	82.0	127.28 ± 5.12	± 5.61
0.20–0.24	0.219	67.1	139.85 ± 5.21	± 5.24	0.219	82.0	116.11 ± 4.78	± 4.20
0.24–0.30	0.268	67.1	127.24 ± 4.12	± 4.23	0.269	82.0	89.46 ± 3.54	± 3.41
0.30–0.36	0.327	67.1	95.86 ± 3.57	± 2.90	0.326	81.7	65.30 ± 2.98	± 2.39
0.36–0.42	0.387	67.1	77.10 ± 3.16	± 2.60	0.387	81.4	40.08 ± 2.32	± 1.76
0.42–0.50	0.456	66.5	49.66 ± 2.18	± 2.21	0.457	81.4	31.18 ± 1.74	± 1.80
0.50–0.60	0.542	67.0	33.53 ± 1.60	± 2.08	0.541	81.1	18.10 ± 1.15	± 1.44
0.60–0.72	0.649	66.8	17.58 ± 1.02	± 1.50	0.648	81.9	7.58 ± 0.67	± 0.82
0.72–0.90	0.785	66.1	6.45 ± 0.47	± 0.80	0.789	81.5	3.16 ± 0.34	± 0.47
0.90–1.25	1.005	67.1	1.23 ± 0.14	± 0.23	1.019	80.3	0.60 ± 0.10	± 0.14
p_T	90 < θ < 105				105 < θ < 125			
	$\langle p_T \rangle$	$\langle \theta \rangle$	$d^2\sigma/dpd\Omega$		$\langle p_T \rangle$	$\langle \theta \rangle$	$d^2\sigma/dpd\Omega$	
			$d^2\sigma/dpd\Omega$	$d^2\sigma/dpd\Omega$			$d^2\sigma/dpd\Omega$	$d^2\sigma/dpd\Omega$
0.13–0.16	0.144	99.0	174.16 ± 37.95	± 21.73	0.145	114.2	92.78 ± 4.46	± 5.14
0.16–0.20	0.179	97.4	106.65 ± 4.60	± 4.51	0.179	113.8	76.83 ± 3.35	± 2.76
0.20–0.24	0.220	97.1	90.48 ± 4.31	± 3.14	0.217	113.5	52.47 ± 2.80	± 1.83
0.24–0.30	0.266	96.7	57.89 ± 2.81	± 2.04	0.265	113.4	33.18 ± 1.83	± 1.51
0.30–0.36	0.326	97.2	38.41 ± 2.29	± 1.75	0.326	113.0	20.55 ± 1.45	± 1.38
0.36–0.42	0.387	96.8	29.19 ± 1.97	± 1.78	0.387	113.0	12.85 ± 1.11	± 1.16
0.42–0.50	0.454	96.8	18.65 ± 1.34	± 1.55	0.452	112.5	7.35 ± 0.73	± 0.87
0.50–0.60	0.539	96.6	8.96 ± 0.81	± 1.02	0.545	112.7	2.50 ± 0.36	± 0.39
0.60–0.72	0.643	96.5	3.56 ± 0.46	± 0.55	0.645	111.3	0.55 ± 0.16	± 0.11
0.72–0.90	0.783	94.9	0.77 ± 0.17	± 0.16	0.829	111.5	0.23 ± 0.09	± 0.06
0.90–1.25	1.017	95.0	0.12 ± 0.04	± 0.04				

Table A.37: Double-differential inclusive cross-section $d^2\sigma/dpd\Omega$ [mb/(GeV/c sr)] of the production of protons in $p + \text{Cu} \rightarrow p + X$ interactions with $+15.0$ GeV/c beam momentum; the first error is statistical, the second systematic; p_T in GeV/c, polar angle θ in degrees.

p_T	20 < θ < 30						30 < θ < 40							
	$\langle p_T \rangle$	$\langle \theta \rangle$	$d^2\sigma/dpd\Omega$				$\langle p_T \rangle$	$\langle \theta \rangle$	$d^2\sigma/dpd\Omega$					
			515.44	\pm	14.55	\pm	49.81		505.59	\pm	11.82	\pm	37.86	
0.20–0.24	0.219	25.1	515.44	\pm	14.55	\pm	49.81	0.269	34.9	505.59	\pm	11.82	\pm	37.86
0.24–0.30	0.268	25.1	479.44	\pm	11.19	\pm	39.68	0.328	34.8	456.14	\pm	10.68	\pm	26.93
0.30–0.36	0.327	25.1	401.51	\pm	10.35	\pm	27.67	0.387	35.0	368.96	\pm	9.81	\pm	17.72
0.36–0.42	0.386	25.2	359.38	\pm	9.91	\pm	20.55	0.454	35.0	313.72	\pm	8.07	\pm	13.24
0.42–0.50	0.454	25.3	285.30	\pm	7.51	\pm	13.32	0.541	35.0	217.80	\pm	6.05	\pm	10.67
0.50–0.60	0.542	25.2	218.05	\pm	5.81	\pm	9.34	0.645	35.1	166.26	\pm	4.89	\pm	11.44
0.60–0.72	0.648	25.1	156.33	\pm	4.40	\pm	9.44	0.788	35.0	92.76	\pm	2.94	\pm	9.98
<hr/>														
p_T	40 < θ < 50						50 < θ < 60							
	$\langle p_T \rangle$	$\langle \theta \rangle$	$d^2\sigma/dpd\Omega$				$\langle p_T \rangle$	$\langle \theta \rangle$	$d^2\sigma/dpd\Omega$					
0.30–0.36	0.328	45.1	462.44	\pm	10.49	\pm	20.38	0.387	55.1	423.52	\pm	9.66	\pm	14.19
0.36–0.42	0.387	45.2	396.25	\pm	9.74	\pm	13.20	0.456	55.1	347.45	\pm	7.99	\pm	11.02
0.42–0.50	0.456	45.0	338.67	\pm	8.09	\pm	10.54	0.543	54.9	235.73	\pm	6.07	\pm	12.31
0.50–0.60	0.544	45.0	238.40	\pm	6.31	\pm	11.82	0.651	54.9	143.18	\pm	4.61	\pm	12.40
0.60–0.72	0.652	44.9	165.20	\pm	4.98	\pm	12.84	0.795	55.0	82.02	\pm	2.95	\pm	10.40
0.72–0.90	0.796	44.9	89.79	\pm	3.07	\pm	10.53	1.026	55.0	24.51	\pm	1.14	\pm	4.88
0.90–1.25	1.024	44.9	29.27	\pm	1.24	\pm	5.61							
<hr/>														
p_T	60 < θ < 75						75 < θ < 90							
	$\langle p_T \rangle$	$\langle \theta \rangle$	$d^2\sigma/dpd\Omega$				$\langle p_T \rangle$	$\langle \theta \rangle$	$d^2\sigma/dpd\Omega$					
0.50–0.60	0.546	67.6	229.15	\pm	4.62	\pm	13.42	0.653	81.7	98.39	\pm	2.77	\pm	13.13
0.60–0.72	0.654	67.4	140.87	\pm	3.54	\pm	14.14	0.794	81.7	41.62	\pm	1.68	\pm	8.19
0.72–0.90	0.795	66.8	64.54	\pm	2.10	\pm	10.50	1.031	81.4	9.13	\pm	0.61	\pm	2.82
0.90–1.25	1.029	66.9	17.44	\pm	0.81	\pm	4.73							
<hr/>														
p_T	90 < θ < 105						105 < θ < 125							
	$\langle p_T \rangle$	$\langle \theta \rangle$	$d^2\sigma/dpd\Omega$				$\langle p_T \rangle$	$\langle \theta \rangle$	$d^2\sigma/dpd\Omega$					
0.42–0.50							0.459	113.8	108.92	\pm	2.98	\pm	10.44	
0.50–0.60							0.544	112.9	59.74	\pm	2.02	\pm	10.43	
0.60–0.72	0.652	97.2	60.37	\pm	2.16	\pm	10.27	0.648	112.9	24.15	\pm	1.30	\pm	6.62
0.72–0.90	0.795	96.9	21.88	\pm	1.21	\pm	5.00	0.788	112.6	6.96	\pm	0.61	\pm	2.89
0.90–1.25	1.026	96.8	3.86	\pm	0.41	\pm	1.30	1.013	112.2	1.22	\pm	0.19	\pm	0.81

Table A.38: Double-differential inclusive cross-section $d^2\sigma/dpd\Omega$ [mb/(GeV/c sr)] of the production of π^+ 's in $p + \text{Cu} \rightarrow \pi^+ + \text{X}$ interactions with +15.0 GeV/c beam momentum; the first error is statistical, the second systematic; p_T in GeV/c, polar angle θ in degrees.

p_T	20 < θ < 30				30 < θ < 40			
	$\langle p_T \rangle$	$\langle \theta \rangle$	$d^2\sigma/dpd\Omega$		$\langle p_T \rangle$	$\langle \theta \rangle$	$d^2\sigma/dpd\Omega$	
			$d^2\sigma/dpd\Omega$	$d^2\sigma/dpd\Omega$			$d^2\sigma/dpd\Omega$	$d^2\sigma/dpd\Omega$
0.10–0.13	0.116	24.8	331.64 ± 15.68	± 38.06	0.115	34.8	263.62 ± 13.12	± 28.46
0.13–0.16	0.145	24.8	386.36 ± 15.10	± 36.09	0.145	34.7	316.28 ± 13.38	± 28.78
0.16–0.20	0.180	24.9	449.85 ± 13.55	± 35.69	0.180	34.7	315.94 ± 11.23	± 24.37
0.20–0.24	0.219	24.9	457.24 ± 13.61	± 30.34	0.219	34.6	350.23 ± 11.81	± 22.24
0.24–0.30	0.268	24.9	416.13 ± 10.29	± 20.72	0.268	34.7	312.53 ± 9.04	± 14.91
0.30–0.36	0.327	24.8	376.04 ± 9.71	± 13.14	0.327	34.7	261.20 ± 8.25	± 8.86
0.36–0.42	0.386	24.7	300.03 ± 8.58	± 8.94	0.386	34.7	215.37 ± 7.34	± 6.51
0.42–0.50	0.453	24.8	234.41 ± 6.58	± 10.06	0.454	34.7	160.99 ± 5.55	± 6.81
0.50–0.60	0.543	24.8	154.73 ± 4.62	± 10.99	0.541	34.8	109.71 ± 3.87	± 7.73
0.60–0.72	0.647	24.8	98.76 ± 3.19	± 11.11	0.647	34.7	65.41 ± 2.64	± 7.24
0.72–0.90					0.789	34.5	33.04 ± 1.43	± 5.67
p_T	40 < θ < 50				50 < θ < 60			
	$\langle p_T \rangle$	$\langle \theta \rangle$	$d^2\sigma/dpd\Omega$		$\langle p_T \rangle$	$\langle \theta \rangle$	$d^2\sigma/dpd\Omega$	
			$d^2\sigma/dpd\Omega$	$d^2\sigma/dpd\Omega$			$d^2\sigma/dpd\Omega$	$d^2\sigma/dpd\Omega$
0.10–0.13	0.116	44.9	230.55 ± 13.07	± 25.70	0.145	55.1	196.26 ± 10.39	± 17.83
0.13–0.16	0.145	44.8	243.66 ± 11.52	± 22.30	0.179	54.9	219.11 ± 9.25	± 16.21
0.16–0.20	0.180	44.9	269.62 ± 10.41	± 20.76	0.219	54.6	201.03 ± 8.68	± 11.99
0.20–0.24	0.220	44.8	268.10 ± 10.30	± 16.98	0.268	54.8	183.19 ± 7.01	± 8.08
0.24–0.30	0.269	44.7	243.35 ± 8.01	± 11.42	0.328	54.6	143.44 ± 6.14	± 4.55
0.30–0.36	0.327	44.7	184.18 ± 6.87	± 6.12	0.387	54.5	110.80 ± 5.30	± 3.97
0.36–0.42	0.387	44.8	156.38 ± 6.26	± 4.97	0.455	54.5	81.80 ± 3.89	± 4.43
0.42–0.50	0.456	44.9	106.05 ± 4.47	± 4.91	0.545	54.7	57.04 ± 2.91	± 4.83
0.50–0.60	0.544	44.7	80.41 ± 3.43	± 5.99	0.650	54.5	29.62 ± 1.78	± 3.79
0.60–0.72	0.650	44.5	45.07 ± 2.25	± 5.14	0.791	54.6	14.05 ± 0.96	± 2.61
0.72–0.90	0.791	44.5	21.92 ± 1.22	± 3.77	1.016	54.7	2.68 ± 0.23	± 0.82
p_T	60 < θ < 75				75 < θ < 90			
	$\langle p_T \rangle$	$\langle \theta \rangle$	$d^2\sigma/dpd\Omega$		$\langle p_T \rangle$	$\langle \theta \rangle$	$d^2\sigma/dpd\Omega$	
			$d^2\sigma/dpd\Omega$	$d^2\sigma/dpd\Omega$			$d^2\sigma/dpd\Omega$	$d^2\sigma/dpd\Omega$
0.13–0.16	0.145	67.3	171.26 ± 8.47	± 16.06	0.147	81.8	142.86 ± 10.46	± 14.94
0.16–0.20	0.179	67.5	171.73 ± 6.50	± 12.87	0.180	81.8	126.57 ± 5.71	± 8.51
0.20–0.24	0.220	67.2	172.21 ± 6.63	± 9.96	0.220	82.1	119.23 ± 5.39	± 5.89
0.24–0.30	0.269	67.0	133.35 ± 4.86	± 5.46	0.267	81.8	88.01 ± 3.96	± 3.32
0.30–0.36	0.329	66.9	90.81 ± 4.00	± 2.87	0.327	81.7	64.88 ± 3.52	± 3.00
0.36–0.42	0.392	66.7	80.12 ± 3.80	± 3.63	0.390	81.6	42.64 ± 2.76	± 2.66
0.42–0.50	0.457	66.4	53.52 ± 2.63	± 3.68	0.456	81.6	29.05 ± 1.99	± 2.75
0.50–0.60	0.548	66.7	35.79 ± 1.87	± 3.84	0.553	81.6	16.61 ± 1.27	± 2.30
0.60–0.72	0.655	66.7	20.55 ± 1.29	± 3.23	0.650	81.5	9.53 ± 0.92	± 1.85
0.72–0.90	0.794	66.4	5.44 ± 0.46	± 1.25	0.792	80.7	2.80 ± 0.34	± 0.77
0.90–1.25	1.028	65.4	1.11 ± 0.12	± 0.39	1.009	81.1	0.47 ± 0.08	± 0.20
p_T	90 < θ < 105				105 < θ < 125			
	$\langle p_T \rangle$	$\langle \theta \rangle$	$d^2\sigma/dpd\Omega$		$\langle p_T \rangle$	$\langle \theta \rangle$	$d^2\sigma/dpd\Omega$	
			$d^2\sigma/dpd\Omega$	$d^2\sigma/dpd\Omega$			$d^2\sigma/dpd\Omega$	$d^2\sigma/dpd\Omega$
0.13–0.16	0.147	98.0	132.66 ± 9.73	± 15.63	0.146	115.2	102.35 ± 5.41	± 6.70
0.16–0.20	0.179	97.1	115.80 ± 5.56	± 6.78	0.179	114.2	77.79 ± 3.69	± 3.77
0.20–0.24	0.219	97.3	93.19 ± 4.71	± 3.75	0.219	113.5	61.80 ± 3.49	± 2.46
0.24–0.30	0.267	97.1	64.74 ± 3.43	± 2.59	0.268	113.8	36.60 ± 2.23	± 2.33
0.30–0.36	0.326	96.7	35.85 ± 2.56	± 2.37	0.328	113.4	18.84 ± 1.57	± 1.99
0.36–0.42	0.389	96.3	29.97 ± 2.33	± 3.02	0.390	112.6	12.02 ± 1.25	± 1.80
0.42–0.50	0.457	97.3	14.63 ± 1.40	± 2.10	0.457	113.3	7.02 ± 0.80	± 1.41
0.50–0.60	0.542	96.0	8.78 ± 0.95	± 1.77	0.537	112.2	4.22 ± 0.61	± 1.14
0.60–0.72	0.650	97.5	3.18 ± 0.48	± 0.87	0.660	111.1	1.13 ± 0.24	± 0.41
0.72–0.90	0.794	97.2	1.48 ± 0.26	± 0.55	0.819	109.5	0.17 ± 0.07	± 0.08
0.90–1.25	1.007	96.5	0.17 ± 0.05	± 0.09	1.024	115.8	0.06 ± 0.03	± 0.04

Table A.40: Double-differential inclusive cross-section $d^2\sigma/dpd\Omega$ [mb/(GeV/c sr)] of the production of protons in $\pi^+ + \text{Cu} \rightarrow p + X$ interactions with +15.0 GeV/c beam momentum; the first error is statistical, the second systematic; p_T in GeV/c, polar angle θ in degrees.

p_T	20 < θ < 30			30 < θ < 40		
	$\langle p_T \rangle$	$\langle \theta \rangle$	$d^2\sigma/dpd\Omega$	$\langle p_T \rangle$	$\langle \theta \rangle$	$d^2\sigma/dpd\Omega$
0.20–0.24	0.221	25.7	434.31 \pm 117.18 \pm 43.62	0.267	34.8	399.52 \pm 87.13 \pm 31.89
0.24–0.30	0.275	25.6	172.89 \pm 58.21 \pm 15.15	0.331	35.3	410.74 \pm 87.94 \pm 26.88
0.30–0.36	0.329	25.3	468.50 \pm 96.58 \pm 35.53	0.387	35.5	246.54 \pm 70.16 \pm 14.11
0.36–0.42	0.388	24.1	250.81 \pm 69.23 \pm 16.34	0.463	34.9	183.84 \pm 53.89 \pm 9.77
0.42–0.50	0.455	26.2	204.26 \pm 56.01 \pm 11.49	0.542	36.0	171.57 \pm 47.54 \pm 10.00
0.50–0.60	0.541	25.7	149.88 \pm 41.63 \pm 7.95	0.648	33.8	57.64 \pm 24.90 \pm 4.35
0.60–0.72	0.639	24.2	68.93 \pm 22.45 \pm 4.71	0.761	35.0	47.23 \pm 18.24 \pm 5.31
0.72–0.90						
p_T	40 < θ < 50			50 < θ < 60		
	$\langle p_T \rangle$	$\langle \theta \rangle$	$d^2\sigma/dpd\Omega$	$\langle p_T \rangle$	$\langle \theta \rangle$	$d^2\sigma/dpd\Omega$
0.30–0.36	0.318	45.7	479.44 \pm 92.69 \pm 25.87	0.385	54.9	367.71 \pm 77.28 \pm 16.59
0.36–0.42	0.391	43.9	290.70 \pm 71.30 \pm 12.84	0.455	54.9	264.65 \pm 60.62 \pm 11.25
0.42–0.50	0.460	46.5	178.64 \pm 52.00 \pm 7.69	0.537	55.5	213.14 \pm 50.73 \pm 12.82
0.50–0.60	0.549	44.1	149.60 \pm 43.26 \pm 8.82	0.670	55.1	58.89 \pm 25.72 \pm 5.44
0.60–0.72	0.653	44.7	135.00 \pm 38.75 \pm 11.34	0.797	55.6	93.71 \pm 27.48 \pm 12.24
0.72–0.90	0.776	45.7	40.84 \pm 18.02 \pm 4.94	1.040	54.9	14.65 \pm 7.73 \pm 2.95
0.90–1.25	1.055	43.8	20.61 \pm 8.97 \pm 4.02			
p_T	60 < θ < 75			75 < θ < 90		
	$\langle p_T \rangle$	$\langle \theta \rangle$	$d^2\sigma/dpd\Omega$	$\langle p_T \rangle$	$\langle \theta \rangle$	$d^2\sigma/dpd\Omega$
0.50–0.60	0.540	67.7	195.47 \pm 37.40 \pm 12.67	0.652	82.0	76.93 \pm 21.45 \pm 10.47
0.60–0.72	0.663	64.8	99.29 \pm 25.71 \pm 10.34	0.793	82.7	49.67 \pm 15.95 \pm 9.81
0.72–0.90	0.794	65.9	17.55 \pm 9.32 \pm 2.89	1.047	82.9	10.14 \pm 5.49 \pm 3.13
0.90–1.25	1.022	65.6	8.43 \pm 4.86 \pm 2.30			
p_T	90 < θ < 105			105 < θ < 125		
	$\langle p_T \rangle$	$\langle \theta \rangle$	$d^2\sigma/dpd\Omega$	$\langle p_T \rangle$	$\langle \theta \rangle$	$d^2\sigma/dpd\Omega$
0.42–0.50				0.460	113.1	60.82 \pm 19.55 \pm 6.03
0.50–0.60				0.547	113.2	69.67 \pm 18.99 \pm 12.27
0.60–0.72	0.650	96.1	33.11 \pm 14.07 \pm 5.69	0.677	113.8	19.56 \pm 10.19 \pm 5.38
0.72–0.90	0.793	91.7	10.11 \pm 7.09 \pm 2.30	0.754	118.4	8.74 \pm 5.75 \pm 3.61

Table A.41: Double-differential inclusive cross-section $d^2\sigma/dpd\Omega$ [mb/(GeV/c sr)] of the production of π^+ 's in $\pi^+ + \text{Cu} \rightarrow \pi^+ + \text{X}$ interactions with +15.0 GeV/c beam momentum; the first error is statistical, the second systematic; p_T in GeV/c, polar angle θ in degrees.

p_T	20 < θ < 30				30 < θ < 40			
	$\langle p_T \rangle$	$\langle \theta \rangle$	$d^2\sigma/dpd\Omega$		$\langle p_T \rangle$	$\langle \theta \rangle$	$d^2\sigma/dpd\Omega$	
0.10–0.13	0.114	27.6	440.28	\pm 166.92	50.52	0.123	34.1	185.00 \pm 90.12 \pm 20.46
0.13–0.16	0.150	23.6	324.27	\pm 120.96	31.57	0.148	33.5	367.59 \pm 127.99 \pm 34.88
0.16–0.20	0.175	25.0	353.93	\pm 108.68	29.73	0.181	34.5	579.48 \pm 134.30 \pm 47.40
0.20–0.24	0.226	23.9	333.45	\pm 98.50	23.91	0.218	33.7	288.00 \pm 90.00 \pm 19.92
0.24–0.30	0.271	25.4	394.57	\pm 88.29	22.53	0.269	34.4	490.59 \pm 98.23 \pm 27.09
0.30–0.36	0.326	25.4	316.78	\pm 78.97	14.20	0.331	34.7	369.81 \pm 86.41 \pm 16.28
0.36–0.42	0.387	24.3	464.48	\pm 91.77	19.07	0.390	36.5	204.05 \pm 62.09 \pm 8.48
0.42–0.50	0.450	24.3	206.78	\pm 54.46	10.62	0.456	33.4	160.91 \pm 48.61 \pm 8.22
0.50–0.60	0.545	25.5	189.59	\pm 45.85	14.51	0.539	33.9	78.45 \pm 28.37 \pm 6.00
0.60–0.72	0.635	23.4	92.02	\pm 25.62	10.70	0.661	35.1	27.77 \pm 15.40 \pm 3.20
0.72–0.90						0.764	33.0	25.24 \pm 11.53 \pm 4.41
p_T	40 < θ < 50				50 < θ < 60			
	$\langle p_T \rangle$	$\langle \theta \rangle$	$d^2\sigma/dpd\Omega$		$\langle p_T \rangle$	$\langle \theta \rangle$	$d^2\sigma/dpd\Omega$	
0.10–0.13	0.116	44.9	246.49	\pm 114.58	27.63	0.155	55.5	167.85 \pm 84.37 \pm 15.80
0.13–0.16	0.143	45.2	244.50	\pm 100.80	23.24	0.177	55.5	192.27 \pm 79.30 \pm 15.08
0.16–0.20	0.179	44.8	218.17	\pm 83.84	17.77	0.221	55.9	173.35 \pm 73.10 \pm 11.27
0.20–0.24	0.227	46.2	175.65	\pm 75.10	12.07	0.269	56.0	205.31 \pm 64.76 \pm 10.42
0.24–0.30	0.269	44.5	132.97	\pm 52.40	7.22	0.316	54.9	150.23 \pm 55.41 \pm 6.25
0.30–0.36	0.321	44.1	222.94	\pm 66.74	9.65	0.397	54.9	77.92 \pm 37.88 \pm 3.51
0.36–0.42	0.379	45.2	122.42	\pm 47.71	5.20	0.459	53.5	75.99 \pm 32.78 \pm 4.62
0.42–0.50	0.450	46.6	92.76	\pm 37.10	5.06	0.546	52.5	28.52 \pm 17.30 \pm 2.55
0.50–0.60	0.551	44.8	89.02	\pm 31.65	7.14	0.657	53.8	32.37 \pm 16.40 \pm 4.27
0.60–0.72	0.666	43.8	60.03	\pm 22.61	7.12	0.811	55.5	11.69 \pm 6.99 \pm 2.22
0.72–0.90	0.786	44.8	28.06	\pm 13.04	4.93	1.090	56.7	0.31 \pm 0.22 \pm 0.09
p_T	60 < θ < 75				75 < θ < 90			
	$\langle p_T \rangle$	$\langle \theta \rangle$	$d^2\sigma/dpd\Omega$		$\langle p_T \rangle$	$\langle \theta \rangle$	$d^2\sigma/dpd\Omega$	
0.13–0.16	0.143	67.7	120.32	\pm 59.36	11.66	0.147	84.5	87.31 \pm 60.93 \pm 8.66
0.16–0.20	0.175	65.9	236.81	\pm 66.69	18.78	0.181	81.9	106.23 \pm 47.40 \pm 7.63
0.20–0.24	0.219	67.5	226.55	\pm 65.19	14.34	0.213	80.3	119.51 \pm 48.93 \pm 6.59
0.24–0.30	0.267	65.7	100.80	\pm 36.78	4.81	0.277	85.0	96.80 \pm 36.88 \pm 4.25
0.30–0.36	0.336	65.1	115.68	\pm 38.75	4.68	0.340	80.3	53.26 \pm 27.59 \pm 2.60
0.36–0.42	0.391	66.5	63.14	\pm 29.52	3.22	0.381	84.2	33.83 \pm 20.54 \pm 2.23
0.42–0.50	0.450	63.6	18.03	\pm 13.13	1.33	0.455	78.1	37.43 \pm 19.58 \pm 3.61
0.50–0.60	0.555	65.4	27.08	\pm 14.21	2.99	0.512	83.9	20.83 \pm 12.51 \pm 2.91
0.60–0.72	0.640	64.2	11.64	\pm 8.51	1.86			
0.72–0.90	0.839	64.8	8.17	\pm 5.06	1.89			
0.90–1.25	1.070	64.3	2.85	\pm 1.99	1.02			
p_T	90 < θ < 105				105 < θ < 125			
	$\langle p_T \rangle$	$\langle \theta \rangle$	$d^2\sigma/dpd\Omega$		$\langle p_T \rangle$	$\langle \theta \rangle$	$d^2\sigma/dpd\Omega$	
0.13–0.16	0.154	94.9	78.87	\pm 55.81	7.03	0.141	121.8	53.47 \pm 30.88 \pm 3.72
0.16–0.20	0.190	98.6	220.31	\pm 66.88	13.96	0.172	108.6	45.72 \pm 26.49 \pm 2.39
0.20–0.24	0.220	96.7	88.60	\pm 40.44	4.10	0.214	113.3	89.36 \pm 36.82 \pm 4.01
0.24–0.30	0.271	95.8	51.79	\pm 26.22	2.32	0.263	114.6	11.68 \pm 10.47 \pm 0.78
0.30–0.36	0.336	99.7	39.40	\pm 23.59	2.67	0.399	112.0	17.96 \pm 13.46 \pm 2.68
0.36–0.42						0.458	114.2	5.14 \pm 4.13 \pm 1.03
0.42–0.50	0.451	92.7	18.31	\pm 13.73	2.64			

Table A.42: Double-differential inclusive cross-section $d^2\sigma/dpd\Omega$ [mb/(GeV/c sr)] of the production of π^- 's in $\pi^+ + \text{Cu} \rightarrow \pi^- + \text{X}$ interactions with +15.0 GeV/c beam momentum; the first error is statistical, the second systematic; p_T in GeV/c, polar angle θ in degrees.

p_T	20 < θ < 30				30 < θ < 40			
	$\langle p_T \rangle$	$\langle \theta \rangle$	$d^2\sigma/dpd\Omega$		$\langle p_T \rangle$	$\langle \theta \rangle$	$d^2\sigma/dpd\Omega$	
0.10–0.13	0.107	25.2	271.22	\pm 127.02	31.78	0.121	36.5	214.72 \pm 100.38 \pm 24.97
0.13–0.16	0.147	25.8	319.44	\pm 114.59	31.77	0.147	34.4	346.29 \pm 121.90 \pm 34.20
0.16–0.20	0.187	25.0	287.09	\pm 93.56	24.25	0.188	36.3	394.85 \pm 111.07 \pm 33.09
0.20–0.24	0.223	24.1	188.07	\pm 70.90	12.93	0.218	34.9	264.27 \pm 89.20 \pm 18.25
0.24–0.30	0.266	24.2	413.59	\pm 86.72	21.70	0.269	35.0	263.30 \pm 71.12 \pm 13.97
0.30–0.36	0.331	26.5	304.68	\pm 78.78	12.52	0.333	35.3	334.19 \pm 79.36 \pm 13.94
0.36–0.42	0.389	22.8	245.56	\pm 65.67	10.85	0.399	34.2	173.20 \pm 55.25 \pm 7.65
0.42–0.50	0.451	23.4	90.96	\pm 34.47	5.65	0.465	33.5	151.68 \pm 43.81 \pm 9.25
0.50–0.60	0.558	26.3	113.12	\pm 37.71	10.69	0.541	36.7	69.77 \pm 28.52 \pm 6.40
0.60–0.72	0.664	25.0	46.79	\pm 20.93	6.47	0.637	32.1	24.89 \pm 14.37 \pm 3.35
0.72–0.90						0.784	33.8	19.37 \pm 9.69 \pm 3.84
p_T	40 < θ < 50				50 < θ < 60			
	$\langle p_T \rangle$	$\langle \theta \rangle$	$d^2\sigma/dpd\Omega$		$\langle p_T \rangle$	$\langle \theta \rangle$	$d^2\sigma/dpd\Omega$	
0.10–0.13	0.113	46.5	305.22	\pm 131.15	36.09	0.154	54.5	118.37 \pm 66.99 \pm 11.55
0.13–0.16						0.173	54.8	90.79 \pm 51.75 \pm 7.33
0.16–0.20	0.177	47.5	108.69	\pm 53.88	9.14	0.235	57.9	63.01 \pm 44.56 \pm 4.13
0.20–0.24	0.221	43.8	107.17	\pm 54.01	7.40	0.266	54.1	159.10 \pm 56.31 \pm 7.90
0.24–0.30	0.266	43.8	104.08	\pm 42.74	5.44	0.327	53.2	82.35 \pm 38.53 \pm 3.38
0.30–0.36	0.327	45.3	137.21	\pm 52.00	5.67	0.409	52.6	111.79 \pm 45.65 \pm 5.37
0.36–0.42	0.393	46.5	128.18	\pm 48.50	5.88			
0.42–0.50	0.470	44.2	80.05	\pm 32.68	5.19	0.551	55.7	20.96 \pm 14.82 \pm 2.16
0.50–0.60	0.559	44.3	98.20	\pm 32.74	9.65	0.663	54.9	15.30 \pm 10.83 \pm 2.31
0.60–0.72	0.659	45.3	17.04	\pm 12.05	2.47	0.729	55.4	11.13 \pm 7.87 \pm 2.38
0.72–0.90	0.844	44.5	16.52	\pm 9.54	3.43			
p_T	60 < θ < 75				75 < θ < 90			
	$\langle p_T \rangle$	$\langle \theta \rangle$	$d^2\sigma/dpd\Omega$		$\langle p_T \rangle$	$\langle \theta \rangle$	$d^2\sigma/dpd\Omega$	
0.13–0.16	0.151	68.2	63.69	\pm 45.06	5.82	0.153	79.1	92.88 \pm 60.05 \pm 8.77
0.16–0.20	0.182	64.0	55.98	\pm 30.25	4.13	0.186	80.6	106.85 \pm 47.79 \pm 7.21
0.20–0.24	0.224	67.8	157.13	\pm 55.69	9.17	0.223	82.7	51.76 \pm 30.38 \pm 2.66
0.24–0.30	0.264	64.8	86.45	\pm 31.94	3.82	0.269	81.7	105.57 \pm 37.48 \pm 4.44
0.30–0.36	0.334	66.1	143.16	\pm 43.17	5.95	0.344	77.7	55.94 \pm 28.00 \pm 3.14
0.36–0.42	0.384	69.3	66.24	\pm 29.63	3.65	0.390	84.7	27.37 \pm 19.36 \pm 2.07
0.42–0.50	0.454	72.0	17.92	\pm 12.68	1.44			
0.50–0.60	0.553	64.2	43.09	\pm 17.59	5.10	0.669	83.3	11.17 \pm 7.90 \pm 2.37
0.60–0.72	0.655	64.6	31.69	\pm 12.94	5.37			
0.72–0.90	0.784	68.9	6.88	\pm 4.86	1.64			
p_T	90 < θ < 105				105 < θ < 125			
	$\langle p_T \rangle$	$\langle \theta \rangle$	$d^2\sigma/dpd\Omega$		$\langle p_T \rangle$	$\langle \theta \rangle$	$d^2\sigma/dpd\Omega$	
0.13–0.16	0.135	102.9	130.07	\pm 109.54	11.82			
0.16–0.20	0.177	96.6	89.41	\pm 42.02	5.63	0.226	119.1	44.17 \pm 25.51 \pm 2.23
0.20–0.24	0.219	97.4	41.62	\pm 29.43	1.91	0.257	116.3	29.42 \pm 17.00 \pm 2.33
0.24–0.30	0.283	91.8	42.68	\pm 24.64	2.02	0.319	111.4	41.18 \pm 20.59 \pm 5.13
0.30–0.36	0.318	92.1	28.34	\pm 20.04	2.16			
0.36–0.42	0.369	96.2	26.45	\pm 18.71	3.00			
0.50–0.60	0.550	93.8	32.10	\pm 16.05	7.14			

Table A.43: Double-differential inclusive cross-section $d^2\sigma/dpd\Omega$ [mb/(GeV/c sr)] of the production of protons in $\pi^- + \text{Cu} \rightarrow p + X$ interactions with -15.0 GeV/c beam momentum; the first error is statistical, the second systematic; p_T in GeV/c, polar angle θ in degrees.

p_T	20 < θ < 30					30 < θ < 40						
	$\langle p_T \rangle$	$\langle \theta \rangle$	$d^2\sigma/dpd\Omega$			$\langle p_T \rangle$	$\langle \theta \rangle$	$d^2\sigma/dpd\Omega$				
			372.72	\pm	8.38	\pm	22.62	354.38	\pm	6.36	\pm	18.37
0.20–0.24	0.221	25.2	372.72	\pm	8.38	\pm	22.62	354.38	\pm	6.36	\pm	18.37
0.24–0.30	0.270	25.2	306.80	\pm	5.94	\pm	16.94	328.84	\pm	5.99	\pm	15.34
0.30–0.36	0.329	25.2	271.26	\pm	5.67	\pm	14.37	248.65	\pm	5.35	\pm	11.47
0.36–0.42	0.390	25.3	223.63	\pm	5.17	\pm	11.54	205.71	\pm	4.33	\pm	10.41
0.42–0.50	0.458	25.2	174.87	\pm	3.92	\pm	9.19	153.48	\pm	3.39	\pm	8.68
0.50–0.60	0.548	25.1	131.92	\pm	3.02	\pm	7.27	105.17	\pm	2.59	\pm	6.89
0.60–0.72	0.656	25.2	98.09	\pm	2.31	\pm	5.58	55.38	\pm	1.50	\pm	4.47
0.72–0.90								0.800	\pm	35.0	\pm	
p_T	40 < θ < 50					50 < θ < 60						
	$\langle p_T \rangle$	$\langle \theta \rangle$	$d^2\sigma/dpd\Omega$			$\langle p_T \rangle$	$\langle \theta \rangle$	$d^2\sigma/dpd\Omega$				
			350.35	\pm	6.06	\pm	14.81	293.11	\pm	5.36	\pm	12.51
0.30–0.36	0.329	45.1	288.98	\pm	5.55	\pm	11.46	230.47	\pm	4.28	\pm	9.07
0.36–0.42	0.389	45.1	222.88	\pm	4.38	\pm	9.52	167.50	\pm	3.43	\pm	8.10
0.42–0.50	0.458	45.1	152.68	\pm	3.38	\pm	8.35	100.85	\pm	2.59	\pm	6.91
0.50–0.60	0.548	45.0	102.84	\pm	2.61	\pm	7.11	50.91	\pm	1.53	\pm	4.57
0.60–0.72	0.655	44.9	55.75	\pm	1.60	\pm	4.89	14.41	\pm	0.59	\pm	1.94
0.72–0.90	0.798	45.1	15.81	\pm	0.59	\pm	1.98	1.034	\pm	55.0	\pm	
0.90–1.25								0.798	\pm	54.9	\pm	
p_T	60 < θ < 75					75 < θ < 90						
	$\langle p_T \rangle$	$\langle \theta \rangle$	$d^2\sigma/dpd\Omega$			$\langle p_T \rangle$	$\langle \theta \rangle$	$d^2\sigma/dpd\Omega$				
			157.21	\pm	2.54	\pm	7.58	68.88	\pm	1.54	\pm	5.27
0.50–0.60	0.546	67.5	93.72	\pm	1.93	\pm	6.20	29.03	\pm	0.93	\pm	3.29
0.60–0.72	0.654	67.2	44.55	\pm	1.17	\pm	4.58	113.0	\pm	0.70	\pm	2.31
0.72–0.90	0.797	67.2	12.11	\pm	0.46	\pm	1.94	112.4	\pm	4.58	\pm	1.02
0.90–1.25	1.033	67.0	3.13	\pm	0.24	\pm	0.60	1.033	\pm	81.5	\pm	
p_T	90 < θ < 105					105 < θ < 125						
	$\langle p_T \rangle$	$\langle \theta \rangle$	$d^2\sigma/dpd\Omega$			$\langle p_T \rangle$	$\langle \theta \rangle$	$d^2\sigma/dpd\Omega$				
			45.80	\pm	1.26	\pm	4.24	113.5	\pm	1.74	\pm	5.64
0.42–0.50	0.458	97.1	14.99	\pm	0.68	\pm	1.95	112.9	\pm	1.10	\pm	3.83
0.50–0.60	0.543	96.8	3.13	\pm	0.24	\pm	0.60	113.0	\pm	0.70	\pm	
0.60–0.72	0.650	96.1	0.794	\pm	0.34	\pm		112.4	\pm	4.58	\pm	
0.72–0.90	0.794											
0.90–1.25	1.015											

Table A.44: Double-differential inclusive cross-section $d^2\sigma/dpd\Omega$ [mb/(GeV/c sr)] of the production of π^+ 's in $\pi^- + \text{Cu} \rightarrow \pi^+ + \text{X}$ interactions with -15.0 GeV/c beam momentum; the first error is statistical, the second systematic; p_T in GeV/c, polar angle θ in degrees.

p_T	20 < θ < 30				30 < θ < 40			
	$\langle p_T \rangle$	$\langle \theta \rangle$	$d^2\sigma/dpd\Omega$		$\langle p_T \rangle$	$\langle \theta \rangle$	$d^2\sigma/dpd\Omega$	
			$\langle p_T \rangle$	$\langle \theta \rangle$			$d^2\sigma/dpd\Omega$	$d^2\sigma/dpd\Omega$
0.10–0.13	0.116	24.8	276.55	\pm 9.11	\pm 22.16	0.116	34.6	217.82 \pm 7.99 \pm 17.24
0.13–0.16	0.145	25.0	321.41	\pm 8.95	\pm 20.79	0.145	35.0	241.02 \pm 7.59 \pm 15.14
0.16–0.20	0.181	24.9	340.37	\pm 7.57	\pm 18.94	0.181	34.7	253.12 \pm 6.45 \pm 13.88
0.20–0.24	0.220	24.8	356.33	\pm 7.65	\pm 17.76	0.220	34.7	265.88 \pm 6.60 \pm 13.00
0.24–0.30	0.270	24.8	337.10	\pm 6.02	\pm 14.85	0.269	34.7	249.92 \pm 5.19 \pm 10.84
0.30–0.36	0.329	24.7	279.19	\pm 5.42	\pm 11.23	0.329	34.8	218.38 \pm 4.88 \pm 8.64
0.36–0.42	0.389	24.9	232.78	\pm 4.89	\pm 9.24	0.389	34.7	179.76 \pm 4.36 \pm 6.98
0.42–0.50	0.458	24.8	183.14	\pm 3.77	\pm 8.14	0.458	34.7	123.18 \pm 3.06 \pm 5.18
0.50–0.60	0.548	24.8	118.32	\pm 2.57	\pm 6.81	0.546	34.7	83.56 \pm 2.17 \pm 4.45
0.60–0.72	0.655	24.8	76.87	\pm 1.82	\pm 6.25	0.655	34.7	48.19 \pm 1.41 \pm 3.64
0.72–0.90						0.798	34.5	24.19 \pm 0.74 \pm 2.80
p_T	40 < θ < 50				50 < θ < 60			
	$\langle p_T \rangle$	$\langle \theta \rangle$	$d^2\sigma/dpd\Omega$		$\langle p_T \rangle$	$\langle \theta \rangle$	$d^2\sigma/dpd\Omega$	
			$\langle p_T \rangle$	$\langle \theta \rangle$			$d^2\sigma/dpd\Omega$	$d^2\sigma/dpd\Omega$
0.10–0.13	0.116	45.0	187.77	\pm 7.73	\pm 15.07	0.145	55.2	158.85 \pm 6.26 \pm 10.44
0.13–0.16	0.145	44.7	207.93	\pm 7.12	\pm 13.20	0.181	54.8	166.34 \pm 5.22 \pm 9.12
0.16–0.20	0.180	44.8	217.39	\pm 6.01	\pm 11.99	0.220	54.8	163.30 \pm 5.11 \pm 7.88
0.20–0.24	0.220	44.7	198.69	\pm 5.72	\pm 9.73	0.269	54.8	142.63 \pm 4.00 \pm 6.13
0.24–0.30	0.270	44.8	182.93	\pm 4.47	\pm 7.92	0.330	54.7	113.75 \pm 3.54 \pm 4.49
0.30–0.36	0.330	44.8	161.81	\pm 4.19	\pm 6.41	0.390	54.7	94.23 \pm 3.23 \pm 3.81
0.36–0.42	0.389	44.8	128.45	\pm 3.73	\pm 5.03	0.458	54.8	71.89 \pm 2.39 \pm 3.22
0.42–0.50	0.457	44.7	97.33	\pm 2.75	\pm 4.13	0.545	54.7	43.96 \pm 1.61 \pm 2.44
0.50–0.60	0.546	44.7	66.24	\pm 1.97	\pm 3.45	0.656	54.6	25.14 \pm 1.09 \pm 1.86
0.60–0.72	0.652	44.7	36.32	\pm 1.27	\pm 2.56	0.797	54.4	10.15 \pm 0.51 \pm 1.08
0.72–0.90	0.794	44.4	16.31	\pm 0.64	\pm 1.74	1.028	54.3	2.43 \pm 0.14 \pm 0.43
p_T	60 < θ < 75				75 < θ < 90			
	$\langle p_T \rangle$	$\langle \theta \rangle$	$d^2\sigma/dpd\Omega$		$\langle p_T \rangle$	$\langle \theta \rangle$	$d^2\sigma/dpd\Omega$	
			$\langle p_T \rangle$	$\langle \theta \rangle$			$d^2\sigma/dpd\Omega$	$d^2\sigma/dpd\Omega$
0.13–0.16	0.146	66.9	129.17	\pm 4.86	\pm 8.61	0.145	84.2	138.99 \pm 43.27 \pm 10.92
0.16–0.20	0.180	67.3	136.46	\pm 3.86	\pm 7.51	0.180	82.0	100.31 \pm 3.39 \pm 5.34
0.20–0.24	0.219	67.1	122.37	\pm 3.60	\pm 5.83	0.220	81.9	88.88 \pm 3.10 \pm 4.05
0.24–0.30	0.269	67.0	102.67	\pm 2.76	\pm 4.29	0.268	81.8	75.59 \pm 2.40 \pm 3.25
0.30–0.36	0.329	66.7	82.04	\pm 2.49	\pm 3.41	0.329	81.6	48.10 \pm 1.92 \pm 2.13
0.36–0.42	0.389	66.6	62.22	\pm 2.16	\pm 2.66	0.388	81.6	37.60 \pm 1.70 \pm 1.90
0.42–0.50	0.457	66.7	45.96	\pm 1.59	\pm 2.28	0.457	81.6	25.56 \pm 1.17 \pm 1.51
0.50–0.60	0.547	66.8	28.92	\pm 1.08	\pm 1.86	0.547	81.8	18.18 \pm 0.86 \pm 1.42
0.60–0.72	0.653	66.7	15.36	\pm 0.70	\pm 1.33	0.652	81.9	8.35 \pm 0.52 \pm 0.86
0.72–0.90	0.794	66.3	6.15	\pm 0.33	\pm 0.76	0.789	81.7	3.30 \pm 0.25 \pm 0.48
0.90–1.25	1.029	66.4	1.35	\pm 0.09	\pm 0.26	1.035	80.6	0.52 \pm 0.06 \pm 0.12
p_T	90 < θ < 105				105 < θ < 125			
	$\langle p_T \rangle$	$\langle \theta \rangle$	$d^2\sigma/dpd\Omega$		$\langle p_T \rangle$	$\langle \theta \rangle$	$d^2\sigma/dpd\Omega$	
			$\langle p_T \rangle$	$\langle \theta \rangle$			$d^2\sigma/dpd\Omega$	$d^2\sigma/dpd\Omega$
0.13–0.16	0.143	98.2	136.90	\pm 47.57	\pm 10.00	0.145	114.5	74.78 \pm 3.04 \pm 4.54
0.16–0.20	0.179	97.5	85.71	\pm 3.11	\pm 4.42	0.179	114.0	63.62 \pm 2.23 \pm 3.22
0.20–0.24	0.219	97.3	72.59	\pm 2.80	\pm 3.15	0.218	113.7	46.11 \pm 1.97 \pm 1.99
0.24–0.30	0.268	97.1	54.21	\pm 2.06	\pm 2.37	0.266	113.8	30.72 \pm 1.34 \pm 1.51
0.30–0.36	0.329	96.6	30.72	\pm 1.54	\pm 1.55	0.329	113.5	16.48 \pm 0.96 \pm 1.06
0.36–0.42	0.387	97.0	20.93	\pm 1.22	\pm 1.30	0.389	113.7	11.24 \pm 0.79 \pm 0.94
0.42–0.50	0.459	96.9	15.15	\pm 0.92	\pm 1.22	0.455	112.7	6.88 \pm 0.53 \pm 0.74
0.50–0.60	0.543	97.2	7.34	\pm 0.55	\pm 0.79	0.542	112.7	2.73 \pm 0.27 \pm 0.39
0.60–0.72	0.653	96.4	3.30	\pm 0.33	\pm 0.47	0.641	111.5	0.74 \pm 0.14 \pm 0.14
0.72–0.90	0.795	96.1	1.28	\pm 0.16	\pm 0.24	0.774	114.0	0.12 \pm 0.04 \pm 0.03
0.90–1.25	1.045	96.8	0.17	\pm 0.03	\pm 0.05	1.030	109.8	0.02 \pm 0.01 \pm 0.01

Table A.45: Double-differential inclusive cross-section $d^2\sigma/dpd\Omega$ [mb/(GeV/c sr)] of the production of π^- 's in $\pi^- + \text{Cu} \rightarrow \pi^- + \text{X}$ interactions with -15.0 GeV/c beam momentum; the first error is statistical, the second systematic; p_T in GeV/c, polar angle θ in degrees.

p_T	20 < θ < 30				30 < θ < 40			
	$\langle p_T \rangle$	$\langle \theta \rangle$	$d^2\sigma/dpd\Omega$		$\langle p_T \rangle$	$\langle \theta \rangle$	$d^2\sigma/dpd\Omega$	
0.10–0.13	0.115	24.7	363.75	± 10.38	28.41	0.115	34.8	253.15 ± 8.52 ± 20.01
0.13–0.16	0.145	24.6	403.10	± 10.03	26.17	0.145	34.7	289.21 ± 8.41 ± 18.70
0.16–0.20	0.180	24.6	458.73	± 8.89	25.54	0.181	34.8	333.24 ± 7.59 ± 18.58
0.20–0.24	0.220	24.6	460.48	± 8.82	22.78	0.220	34.8	313.42 ± 7.17 ± 15.33
0.24–0.30	0.269	24.8	437.88	± 6.95	18.66	0.269	34.7	300.24 ± 5.79 ± 12.83
0.30–0.36	0.329	24.7	366.60	± 6.36	14.27	0.329	34.7	248.28 ± 5.16 ± 9.65
0.36–0.42	0.389	24.7	305.15	± 5.80	12.03	0.389	34.7	202.97 ± 4.68 ± 7.95
0.42–0.50	0.458	24.6	221.21	± 4.24	9.94	0.459	34.8	146.78 ± 3.41 ± 6.47
0.50–0.60	0.546	24.7	148.59	± 3.13	8.49	0.547	34.7	101.91 ± 2.54 ± 5.66
0.60–0.72	0.653	24.8	90.25	± 2.21	6.86	0.656	34.8	59.29 ± 1.76 ± 4.37
0.72–0.90	0.796	24.8	90.25	± 2.21	6.86	0.796	34.6	32.42 ± 1.08 ± 3.28
p_T	40 < θ < 50				50 < θ < 60			
	$\langle p_T \rangle$	$\langle \theta \rangle$	$d^2\sigma/dpd\Omega$		$\langle p_T \rangle$	$\langle \theta \rangle$	$d^2\sigma/dpd\Omega$	
0.10–0.13	0.115	45.0	201.30	± 7.59	16.28	0.145	55.0	194.12 ± 6.95 ± 12.96
0.13–0.16	0.145	44.9	255.49	± 7.97	16.66	0.180	54.9	200.17 ± 5.84 ± 11.17
0.16–0.20	0.180	44.8	245.09	± 6.46	13.75	0.220	54.9	196.42 ± 5.75 ± 9.50
0.20–0.24	0.219	44.8	231.22	± 6.25	11.40	0.269	54.8	166.88 ± 4.33 ± 7.03
0.24–0.30	0.270	44.7	217.67	± 4.91	9.29	0.328	54.9	132.74 ± 3.82 ± 5.19
0.30–0.36	0.330	44.6	177.02	± 4.39	6.90	0.390	54.6	105.02 ± 3.41 ± 4.29
0.36–0.42	0.389	44.7	144.72	± 3.95	5.77	0.457	54.7	75.93 ± 2.44 ± 3.59
0.42–0.50	0.459	44.5	106.38	± 2.88	4.86	0.546	54.7	53.26 ± 1.86 ± 3.22
0.50–0.60	0.546	44.8	71.12	± 2.12	4.15	0.653	54.7	30.16 ± 1.25 ± 2.42
0.60–0.72	0.654	44.8	41.61	± 1.45	3.26	0.791	54.6	11.63 ± 0.61 ± 1.31
0.72–0.90	0.793	44.8	18.84	± 0.80	2.02	1.037	54.5	2.23 ± 0.15 ± 0.41
p_T	60 < θ < 75				75 < θ < 90			
	$\langle p_T \rangle$	$\langle \theta \rangle$	$d^2\sigma/dpd\Omega$		$\langle p_T \rangle$	$\langle \theta \rangle$	$d^2\sigma/dpd\Omega$	
0.13–0.16	0.145	67.5	166.04	± 5.32	10.85	0.147	81.8	150.06 ± 8.07 ± 14.04
0.16–0.20	0.180	67.3	153.81	± 4.14	8.18	0.179	81.9	121.33 ± 3.74 ± 6.26
0.20–0.24	0.219	67.1	141.39	± 3.94	6.52	0.220	82.3	108.18 ± 3.51 ± 4.86
0.24–0.30	0.269	66.8	120.64	± 3.05	5.15	0.269	81.9	86.25 ± 2.61 ± 3.78
0.30–0.36	0.330	66.9	93.32	± 2.68	3.78	0.328	81.9	61.23 ± 2.22 ± 2.89
0.36–0.42	0.389	66.8	73.33	± 2.35	3.16	0.389	81.8	45.19 ± 1.87 ± 2.33
0.42–0.50	0.457	67.0	50.43	± 1.65	2.62	0.456	81.9	30.88 ± 1.32 ± 1.96
0.50–0.60	0.545	66.8	31.25	± 1.14	2.11	0.545	81.7	19.52 ± 0.92 ± 1.64
0.60–0.72	0.653	66.6	16.18	± 0.73	1.47	0.653	81.6	8.06 ± 0.51 ± 0.91
0.72–0.90	0.799	66.5	6.30	± 0.36	0.78	0.796	81.1	2.69 ± 0.25 ± 0.40
0.90–1.25	1.026	66.1	1.15	± 0.10	0.22	1.025	81.0	0.41 ± 0.06 ± 0.09
p_T	90 < θ < 105				105 < θ < 125			
	$\langle p_T \rangle$	$\langle \theta \rangle$	$d^2\sigma/dpd\Omega$		$\langle p_T \rangle$	$\langle \theta \rangle$	$d^2\sigma/dpd\Omega$	
0.13–0.16	0.147	97.5	127.02	± 6.25	11.18	0.145	114.4	88.97 ± 3.31 ± 5.51
0.16–0.20	0.179	97.4	103.21	± 3.41	5.27	0.178	114.2	75.85 ± 2.54 ± 3.41
0.20–0.24	0.219	97.3	82.99	± 3.10	3.58	0.219	113.6	51.27 ± 2.10 ± 2.26
0.24–0.30	0.268	96.7	61.30	± 2.21	2.79	0.266	113.7	34.76 ± 1.44 ± 1.85
0.30–0.36	0.329	96.9	41.20	± 1.79	2.13	0.329	113.5	18.81 ± 1.04 ± 1.35
0.36–0.42	0.389	97.0	29.06	± 1.49	1.95	0.388	113.2	11.59 ± 0.78 ± 1.09
0.42–0.50	0.458	96.3	16.59	± 0.96	1.45	0.460	112.1	7.42 ± 0.55 ± 0.90
0.50–0.60	0.542	97.0	9.21	± 0.61	1.08	0.543	111.7	2.82 ± 0.30 ± 0.44
0.60–0.72	0.651	96.6	4.66	± 0.41	0.72	0.651	112.7	0.69 ± 0.13 ± 0.14
0.72–0.90	0.792	95.7	0.93	± 0.14	0.19	0.790	110.8	0.21 ± 0.06 ± 0.06
0.90–1.25	0.989	96.4	0.18	± 0.04	0.06	1.052	110.8	0.04 ± 0.02 ± 0.02